

In vitro and *in silico* studies elucidating
pharmacodynamic interactions of
 β -lactam/ β -lactamase-inhibitor
combinations with last-resort antibiotics

Dissertation

to obtain the academic degree
Doctor rerum naturalium (Dr. rer. nat.)

submitted to the Department of Chemistry,
Clinical Pharmacy,
Institute of Pharmacy,
Faculty of Mathematics, Informatics and Natural Sciences
University of Hamburg

by

Niklas Krömer

born in Borken

Hamburg 2024

The results presented in this dissertation were obtained from January 2020 until April 2023 supervised by Prof. Dr. Sebastian G. Wicha at the Department of Clinical Pharmacy, Institute of Pharmacy, University of Hamburg.

First Reviewer: Prof. Dr. Sebastian G. Wicha

Second Reviewer: Priv.-Doz. Dr. Claudia Langebrake

Thesis defence committee: Prof. Dr. Sebastian G. Wicha

Prof. Dr. Peter Heisig

Prof. Dr. Wolfgang Maison

Date of thesis defence and approval: 22nd March 2024

One sometimes finds what one is not looking for.

Sir Alexander Fleming (1881-1955)

I. List of publications

Original articles included in the cumulative dissertation

Niklas Kroemer, Romain Aubry, William Couet, Nicolas Grégoire, Sebastian G. Wicha. Optimized rhombic experimental dynamic checkerboard designs to elucidate pharmacodynamic drug interactions of antibiotics. *Pharmaceutical Research*. 39, 3267-3277. 2022. doi: 10.1007/s11095-022-03396-7

Niklas Kroemer, Miklas Martens, Jean-Winoc Decousser, Nicolas Grégoire, Patrice Nordmann, Sebastian G. Wicha. Evaluation of *in vitro* pharmacodynamic drug interactions of ceftazidime/avibactam and fosfomycin in *Escherichia coli*. *Journal of Antimicrobial Chemotherapy*. 78(10), 2524-2534. 2023. doi: 10.1093/jac/dkad264

Niklas Kroemer, Lisa F. Amann, Aneeq Farooq, Christoph Pfaffendorf, Miklas Martens, Jean-Winoc Decousser, Nicolas Grégoire, Patrice Nordmann, Sebastian G. Wicha. Pharmacokinetic/pharmacodynamic analysis of ceftazidime/avibactam and fosfomycin combinations in an *in vitro* hollow fiber infection model against multidrug-resistant *Escherichia coli*. *Microbiology Spectrum*. 12(1), e03318-23. 2024. doi: 10.1128/spectrum.03318-23

Original articles

Anna K. Tietjen, **Niklas Kroemer**, Dario Cattaneo, Sara Baldelli, Sebastian G. Wicha. Population pharmacokinetics and target attainment analysis of linezolid in multidrug-resistant tuberculosis patients. *British Journal of Clinical Pharmacology*. 88(4), 1835-1844. 2021.

doi: 10.1111/bcp.15102

Conference abstracts (oral/poster)

Aneeq Farooq, **Niklas Kroemer**, Jean-Winoc Decousser, Sebastian G. Wicha. *In vitro* pharmacokinetic/pharmacodynamic interaction model assessing the synergy between meropenem and fosfomycin in a clinical multi-resistant *K. pneumoniae* isolate. Population Approach Group Europe (PAGE) Meeting 2023. A Coruña, Spain. 27th - 30th June 2023.

(poster presentation)

Niklas Kroemer, Aneeq Farooq, Jean-Winoc Decousser, Julien Buyck, Nicolas Grégoire, Patrice Nordmann, Sebastian G. Wicha. Hollow fiber study assessing synergy of ceftazidime/avibactam and fosfomycin in a clinical *E. coli* expressing beta-lactamase and carbapenemase genes. 33rd European Congress of Clinical Microbiology and Infectious Diseases (ECCMID). Copenhagen, Denmark. 15th - 18th April 2023.

(poster presentation)

Aneeq Farooq, **Niklas Kroemer**, Jean-Winoc Decousser, Julien Buyck, Nicolas Grégoire, Patrice Nordmann, Sebastian G. Wicha. *In vitro* evaluation of the interaction between meropenem-fosfomycin and meropenem-vaborbactam-fosfomycin in a clinical multi-drug resistant *K. pneumoniae* strain expressing KPC-2. 33rd European Congress of Clinical Microbiology and Infectious Diseases (ECCMID). Copenhagen, Denmark. 15th - 18th April 2023.

(poster presentation)

Aneeq Farooq, **Niklas Kroemer**, Jean-Winoc Decousser, Julien Buyck, Nicolas Grégoire, Patrice Nordmann, Sebastian G. Wicha. Pharmacokinetic/pharmacodynamic studies of meropenem combined with fosfomycin in a clinical *K. pneumoniae* isolate expressing KPC-2 carbapenemase and fosfomycin resistance. Hengstberger-Symposium. Heidelberg, Germany. 17th - 19th March 2023.

(oral presentation)

Niklas Kroemer, Jean-Winoc Decousser, Julien Buyck, Patrice Nordmann, Sebastian G. Wicha. Systematic in vitro interaction study on ceftazidime/avibactam and fosfomycin. 32nd International Congress of Antimicrobial Chemotherapy (ICC). Perth, Australia. 27th - 30th November 2022. Published in: Journal of Global Antimicrobial Resistance. 31 (S1), S21-S22. 2022. doi: 10.1016/S2213-7165(22)00313-7

(poster presentation)

Niklas Kroemer, Jean-Winoc Decousser, Patrice Nordmann, Sebastian G. Wicha. A general pharmacodynamic interaction modelling approach to assess semi-mechanistic synergy of ceftazidime/avibactam and fosfomycin in time kill experiments. Population Approach Group Europe (PAGE) Meeting 2022. Ljubljana, Slovenia. 28th June - 1st July 2022.

(poster presentation)

Niklas Kroemer, Jean-Winoc Decousser, Julien Buyck, Nicolas Grégoire, Patrice Nordmann, Sebastian G. Wicha. Systematic pharmacodynamic interaction screening of meropenem-vaborbactam and fosfomycin in isogenic and clinical *E. coli* and *K. pneumoniae* isolates expressing ESBL or carbapenemases. 32nd European Congress of Clinical Microbiology and Infectious Diseases (ECCMID). Lisbon, Portugal. 23th - 26th April 2022.

(poster presentation)

Aneeq Farooq, **Niklas Kroemer**, Jean-Winoc Decousser, Julien Buyck, Nicolas Grégoire, Patrice Nordmann, Sebastian G. Wicha. Interaction screening of ceftazidime-avibactam and tigecycline against six clinical and nine isogenic *E. coli* and *K. pneumoniae* strains expressing carbapenemases. 32nd European Congress of Clinical Microbiology and Infectious Diseases (ECCMID). Lisbon, Portugal. 23th - 26th April 2022.
(poster presentation)

Niklas Kroemer, Jean-Winoc Decousser, Julien Buyck, Nicolas Grégoire, Patrice Nordmann, Sebastian G. Wicha. Systematic 'dynamic' checkerboard screening of eight isogenic *E. coli* strains against ceftazidime-avibactam and fosfomycin. Annual Meeting of the German Pharmaceutical Society (DPhG). Virtual meeting. 28th September - 1st October 2021.
(poster presentation)

Niklas Kroemer, Romain Aubry, Nicolas Grégoire, William Couet, Sebastian G. Wicha. Development and evaluation of D-optimal 2x2 checkerboard designs for identification of pharmacodynamic drug interactions. Population Approach Group Europe (PAGE) Meeting 2021. Virtual meeting. 2nd - 7th September 2021.
(poster presentation)

Niklas Kroemer, Jean-Winoc Decousser, Julien Buyck, Nicolas Grégoire, Patrice Nordmann, Sebastian G. Wicha. Systematic interaction screening of ceftazidime-avibactam and fosfomycin against eight isogenic *E. coli* strains. 31st European Congress of Clinical Microbiology and Infectious Diseases (ECCMID). Virtual meeting. 9th - 12th July 2021.
(poster presentation)

Presentations without abstract

Niklas Kroemer, Sebastian G. Wicha. Rationale Kombinationstherapien von neuen β -Laktam- β -Laktamase-Inhibitoren mit Reserveantibiotika gegen Gram-negative Problemkeime. Tag der Pharmazie. Hamburg, Germany. 22th June 2022.

(oral presentation)

Niklas Kroemer, Sebastian G. Wicha. Adaptive optimal design to support efficient high throughput screening of in vitro pharmacodynamic drug interaction studies. Virtual International Society of Anti-Infective Pharmacology (ISAP) Meeting. 18th September 2020.

(oral presentation)

II. Contents

I.	List of publications	I
II.	Contents.....	VII
III.	List of abbreviations.....	IX
IV.	Zusammenfassung.....	XI
V.	Abstract.....	XV
1	Introduction.....	1
1.1	Antimicrobial resistance – the hidden pandemic	1
1.2	Need for innovative treatment options.....	1
1.3	Drug interactions.....	3
1.4	Key antibiotics in the present thesis.....	4
1.4.1	Ceftazidime/avibactam.....	5
1.4.2	Fosfomycin	6
1.5	Key pharmacological elements in the present thesis.....	7
1.5.1	Pharmacokinetics.....	8
1.5.2	Pharmacodynamics	8
1.6	Pharmacometrics	9
1.6.1	Pharmacometric modelling	9
1.6.2	Pharmacometric simulations	12
1.6.3	Optimal experimental design	13
1.7	<i>In vitro</i> infection models.....	14
1.7.1	Susceptibility testing methods	14
1.7.2	Checkerboard assay	15
1.7.3	Static time kill experiment.....	16

1.7.4	Dynamic Hollow Fiber experiment	17
2	Objectives	19
3	Cumulative part.....	23
3.1	Publication I.....	25
3.2	Publication II.....	39
3.3	Publication III.....	53
4	Discussion	67
4.1	Design of experiments.....	67
4.2	Evaluation of drug interactions	69
4.3	Extrapolation of <i>in vitro</i> results	73
4.3.1	<i>In vitro-in vitro</i> transfer.....	74
4.3.2	<i>In vitro-in vivo</i> translation	77
4.4	Combination therapy in clinical practice.....	81
4.5	Guidance of clinical decision making	83
5	Limitations and Perspectives	87
6	References	89
7	Appendix.....	107
7.1	Supplementary material of Publication I	107
7.2	Supplementary material of Publication II	111
7.3	Supplementary material of Publication III	121
8	Hazardous materials	141
9	Acknowledgements.....	143
10	Eidesstattliche Versicherung	145

III. List of abbreviations

AmpC	AmpC beta-lactamase
AMR	antimicrobial resistance
AUC	area under the concentration-time curve
CLSI	Clinical and Laboratory Standards Institute
CTX-M	Cefotaxime-Munich-beta-lactamase
EC	effective concentrations
EC50	drug potency
<i>E. coli</i>	<i>Escherichia coli</i>
E _{max}	maximum drug effect
Etest	Epsilometer test
EUCAST	European Committee on Antimicrobial Susceptibility Testing
FIC	fractional inhibitory concentration
FosA	enzyme mediating fosfomycin resistance
GlpT	L-alpha- glycerophosphate transporter
GPDI	general pharmacodynamic interaction
<i>K. pneumoniae</i>	<i>Klebsiella pneumoniae</i>
KPC	<i>Klebsiella pneumoniae</i> carbapenemase
MIC	minimum inhibitory concentration
MurA	UDP-N-acetylglucosamine enolpyruvyl transferase
NDM	New Delhi metallo-β-lactamase
NLME	non-linear mixed effects
OXA	oxacillinase
<i>P. aeruginosa</i>	<i>Pseudomonas aeruginosa</i>
PBPK	physiologically based pharmacokinetic(s)
PD	pharmacodynamic(s)

PK	pharmacokinetic(s)
q8h	every 8 h
SSE	Stochastic Simulation and Estimation
TEM	Temoniera
UhpT	hexose-6-phosphate transporter
VIM	Verona integron-encoded metallo-beta-lactamase
WHO	World Health Organisation

IV. Zusammenfassung

Das Vorkommen von Antibiotikaresistenzen stellt eine große Bedrohung für hospitalisierte Patienten dar. Vor allem das vermehrte Auftreten von resistenten gram-negativen *Enterobacteriaceae* wie *Klebsiella pneumoniae* oder *Escherichia coli* sind besorgniserregend. Aufgrund dessen hat die Weltgesundheitsorganisation (WHO) der Forschung und Entwicklung neuer Antibiotika gegen diese Erreger eine sehr hohe Priorität zugeordnet.[1] Neben der Entwicklung von neuen antimikrobiellen Wirkstoffen, kann das Umwidmen und Kombinieren von bereits zugelassenen Substanzen dazu beitragen, Antibiotikaresistenzen zu überwinden und mögliche vorteilhafte Arzneistoff-interaktionen auszunutzen.[2], [3] Die wirkungsvollsten Methoden, um *in vitro* Arzneistoffinteraktionen umfassend zu analysieren, zu quantifizieren und deren klinisches Potential abzuschätzen, sind pharmakometrische *in silico* Modellierungs- und Simulationstechniken.[4]

Neue Hoffnungen für die Therapie von multiresistenten Erregern stellen in den letzten Jahren Zulassungen von neuen Beta-Laktam/Beta-Laktamase-Inhibitor-Kombinationen dar. Einer dieser Vertreter ist Ceftazidim/Avibactam, gegen welchen trotz seines limitierten Einsatzes bereits Resistenzen beschrieben worden sind.[5] Daher kann die Entwicklung von Kombinationstherapien beim Schutz vor weiteren Resistenz-entwicklungen und zur Erhöhung der Wirksamkeit unterstützen.[6] Einen möglichen Kombinationspartner stellt das Antibiotikum Fosfomycin dar, für welches bereits synergistische Arzneistoffinteraktionen mit Beta-Laktam/Beta-Laktamase-Inhibitor-Kombinationen bekannt sind. Eine mechanistische und quantitative Untersuchung in der Kombination mit Ceftazidim/Avibactam in *E. coli* steht allerdings noch aus.[7]

Daher ist das Ziel des vorliegenden Promotionsprojekts die pharmakodynamischen Arzneistoffinteraktionen von Ceftazidim/Avibactam und Fosfomycin in verschiedenen *E. coli* Stämmen, die klinisch relevante Beta-Laktamasen mit erweitertem Spektrum oder Carbapenemasen exprimieren, aufzuklären. Dazu sollten systematische *in vitro* Experimente mittels aussagekräftiger pharmakometrischer Methoden ausgewertet

werden, um Arzneistoffinteraktionen semi-mechanistisch zu beschreiben, zu quantifizieren und die Erkenntnisse letztlich ins klinische Umfeld zu übertragen.

In der Publikation I wurden dazu experimentelle Checkerboard-Designs mittels D-optimaler Design Strategie entwickelt, die eine Testung von Interaktionen effizienter und rationaler gestalten. Die *in silico* Optimierung führte zu rhombischen Designs, welche nur vier getestete Kombinationen umfassen, die auf Arzneistoffpotenzen basieren. Stochastische Simulationen und Schätzungen wurden durchgeführt, um die entwickelten Designs statistisch mit Referenzdesigns mit bis zu 81 Kombination im Hinblick auf Richtigkeit, Präzision und Klassifikationsraten von Interaktionen zu vergleichen. Zweifelsohne führte die Reduktion der experimentellen Designs zu einem Informationsverlust, allerdings steigerten die rhombischen Designs im Vergleich zu aufwändigeren Experimenten die Effizienz deutlich.

In Publikation II wurde das entwickelte rhombische experimentelle Design in einem Interaktions-Screening eingesetzt, welches vierzehn isogene und klinische *E. coli* Isolate umfasste. Expositions-Effekt-Oberflächen-Analysen identifizierten starke synergistische Interaktionen in 70% der untersuchten Bakterienstämme. In den meisten Fällen verstärkte Ceftazidim/Avibactam die Fosfomycin-Effekte, wenngleich ein eindeutiger Zusammenhang zwischen dem genetischen Profil der Isolate und den jeweiligen Arzneistoffinteraktionen nicht identifiziert werden konnte. Die Interaktionen wurden in statischen Time-Kill-Experimenten in drei klinischen *E. coli* Stämmen bestätigt. Anschließende pharmakokinetisch-pharmakodynamische (PK/PD) Modellierungen quantifizierten bis zu 97% erhöhte Arzneistoffpotenzen in Kombination und bekräftigten die Art und Richtung der Synergien, die in den Checkerboard-Experimenten festgestellt wurden. Zusätzlich konnte mit Hilfe der semi-mechanistischen Modelle die Hypothese entwickelt werden, dass Ceftazidim/Avibactam und Fosfomycin in Kombination eine verstärkte abtötende Wirkung von Bakterien erzielen und dadurch zusätzlich die Entwicklung von Resistenzen unterdrücken.

Um die Arzneistoffinteraktionen bei dynamischer Pharmakokinetik zu untersuchen, wurden in Publikation III zunächst die Interaktionen von Ceftazidim und Avibactam untersucht. Die vorangegangenen Modellierungen wurden daraufhin genutzt, um

dynamische Hollow-Fiber-Experimente, die die Pharmakokinetik klinischer Dosierschemata in einem *in vitro* Infektionsmodell imitieren, vorzubereiten. Ein PK/PD Modell mit semi-mechanistischen und subpopulations-synergistischen Elementen wurde entwickelt, um die bakteriellen Dynamiken und das Aufkommen phänotypisch resistenter Subpopulationen zu beschreiben. Simulationen hoben das Potential der Synergie im Hinblick auf Dosis-Reduktionen in einer Kombinationstherapie hervor, da sich eine simulierte Kombination von 0.5 g alle 8 h (q8h) Fosfomycin und 0.25/0.06 g q8h Ceftazidim/Avibactam genauso wirksam zeigte wie eine vergleichbare Monotherapie von 6 g q8h Fosfomycin oder 1.5/0.375 g q8h Ceftazidim/Avibactam.

V. Abstract

The emergence of antimicrobial resistance (AMR) represents a major threat to hospitalised patients. Especially rising resistances in gram-negative *Enterobacteriaceae* such as *Klebsiella pneumoniae* or *Escherichia coli* are of concern. Therefore, those pathogens were assigned with a ‘critical’ priority for research and development of new antibiotics by the World Health Organisation (WHO).[1] Besides the development of new antimicrobial agents, the repurposing and combination of approved drugs can allow to overcome antimicrobial resistance and exploit beneficial drug interactions.[2], [3] The most potent tools in order to thoroughly analyse and quantify *in vitro* drug interactions as well as to translationally predict their clinical potential are *in silico* pharmacometric modelling and simulation techniques.[4]

New hope for the treatment of resistant pathogens was brought by the approval of novel beta-lactam/beta-lactamase inhibitor combinations in the recent years. Ceftazidime/avibactam is one of those representatives, but despite its limited application resistances were already described.[5] Therefore, the development of combination therapies can support to protect against the further development of resistances and to increase efficacy.[6] A potential combination partner is fosfomycin, for which beneficial drug interactions with beta-lactam/beta-lactamase inhibitor combinations are known, but a mechanistic and quantitative evaluation of the combination with ceftazidime/avibactam in *E. coli* is lacking.[7]

Hence, the present PhD project aims to elucidate the pharmacodynamic drug interactions of ceftazidime/avibactam and fosfomycin in different *E. coli* strains expressing clinically relevant extended-spectrum beta-lactamases or carbapenemases. Systematic *in vitro* experiments should be evaluated by meaningful pharmacometrics to semi-mechanistically describe and quantify drug interactions and to ultimately translate the knowledge into the clinical setting.

In Publication I, optimal experimental checkerboard designs were developed by means of D-optimal design theorem to enable an efficient and streamlined interaction testing.

The *in silico* optimisation led to designs comprising solely four tested combinations based on drug potency values arranged in a rhombic fashion. Stochastic Simulation and Estimation (SSE) was used to statistically compare the developed designs to reference designs including up to 81 combinations with regard to accuracy, precision and classification rates of drug interactions. Apparently, the extensive reduction of the experimental designs led to a loss of information, but the rhombic designs indicated to be considerably more efficient than more cumbersome experiments.

In Publication II, the developed rhombic experimental design was applied in an interaction screening including fourteen isogenic and clinical *E. coli* isolates. Exposure-response-surface-analyses identified strong synergistic interactions increasing the drug potencies in 70% of the evaluated strains. In most cases ceftazidime/avibactam enhanced the fosfomycin effects, but a distinct correlation between the genetics of the isolates and the respective drug interactions could not be identified. The interactions were corroborated in detailed static time kill experiments against three clinical *E. coli* strains. Subsequent pharmacokinetic-pharmacodynamic (PK/PD) modelling quantified up to 97% increased drug potencies in combination and confirmed the type and directions of the synergies identified in the checkerboard experiments. Additionally, the semi-mechanistic modelling evolved the hypothesis, that in combination ceftazidime/avibactam and fosfomycin enhance bacterial killing effects, which also suppresses the emergence of resistance.

In order to translate the drug interaction into dynamic pharmacokinetics the interactions of ceftazidime and avibactam were firstly explored in Publication III. The preceding modelling guided dynamic Hollow Fiber experiments mimicking the pharmacokinetics of clinical dosing regimens in an *in vitro* infection model. A PK/PD model with elements of semi-mechanistic and subpopulation synergy was able to describe the bacterial dynamics and the emergence of phenotypic resistant subpopulations. Simulations revealed the potential of the synergy for dose reductions since a simulated combination of doses of 0.5 g every 8 h (q8h) fosfomycin and 0.25/0.06 g q8h ceftazidime/avibactam showed to be as efficacious as a respective monotherapy of 6 g q8h fosfomycin or 1.5/0.375 g q8h ceftazidime/avibactam.

1 Introduction

1.1 Antimicrobial resistance – the hidden pandemic

Antibiotic resistances are as old as the discovery of antibacterial agents. Sir Alexander Fleming already foresaw the menace of antimicrobial resistance when receiving his Nobel Prize in 1945.[8] Today, nearly 80 years later, antibiotic resistances represent a severe threat for public health and a ‘postantibiotic era’ is hypothesised.[6], [9] In 2019, 1.27 million deaths were estimated to be directly linked to antimicrobial resistance, which is comparable to the combined number of deaths associated with HIV and malaria.[10] In order to streamline the urgent need for effective therapies the World Health Organisation (WHO) defined priorities for research and development.[1] A ‘critical’ priority was assigned to gram-negative *Enterobacteriaceae* like *E. coli* and *K. pneumoniae*, which are amongst the leading antimicrobial resistant pathogens responsible for preventable deaths in 2019.[1], [9] As in many areas of health care, there is an imbalance of the antimicrobial resistance burden from low to high income countries. Nevertheless, also the European Centre for Disease Prevention and Control stated for 2021, that 53.1% of all reported *E. coli* cases and 34.3% of all reported *K. pneumoniae* in Europe were resistant to at least one antimicrobial group under surveillance.[11] This highlights that antimicrobial resistance is a global health concern, but in contrast to the raging pandemic of COVID-19, the pandemic of antimicrobial resistance proceeds hidden.[10], [12] Thus, new and innovative treatment options are urgently required to ensure efficacious antimicrobial therapies to limit further emergence of resistance and prevent avoidable deaths.

1.2 Need for innovative treatment options

Development of new compounds represents the most apparent way to combat resistant pathogens. Nevertheless, the repurposing of already approved drugs with regard to label expansions or development of innovative combination therapies can establish new treatment options as well.[2] The most prominent antibiotic drugs in the research

and development pipelines are direct-acting small molecules encountering known or new bacterial targets like the bacterial cell wall or protein biosynthesis. Other investigated strategies are modulations of the host immune system, alterations of the pathogenicity of the bacteria or phage therapy.[2] In the 'arms race' of researchers and clinicians against the pathogens the development of new potentiators of anti-infective drugs can be another mechanism to tackle resistant bacteria.[2], [13] A well-known example for potentiators in antibiotic therapy are beta-lactamase inhibitors protecting beta-lactam antibiotics against degradation by upcoming beta-lactamases and restoring their activity against bacteria which became resistant.

Although these various research approaches are pursued and the discovery of new drugs is promoted, the development of new compounds is challenging. Reasons are remaining deficits in funding and complex translations from preclinical to clinical research.[2] Additionally, the classic antibiotic targets have often been exploited extensively and new identified targets are less easy druggable. Hence, often lower-risk paths such as modifications of already existing drug classes are followed.[2] That is also the reason, why the WHO warns that in the upcoming years only few innovative antibiotic agents will recharge the antibiotic armouries.[14] Therefore, a repurposing and combination of available drugs seem to offer the most immediate benefit from the options introduced above. Motives of an application of combination therapy are mainly the following: I) expansion of the antibacterial spectrum in the initiation phase of an empirical therapy, when the identity and susceptibility of the pathogen is still unknown, II) the suppression of emergence of resistances, III) the exploitation of drug interactions (e.g. synergies) to increase efficacy or IV) to re-sensitise bacteria, which would be resistant against a monotherapy.[3] Moreover, reductions of dose levels in combination with maintained efficacy could be conceivable in order to avoid or reduce exposure driven toxicities and adverse effects.[15]

1.3 Drug interactions

When two or more drugs are administered in parallel, an immediate potential of interactions arises. This comprises intended combination therapy (e.g. in treatment of tuberculosis or hypertension) as well as polypharmacy in critically ill or geriatric patients. When speaking of rational combination therapy of antibiotics, the drug interactions are intentionally considered and utilised on purpose. This chapter introduces the main forms and concepts of how drugs can interact.

Drug interactions can be distinguished by their pharmacology and their type of interaction. Firstly, pharmacokinetic interactions can be discriminated against pharmacodynamic interactions. Pharmacokinetic interactions occur, when the absorption, metabolism, distribution or elimination of one drug is altered by the combination partner (see 1.5.1). Pharmacodynamic interactions, which are the focus of the present PhD project, display interactions, where the concentration-effect relation of a drug is altered by another in an allosteric (i.e. regarding the maximum effect) or competitive (i.e. regarding the potency) manner (see 1.5.2).[15]–[17] Secondly, drug interactions can be discriminated by the deviation of the observed combined drug effect from the expected additivity in combination. For this differentiation the underlying criterion describing additivity is crucial.[18] The two most common used additivity criteria are Bliss Independence and Loewe Additivity. Bliss Independence assumes that two drugs act independently from the presence of the other drug.[19]–[21] In opposite, Loewe additivity considers that two drugs have the same or a very similar target and in combination they act like a drug, which is added to itself.[19], [20], [22] Based on those criteria, deviations to higher effect sizes are defined as synergies and deviations to lower effect sizes are defined as antagonism.[23] It is important to note, that those deviations are concentration dependent. That means, that there will be areas in the concentration-effect relation of two drugs, where the drug interactions manifest and others were additivity prevails.

Special cases of synergy are described by coalism (i.e. two inactive drugs become active in combination) and syncretism (i.e. one inactive drug potentiates the effect of an

active one).[3] In opposite, a special case of antagonism is displayed by a suppressive drug interaction (i.e. the combined effect is weaker than one single drug effect).[19] The appearance of syncretism highlights, that, in theory, drug interactions are directional. That includes monodirectional interactions like potentiation, but also bidirectional interactions with both drugs enhancing or mitigating each other. Therefore, asymmetric interactions with one drug lowering the effect of a combination partner while being enhanced are mechanistically conceivable as well.[16]

From this variety of drug interactions, one might assume intuitively that synergies with enhanced effect sizes and faster killing are the most beneficial ones, but there is also evidence, that suppressive interactions can prevent or reverse the emergence of resistances.[13], [19] The rational utilisation of drug interactions could therefore also include the weighing of an immediate high (synergistic) effect size against a future development of resistances.[19] In this context it is also important to note, that, when drug interactions are investigated in preclinical *in vitro* or *in vivo* models, the ultimate clinical relevance of a drug interaction has to be translated.[17] This covers evaluations whether the magnitude of the interactions has a therapeutic impact and whether the relevant concentration ranges for the interactions are clinically achievable.[17], [24]

1.4 Key antibiotics in the present thesis

Considering the possible benefits of drug interactions introduced above, novel and innovative antibiotics provide a higher demand for protection against the emergence of resistances. Additionally, agents with a likely synergistic potential can be of interest, when it comes to a systematic evaluation of drug interactions.

Among the newly approved drugs in the recent years, some beta-lactam/beta-lactamase inhibitor combinations entered the markets. One of the new beta-lactamase inhibitors is avibactam, which was approved by the European Medicines Agency in 2016 in a fixed combination with ceftazidime.

When it comes to the rational design of antibiotic combinations, there are considerations, that two drugs combatting the same target on different pathways have

an increased likelihood for synergy.[19], [25] A prominent companion meeting these prerequisites for beta-lactams is fosfomycin, which is an established drug and was rediscovered as partner for combination therapy.[26] Additionally, it already indicated a synergistic potential not only together with ceftazidime/avibactam but also in combination with other beta-lactam and non-beta-lactam antibiotics.[27]–[30] The following two sections introduce the key antibiotics investigated in the present PhD project.

1.4.1 Ceftazidime/avibactam

Ceftazidime/avibactam is a fixed combination of a beta-lactam antibiotic and a beta-lactamase inhibitor and is approved for the treatment of complicated intra-abdominal infections, complicated urinary tract infections, including kidney infections, and hospital-acquired pneumonia, including ventilator-associated pneumonia.[31] The standard dose comprises the thrice daily administration of a fix combination of 2 g ceftazidime and 0.5 g avibactam by intravenous infusion over 2 h.[31] The clinical dose is reduced for children and renally impaired patients.[31] Ceftazidime/avibactam is generally well tolerated, except the risk of beta-lactam related allergic reactions and potential neurotoxicity.[20], [32]–[34]

Ceftazidime is the beta-lactam component in the fix combination and represents a third-generation cephalosporine with enhanced binding activity against penicillin-binding-protein 3 and improved stability against some beta-lactamases.[6] However, it is still unstable in the presence of extended-spectrum beta-lactamases and carbapenemases.[6] Its inhibition of penicillin-binding-proteins is a shared mode of action of all beta-lactam antibiotics and leads to an inhibition of the bacterial cell wall synthesis and ultimately to cell death.[35]

Avibactam is an innovative beta-lactamase inhibitor and in contrast to other beta-lactamase inhibitors the molecule is not characterised by a beta-lactam ring.[6] Avibactam inhibits Ambler class A (e.g. KPC, TEM, CTX-M) and Ambler class C (e.g. AmpC) beta-lactamases as well as some Ambler class D (e.g. OXA) enzymes by covalent binding

to the active sites of the beta-lactamases.[32], [36] Additionally, *in vitro* studies identified own antibacterial drug effects of avibactam at high concentrations.[37], [38] In combination ceftazidime/avibactam is highly active against different *Enterobacteriaceae* and *Pseudomonas aeruginosa* strains. Although the combination is only in use since 2016, resistances related to mutations in beta-lactamase genes, efflux pumps or altered membrane permeability were already described.[5], [39] Therefore, it is important to preserve ceftazidime/avibactam as a treatment option and its protection against the development of resistance is of high interest.[6], [40]

1.4.2 Fosfomycin

Fosfomycin was discovered in 1969 and is therefore already considered an ‘old’ antibiotic.[41] Its chemical structure is derived from phosphonic acid and the mechanism of action is based on the imitation of phosphoenolpyruvate.[7], [26] In particular, fosfomycin combats bacteria by irreversible binding to the active site of the UDP-*N*-acetylglucosamine enolpyruvyl transferase (MurA) and thereby inhibits the first step in the synthesis of UDP-*N*-acetylmuramic acid, a precursor molecule for the bacterial cell wall formation.[26] The uptake of fosfomycin into the bacterial cell is mediated by two transport mechanisms: the L-alpha-glycerophosphate transporter (GlpT) and the hexose-6-phosphate transport (UhpT) system.[7] The activity of the UhpT system is induced by physiologically available glucose-6-phosphate.[26], [42] In order to closer correlate *in vitro* results to the *in vivo* activity of fosfomycin, the transporter system is extrinsically activated by the addition of 25 mg/L glucose-6-phosphate to the bacterial growth media, when *in vitro* testing is performed.[7], [42], [43]

Because of the broad spectrum of fosfomycin against gram-negative and gram-positive pathogens and the activity against bacteria expressing Ambler class B metallo-beta-lactamases (e.g. NDM, VIM), which are not inhibited by most beta-lactamase inhibitors, the intravenous administration of fosfomycin attracted clinicians worldwide.[26], [36], [42], [44], [45] Its dosing depends of the type and severity of infection and ranges from 12 g to 24 g daily divided on 2 to 4 infusions with adjustments needed for children and

renally impaired patients.[26] Those high drug amounts are not unproblematic. Fosfomycin is a generally well-tolerated drug, but when administered as fosfomycin-sodium salt one gram drug comes with 330 mg sodium.[46] The sodium load can lead to direct hypernatremia and via a electrolyte shift to hypokalemia.[46]

When it comes to the emergence of resistance against fosfomycin, several different mechanisms are described. The main ones are mutations in the transporter structures outlined above, alterations of the target enzyme MurA and the expression of fosfomycin modifying enzymes like glutathione S-transferases (e.g. FosA).[26], [43], [47] Especially, those resistances emerge rapidly *in vitro*, but it seems to be inconsistent whether this can be translated into the clinical setting.[47], [48] Yet, to avoid resistance development during monotherapy and ensure efficacy for infections with variable pathogens, fosfomycin is mainly used in combination. Also, the European Medicines Agency recommended in 2020 to restrict the intravenous use in monotherapy to serious infections when other treatments are not available.[44], [46], [49] The updated recommendation for intravenous fosfomycin comprised among other indications the use against complicated urinary tract infections, hospital-acquired pneumonia including ventilator-associated pneumonia and complicated intra-abdominal infections.[49] Nevertheless, due to the unique mode of action and the unique chemical structure of fosfomycin the development of cross resistances is uncommon and fosfomycin is a prominent partner in efficacious antibiotic combination therapy.[7], [26]

1.5 Key pharmacological elements in the present thesis

Pharmacology summarises the studies of how tissues and organ functions of a living organism are affected by xenobiotics (e.g. pharmacological active substances) or endogenous agents.[50] The two main branches of pharmacology are pharmacokinetics and pharmacodynamics. As they are also important components of a pharmacometric model (see 1.6.1), they will be introduced in the following chapters.

1.5.1 Pharmacokinetics

Pharmacokinetics are often related to as how the drug is affected by the body.[17] They can be summarised by the analysis of the 'ADME' principle, which includes all mechanisms and paths of a drug passing through an organism.[51], [52] This acronym comprises the description of absorption, distribution, metabolism and excretion of a drug or its metabolites over time.[51]–[53] The pharmacokinetics of a drug can be influenced externally by adjustable factors like changes of the dose, route and interval of administration. Conversely, pharmacokinetics can also be subject to intended or unintended drug interactions altering for instance the distribution or metabolism of agents.[15], [17]

Within the framework of *in vitro* assays conducted in the present PhD project, experiments can be differentiated in static and dynamic pharmacokinetic conditions (see 1.7). Static *in vitro* experiments are assays with no changes in the drug concentration over the investigation period. In opposite, in more elaborate dynamic time kill experiments alterations in the drug concentration over time are realised to mimic *in vivo* 'ADME' conditions.

1.5.2 Pharmacodynamics

Besides pharmacokinetics, pharmacodynamics are the second main branch of pharmacology and can be described as the relationship of how the drug affects the body.[17] Complementary to pharmacokinetic evaluations, a pharmacodynamic analysis comprises an evaluation of the relationship of a certain drug exposure to a response variable, such as blood pressure or heart rate.[53]

In the field of antibiotics, a pharmacodynamic response of a drug can be measured by its impact on a bacterial population or by the influence on the emergence of resistances. In particular, antibiotic agents can be divided in bactericidal or bacteriostatic drugs. Bacteriostatic agents inhibit the bacterial growth, whereas bactericidal antibiotics like the key antibiotics in the present thesis, ceftazidime/avibactam and fosfomycin, introduced above (see 1.4), are able to kill a bacterial population.

1.6 Pharmacometrics

Quantitative mathematical analyses of pharmacokinetics and pharmacodynamics can contribute to an in-depth understanding of the pharmacology of drugs. Pharmacometrics displays a multidisciplinary science, that unites mathematical and statistical methods with knowledge on pharmacology and medicine.[54] A pharmacometric evaluation aims to characterise, understand and predict the pharmacokinetics (see 1.5.1) and/or pharmacodynamics (see 1.5.2) of a drug whilst informing about the uncertainty of this knowledge as well.[53], [55] The discipline has its origins in the midst of the 20th century in the description of pharmacokinetics in laboratory experiments.[56] Over the years, it evolved to the population pharmacokinetic approach and to complex models to even describe exposure-response relationships.[55], [56] Therefore, it is described as the science of quantitative pharmacology.[55]

The different mathematical and statistical approaches enable quantitative descriptions of drug concentration-time profiles, drug effects, biomarkers or surrogate endpoints and progression of diseases.[53], [55], [57] Nowadays pharmacometrics is an important tool to rationalise decision-making in drug development or optimise individual pharmacotherapy.[53], [55], [57] Due to its versatile application areas, it is no longer just applied to the evaluation of routine clinical data, but widely used from pharmaceutical industry over academia to clinics.[56], [58], [59] Additionally, pharmacometric considerations became pivotally requested by regulatory authorities to guide their decision making.[56], [58], [60]

The following chapters introduce different pharmacometric techniques and how they were applied in the present PhD project.

1.6.1 Pharmacometric modelling

Pharmacometric modelling together with simulations (see 1.6.2) summarises some of the main pharmacometric techniques and provide the tools for a combined pharmacokinetic and pharmacodynamic analysis. In frame of pharmacometrics a model

can be described as *'how you think your data were generated'* (Bonate, 2011).[61] The concepts of traditional pharmacokinetic modelling and the constructions of non-linear mixed effects (NLME) models go back to the early 1970s.[62] In the past as well as today, a typical population model combines different elements: a structural model, a variability model and a covariate model.[58] The structural model usually comes with a compartmental structure and defines the functional form of a model. The variability model introduces mainly interindividual and residual variability components, whereas the covariate model introduces patient specific relations between a structural model parameter (e.g. clearance, volume of distribution) and a patient specific characteristic (e.g. renal function, weight, age).[58] The terminology 'mixed effects' refers to fixed effects like structural model parameters and random effects like the variability components mentioned above.[63]

That concept can be used to describe pharmacokinetic drug concentration-time-profiles as well as pharmacodynamic observations (e.g. biomarker concentrations, bacterial counts). It applies, that if the developed model structure is data-driven but influenced by (micro-) biological considerations and mechanistic knowledge, they are often called semi-mechanistic models as they are always simplifications of the more complex 'real world'.[61], [64]

Pharmacodynamic models

The focus of the present PhD project with regard to modelling was the elucidation of concentration-effect-relationships as well as pharmacodynamic drug interactions. In terms of antibiotics, a mathematically calculated effect could be a killing rate of a bacterial population or an inhibition of its growth rate. There are several ways to relate a drug concentration to a certain effect size. The most common approach is a calculation of an effect as a function of a drug concentration by a sigmoidal maximum effect model.[60] This type of model describes a saturable function and informs about a maximum drug effect (E_{max}) and a drug potency, also known as EC_{50} or the concentration at which the drug effect is half-maximum.[58] For concentrations

noticeably below the EC50 the sigmoidal maximum effect model collapses to a linear or power model.[58]

Pharmacodynamic interaction models

Pharmacodynamic interaction models can support an in-depth understanding of drug interactions by mapping of combined effects as enhanced or reduced effect sizes compared to the drugs in monotherapy. The most common concepts to describe pharmacodynamic interactions of antibiotics are semi-mechanistic or subpopulation synergy models.[65], [66] The semi-mechanistic modelling approach applied in the present PhD project was based on the general pharmacodynamic interaction (GPDI) model.[16] The GPDI model describes interactions as consequences of shifts of pharmacodynamic parameters (i.e. Emax or EC50) driven by the present concentration of an interaction partner.

In opposite, a subpopulation synergy model captures drug interactions via the introduction of different subpopulations with separate susceptibilities to the combination partners.[65], [66] Both techniques can elucidate combined drug effects and inform about interaction directions as well as about interaction potencies and magnitudes.

Pharmacokinetic-pharmacodynamic models

Elaborate pharmacokinetic-pharmacodynamic (PK/PD) models enable an analysis of a drug response over time. Thereto, the pharmacokinetics are linked indirectly or directly to a pharmacodynamic effect to account for different shapes of their relationship or temporal relations (i.e. delayed or immediate effects).[17], [53], [60] Indirect pharmacodynamic links use turnover models or effect-compartments to mimic time delays in the concentration-response-relation or the development of tolerances.[60], [67] Direct links assume a fast distribution to the site of action and an immediate onset of the effect without time delays.[60] To provide an example, the prompt responses of

bacteria against antibiotics in the present PhD project were introduced as direct response pharmacodynamic models.

The combined analysis of pharmacokinetics and pharmacodynamics unfolds the full potential of a pharmacometric analysis connecting clinical doses to a likely treatment outcome.[17], [53] An example is the concept of PK/PD indices in antibiotic therapy. PK/PD indices link a drug exposure and a microbiological measure (i.e. the minimum inhibitory concentration (MIC)(see 1.7.1)) to a clinical outcome.[68] Thus, antibiotics are commonly assigned to one of three different indices, which define the pharmacokinetic driver for clinical efficacy.[69] It was identified, that the efficacy of some antibiotics can be linked to a time period of the dosing interval, where the drug concentration is above the MIC ($\%T > MIC$), whereas others depend from a certain ratio between the peak concentration and the MIC (C_{max}/MIC).[68] For antibiotics assigned to the third PK/PD index the efficacy is driven by the ratio of a certain exposure calculated as the area under the concentration-time curve (AUC) and the MIC (AUC/MIC).[68] The key antibiotics of the present thesis ceftazidime/avibactam and fosfomycin can also be assigned to one PK/PD index, respectively. Beta-lactam antibiotics as ceftazidime are commonly time-dependent antibiotics ($\%T > MIC$), while the fosfomycin efficacy was identified to be exposure driven (AUC/MIC).[44], [70]

1.6.2 Pharmacometric simulations

After establishing a pharmacometric model, it can be used for simulations. Simulations require one or more models and represent an application for evaluation or comparison of models. Additionally, they offer the platform for model predictions and give answers to 'what if' questions as for instance required in model informed precision dosing.[53], [57], [61]

Among various techniques, which require simulations, especially Stochastic Simulation and Estimation (SSE) is used in the present PhD project for comparison of different models. In an SSE study, firstly data is generated by stochastic simulations and in a second step model parameters are estimated based on the simulated dataset. Finally,

statistical analyses like calculations of accuracy and precision of parameter estimates or comparisons of different models with regard to power calculations can be performed. Hence, SSE can be used for hypothesis testing and can contribute to the evaluation and comparison of study designs.

1.6.3 Optimal experimental design

To inform complex pharmacometric models a sufficient amount of data is required, especially when drug interactions are to be characterised. Detailed *in vitro* studies can become time and resource intensive and therefore a rational planning of experiments can be requested. A mathematical strategy to improve the experimental design with regard to efficiency and the information content of the obtained data is the application of optimal experimental design techniques.[71] Assuming that a mathematical model characterised by a defined parameter set describes an experiment, an optimal design strategy will minimise the variance of the estimates of these parameters and thus increase their accuracy and precision. A measure of this variance and thereby of the amount of information about a parameter, which comes with a given set of samples, is the Fisher information matrix.[72] In essence, optimal design approaches minimise different features of the Fisher information matrix with regard to design variables of an experiment. Design variables of interest can be optimal sampling time points in a pharmacokinetic analysis or optimal drug concentrations tested when evaluating antibiotic effects or pharmacodynamic drug interactions. The most important and best-known optimal design criterion reduces the general variance by minimising the determinant of the inverse Fisher information matrix and is named D-optimality.[73], [74] The D-optimality criterion is estimation oriented.[75] Therefore, it is suited for the design of screening experiments and was also applied in the present PhD project to optimise experimental checkerboard designs.[75]

1.7 *In vitro* infection models

The preclinical research in the present PhD project focuses on data obtained in various *in vitro* infection models. The applied *in vitro* assays are not only research but also diagnostic tools to facilitate clinical decision making for antibiotic therapies and are introduced in the following chapters.

1.7.1 Susceptibility testing methods

Susceptibility testing of bacteria represents a routine measure in clinical microbiology.[76] The main metric for antimicrobial susceptibility is the MIC. Surveillance networks like the European Committee on Antimicrobial Susceptibility Testing (EUCAST) collect global MIC data to link a bacterial susceptibility to a probable treatment outcome and thereby provide guidance for clinical decision making (i.e. MIC breakpoints).

There are several different methods for susceptibility testing. Two common ones are the Epsilon meter test (Etest) and the broth microdilution assay. Both methods have in common, that the readout of the experiment is not a surrogate for bacterial susceptibility, but a direct MIC.

For the Etest, numeric labelled plastic strips carrying a predefined antibiotic gradient are placed on inoculated agar plates. The antibiotic agents diffuse into the agar and lead to an elliptical zone of inhibition around the strip after a pre-defined incubation period. The intersect of this zone of inhibition and the plastic strip is directly read as MIC.[77] The Etest strips can also be used for the evaluation of pharmacodynamic drug interactions. For this purpose, the combined zones of inhibition of two strips placed perpendicular to each other, intersecting at the MIC of each drug, are evaluated.[78]

For broth microdilution, bacteria are incubated with standard two-fold drug concentration tiers usually centred around 1 mg/L. After a pre-defined incubation time, the lowest concentration not allowing bacterial growth evaluated by visual inspection of turbidity of the liquid growth medium is defined to be the MIC.[79] This can be sufficient to assist clinical decisions, but with a lower limit of quantification of

approximately $> 10^7$ cfu/mL the visual evaluation lacks sensitivity for research purposes and cannot discriminate between bacteriostatic or bactericidal effects.[20], [60], [80] Therefore, the quantification of the bacteria in a similar experiment combined with modelling of the drug effect (e.g. with a sigmoidal maximum effect model (see 1.6.1)) provides more sophisticated information about the antibiotic pharmacodynamics (e.g. maximum effect and EC50 values) and can guide the rational planning of series of experiments.[20], [58]

However, to reduce external influences on the MIC measures and increase the interlaboratory comparability of susceptibility testing, EUCAST among other organisations sets standards for susceptibility testing and assigned broth microdilution to be the reference method.[20]

1.7.2 Checkerboard assay

The checkerboard assay is a popular and simple method to assess pharmacodynamic drug interactions of antimicrobials.[81] The assay is performed similar to a broth microdilution MIC determination but in two-dimensions, evaluating combined drug effects by calculations of a fractional inhibitory concentration (FIC) index.[82] Alike in the broth microdilution MIC determination, the turbidity-based evaluation of arbitrary two-fold concentrations tiers lacks sensitivity, limits the outcome to the qualitative and does not allow mechanistic insights into pharmacodynamic drug interactions.[20] Therefore, the 'dynamic' checkerboard provides remedy in contrast to the illustrated 'conventional' approach, because it adds the quantification of bacteria as endpoint measure to overcome the turbidity threshold.[80] This quantitative data is more sensitive and enables an exposure-response-surface analysis, which is more robust and less biased than a classical index calculation.[83] Nevertheless, the quantification of bacteria leaves the assay noticeably more elaborate and hinders efficient streamlined interaction testing. Considering that most pharmacodynamic drug interactions can be observed in concentration ranges where the exposure-effect relationship is changing most (i.e. around the EC50), the experimental designs can be rationalised from standard

concentrations with two-fold increments to adaptive experimental designs based on drug potencies. As a consequence, the interaction testing will be more efficient and informative.[84]

1.7.3 Static time kill experiment

'Time kill experiment' is the term of a series of *in vitro* assays observing the growth and kill kinetics of bacteria exposed to antibiotic agents alone or in combination.[60] In a static time kill experiment, which is usually conducted over 24 to 30 h, the concentrations of the drugs do not change over the time course of the experiment. In opposite to the endpoint-based susceptibility and checkerboard assays introduced above, a series of samples can be drawn to quantify the bacterial load throughout the incubation time. Therefore, the observed drug effect is not only a function of drug exposure but also of time.[20] This inclusion of an additional layer provides mechanistic insights and when coupled with PK/PD modelling techniques, semi-mechanistic and quantitative features of the bacterial population dynamics as well as drug effects and emergence of resistances can be elucidated.[60] Due to these benefits, static time kill experiments are the most commonly applied technique to assess pharmacodynamic drug interactions, although there is no real assigned 'gold standard'.[78]

1.7.4 Dynamic Hollow Fiber experiment

The Hollow Fiber experiment can also be referred to as a two-compartment dynamic time kill experiment.[20] 'Dynamic' refers to the change of the drug concentration over time, which is implemented by a system of pumps, that continuously supplies a central compartment with fresh bacterial growth medium from a drug-free reservoir and removes the same volume to a waste container. Thereby administered antibiotic doses to the central compartment are diluted over time. This setup allows to mimic any conceivable pharmacokinetic profile like different dosing schemes of mono- and combination therapy or different modes of administration as well as variable infusion lengths (Figure 1).[85] The

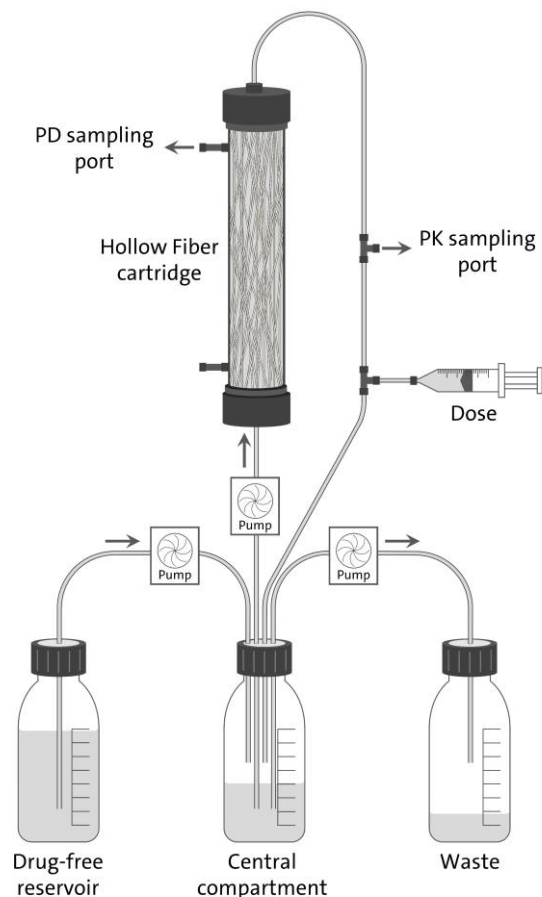


Figure 1: Sketch of the two-compartment Hollow Fiber system. PK: pharmacokinetics; PD: pharmacodynamics

second compartment is represented by a bioreactor containing thousands of semi-permeable hollow fibres with 200 μm of diameter which physically separate the central compartment from an extra-capillary space.[85] The bacteria are cultured in that extra-capillary volume, retained in the cartridge and supplied with oxygen, nutrients and drugs by a circulation from the central compartment. In comparison to other established dynamic one-compartment time kill experiments, in this set-up the bacteria are contained and are not removed during the experiment.[20] This increases the safety of the system, decreases contaminations and enables a more accurate evaluation of mechanisms of resistance.[85] Therefore, among the various *in vitro* assays, the dynamic Hollow Fiber experiment is the most elaborate one to simulate and predict potential clinical outcome of antibiotic therapy.[60]

2 Objectives

Rational combination therapy of already approved antibiotic agents was introduced as an option to increase efficacy or to suppress the emergence of resistance (see 1.2). Especially, novel drugs are the most important agents to be protected from development of resistances to preserve them for future use. One of the newer beta-lactam/beta-lactamase inhibitor combinations is ceftazidime/avibactam. It displays a more recent innovative treatment option against carbapenem resistant bacteria.[6] Nevertheless, resistances have been already described and a call for protection against resistance development to prolong its shelf-life emerged.[5] An elderly potential combination partner to increase efficacy and protect against the emergence of resistances is fosfomycin, which was rediscovered by clinicians and for which synergistic interactions with other cell wall mediating antibiotics have been reported.[26], [29] Yet, a systematic evaluation of the combination in clinically relevant *E. coli* is lacking.

The aim of the German-French consortium project called 'CO-PROTECT', in which frame the present PhD project was conducted, was to rationally explore drug interactions and derive combination therapies of beta-lactam/beta-lactamase inhibitor combinations with several last-resort antibiotics. This thesis addressed a subset of the studied drug combinations from 'CO-PROTECT' in detail. Hence, the objective of the present thesis was to systematically elucidate *in vitro* pharmacodynamic drug interactions of ceftazidime/avibactam and other newer beta-lactam/beta-lactamase-inhibitor combinations with fosfomycin in different *E. coli* and *K. pneumoniae* strains. The analysis was designed to follow a bottom-up approach starting with an efficient broad interaction screening (S), followed by a confirmation (C) of the identified pharmacodynamic interactions in selected strains and an application (A) study in dynamic pharmacokinetic conditions providing a clinical translation of the previous findings (Figure 2).

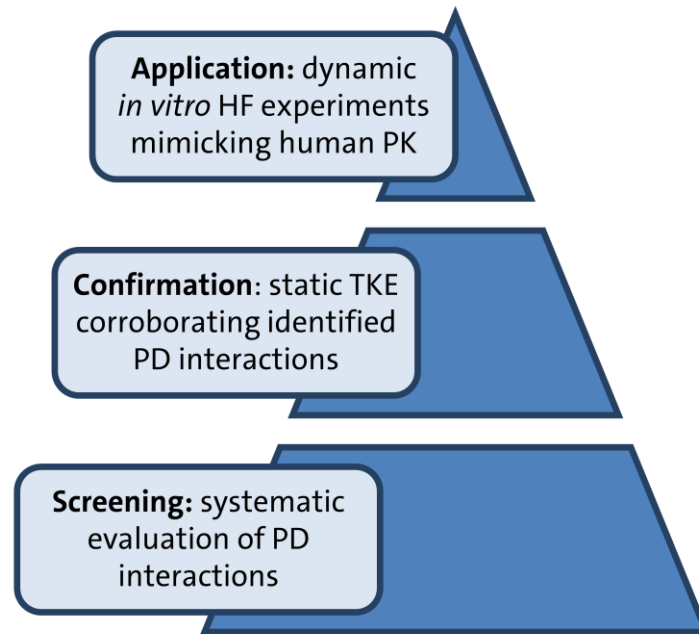


Figure 2: Overview of the consecutive project levels of the present PhD thesis. HF: Hollow Fiber; TKE: time kill experiment; PK: pharmacokinetics; PD: pharmacodynamics

The experimental data should be obtained in different *in vitro* assays and quantitatively and qualitatively evaluated by means of different pharmacometric modelling and simulation techniques. The three publications aimed to gain an in-depth understanding of the interactions and evolve a perspective of the clinical benefit of the combination of ceftazidime/avibactam with fosfomycin with regard to increased efficacy, suppression of the emergence of resistances and to allow for dose reductions to avoid toxicity.

In detail, the Publications I, II and III aimed for:

Publication I: Optimized Rhombic Experimental Dynamic Checkerboard Designs to Elucidate Pharmacodynamic Drug Interactions of Antibiotics

- Rational development of an experimental dynamic checkerboard design with considerably reduced workload compared to reference experimental designs (S)
- Application of D-optimal design theorem to *in silico* identify highly informative effective concentration tiers to support efficient *in vitro* pharmacodynamic interaction screening (S)

- Evaluation of the accuracy and precision of interaction parameter estimations and classification rates of the proposed designs compared to reference designs in SSE studies (S)

Publication II: Evaluation of *in vitro* pharmacodynamic drug interactions of ceftazidime/avibactam and fosfomycin in *Escherichia coli*

- Systematic screening of pharmacodynamic interactions of ceftazidime/avibactam and fosfomycin in different isogenic and clinical *E. coli* isolates utilising the experimental design derived in Publication I (S)
- Application of static exposure-response-surface modelling to elucidate mechanisms and magnitude of the observed pharmacodynamic interactions (S)
- Performance of detailed static time kill experiments coupled with semi-mechanistic modelling in selected strains to confirm the identified interactions (C)

Publication III: Pharmacokinetic/pharmacodynamic analysis of ceftazidime/avibactam and fosfomycin combinations in an *in vitro* hollow fiber infection model against multidrug-resistant *Escherichia coli*

- Translation of the observed pharmacodynamic drug interactions from static into dynamic time kill experiments (C, A)
- *In vitro* Hollow Fiber experiments mimicking human pharmacokinetics of mono- and combination-therapies (A)
- Bioanalytical confirmation of antibiotic pharmacokinetics in bacterial growth medium during the *in vitro* Hollow Fiber experiments (A)
- Combination of semi-mechanistic and subpopulation modelling techniques to describe and quantify the pharmacodynamic drug interactions with their impact on antibiotic efficacy and resistance development (A)
- Simulations to evaluate the clinical potential of the observed drug interactions with regard to allow for dose reductions in combination (A)

3 Cumulative part

The following cumulative part introduces and presents three peer-reviewed original publications. The articles represent the key results of this thesis.

The articles were published in *Pharmaceutical Research*, *Journal of Antimicrobial Chemotherapy* and *Microbiology Spectrum*. [86]–[88]

3.1 Publication I

Optimized Rhombic Experimental Dynamic Checkerboard Designs to Elucidate Pharmacodynamic Drug Interactions of Antibiotics

Niklas Kroemer, Romain Aubry, William Couet, Nicolas Grégoire,
Sebastian G. Wicha

Pharmaceutical Research (2022)

Impact Factor: 4.580 (2021)

Synopsis

Mechanistic understanding of pharmacodynamic drug interactions is essential to develop rational combination therapies. Popular approaches for interaction testing are different variants of the checkerboard assay (see 1.7.2).[81] In brief, ‘dynamic’ checkerboard experiments including a quantification of viable bacteria enable a more sophisticated analysis of pharmacodynamic drug interactions than traditional checkerboards based on visual turbidity of bacterial growth medium, but are considerably more laborious.[80] To combine the benefits of the ‘dynamic’ checkerboard approach with the requirements of a high-throughput screening of pharmacodynamic drug interactions the *in silico* study in Publication I aimed to use the D-optimal design theorem to develop optimal experimental designs and evaluate them against commonly applied reference designs.

Like in considerations of Chen *et al.*, the design development focused on concentration tiers based on drug potencies (e.g. EC50) instead of standard two- or eight-fold concentrations.[84] Firstly, rhombic designs comprising solely four highly informative combinations were developed. Potential reference designs covering nine (i.e. a design by Chen *et al.* or a ‘conventional’ sparse design) or 81 combinations (i.e. a ‘conventional’ rich design) would be substantially more cumbersome in high-throughput *in vitro* experiments.

Secondly, the accuracy and precision of the interaction parameter estimation and the classification rates of the newly proposed designs were evaluated in SSE studies and compared to the reference designs. There the proposed designs showed to be highly efficient. Apparently, the reduction of tested combinations was linked to a loss of information but the potency-based designs were superior to standard concentrations. Hence, the rhombic designs showed to be applicable to streamline testing in a high-throughput interaction screening.



ORIGINAL RESEARCH ARTICLE

Optimized Rhombic Experimental Dynamic Checkerboard Designs to Elucidate Pharmacodynamic Drug Interactions of Antibiotics

Niklas Kroemer¹ · Romain Aubry^{2,3} · William Couet^{2,3,4} · Nicolas Grégoire^{2,3,4} · Sebastian G. Wicha¹ Received: 10 June 2022 / Accepted: 9 September 2022
© The Author(s) 2022

Abstract

Purpose Quantification of pharmacodynamic interactions is key in combination therapies, yet conventional checkerboard experiments with up to 10 by 10 combinations are labor-intensive. Therefore, this study provides optimized experimental rhombic checkerboard designs to enable an efficient interaction screening with significantly reduced experimental workload.

Methods Based on the general pharmacodynamic interaction (GPDI) model implemented in Bliss Independence, a novel rhombic ‘dynamic’ checkerboard design with quantification of bacteria instead of turbidity as endpoint was developed. In stochastic simulations and estimations (SSE), the precision and accuracy of interaction parameter estimations and classification rates of conventional reference designs and the newly proposed rhombic designs based on effective concentrations (EC) were compared.

Results Although a conventional rich design with 20-times as many combination scenarios provided estimates of interaction parameters with higher accuracy, precision and classification rates, the optimized rhombic designs with one natural growth scenario, three monotherapy scenarios per combination partner and only four combination scenarios were still superior to conventional reduced designs with twice as many combination scenarios. Additionally, the rhombic designs were able to identify whether an interaction occurred as a shift on maximum effect or EC50 with > 98%. Overall, effective concentration-based designs were found to be superior to traditional standard concentrations, but were more challenged by strong interaction sizes exceeding their adaptive concentration ranges.

Conclusion The rhombic designs proposed in this study enable a reduction of resources and labor and can be a tool to streamline higher throughput in drug interaction screening.

Keywords checkerboard design · drug interaction testing · optimized experimental design · stochastic simulation and estimation · synergy

Introduction

Resistant bacteria with decreased susceptibility towards antibiotics represent a major threat to human health. One strategy to treat less susceptible strains is to use combination

therapies in order to attain a synergistic killing effect or to prevent resistance development and thereby protect the drugs for future use [1].

Methods are required to investigate pharmacodynamic interactions in a simple and efficient manner. Besides Etest, multiple-combination bacterial test (MCBT) and time-kill assays, checkerboard assays are a common method to investigate pharmacodynamic drug interactions [2]. Checkerboard experiments are based on the microdilution technique and utilize turbidity as a surrogate of bacterial growth in the broth for calculation of indices which are then translated into synergistic, antagonistic or indifferent combinational effects [3]. Conventional experimental checkerboard designs covering multiple concentrations chosen as twofold dilutions with up to 10 by 10 concentration levels can be disadvantageous due to a high number of reagents and resources needed [2].

✉ Sebastian G. Wicha
sebastian.wicha@uni-hamburg.de

¹ Department of Clinical Pharmacy, Institute of Pharmacy, University of Hamburg, Hamburg, Germany

² Inserm U1070, Poitiers, France

³ Université de Poitiers, UFR de Médecine Pharmacie, Poitiers, France

⁴ CHU de Poitiers, Laboratoire de Toxicologie-Pharmacologie, Poitiers, France

In addition, the criterion of evaluating the turbidity of the broth as endpoint criterion lacks sensitivity, is subjective and does not display a continuous effect read out and only informs about bacteriostatic effects and interactions beyond the turbidity threshold. To overcome this limitation, the quantification of colony forming units (CFU) as determined in 'dynamic' checkerboard experiments, can provide more detailed and specific insights into pharmacodynamics of single drugs and their interactions [4]. Together with modelling and simulation techniques the bacterial count can be a strong tool for interaction screening and for quantification of interaction parameters [4].

In order to reduce the workload, a rational reduced design based on effective concentrations (EC) was proposed by Chen *et al.* [5]. Their EC-4×4 checkerboard design, including one scenario of natural growth, six scenarios of mono-treatment and nine combination scenarios provided higher accuracy and precision than a conventional reduced design with same number of scenarios, but unoptimized concentrations [5]. Associated with checkerboard designs, a scenario was defined as an experimental combination of two drugs with distinct concentrations whereas the growth scenario contains no drug and in the mono testing scenarios solely one drug was present.

The objective of the present study was to further optimize and reduce the design of Chen *et al.* [5]. The optimization of those designs was inspired by a D-optimal design approach. D-optimality is beside other optimality criteria one of the most important ones and a design is considered optimal when it is minimizing the determinant of the inverse Fisher Information matrix [6, 7]. Such reduced designs should still be able to classify drug interactions accurately, but should be highly efficient to comply with the requirements of high-throughput analyses. The general pharmacodynamic interaction (GPDI) model implemented in Bliss Independence was used for interaction modelling in the course of the experimental design development and design evaluation [8, 9]. The applied GPDI model enables elucidation of synergistic (syn), antagonistic (ant) or asymmetric (asym) drug interactions and describes the direction of an interaction via identification of perpetrator and victim drugs [8]. Furthermore, it can distinguish between allosteric and competitive interacting drugs, i.e. interactions on the level of the maximum effect (Emax) or potency (EC50) [8].

Materials and Methods

Conceptual Workflow of Design Development and Evaluation

The workflow of the development and evaluation of the experimental designs is illustrated on Fig. 1.

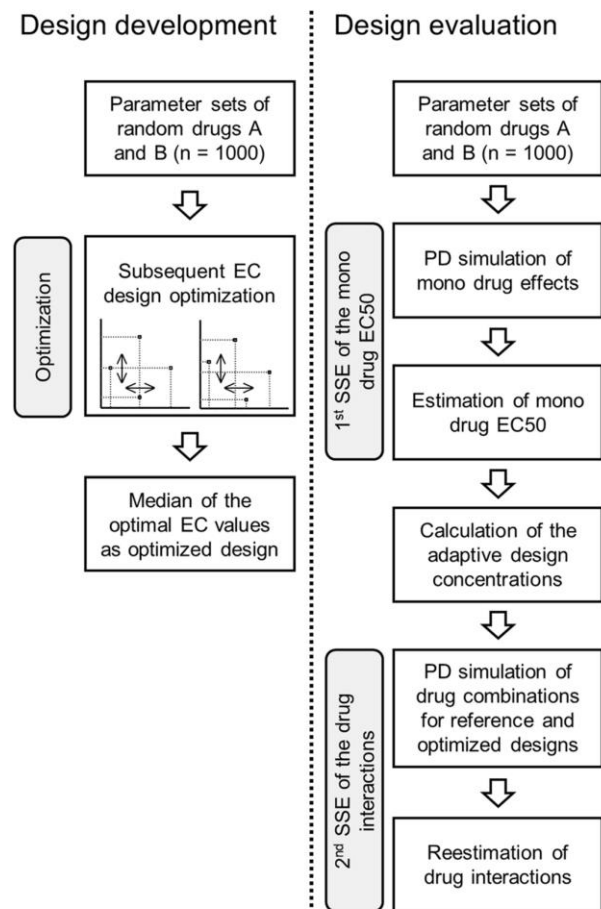


Fig. 1 Flowchart illustrating the workflow of the experimental design development and evaluation. EC: effective concentration, SSE stochastic simulation and estimation, PD: pharmacodynamic.

The optimized experimental designs were planned as adaptive designs based on EC with solely four combination scenarios. For the design development 1000 parameter sets of random drugs A and B were generated and for each drug combination an optimal set of adaptive EC-values forming an experimental design layout for estimation of the drug interactions was determined inspired by D-optimality. The median of the 1000 individual optimal designs was considered to be the optimized design layout.

In a second step, the developed designs were evaluated in stochastic simulations and estimations (SSE) and compared with reference designs with respect to their predictive performance. Therefore, an experimental screening was simulated. 1000 parameter sets of random drugs A and B were generated and in a first simulation the mono drug effects were simulated in an ordinary differential equation system. The drug EC50 were re-estimated and used to calculate the concentrations for the EC-based adaptive experimental designs. The ordinary differential equation system was then used again to simulate dynamic checkerboard experiments

utilizing the reference and optimized designs. From these simulations the pharmacodynamic drug interactions were re-estimated. Finally, the misclassification of interactions, the precision and the accuracy of the interaction estimation of the different designs were compared.

General Pharmacodynamic Interaction (GPDI) Model

The GPDI model was used for design development, simulation and estimation of drug interactions. In the GPDI model, interactions caused by a perpetrator drug at the concentration C are described as shifts of pharmacodynamic parameters (θ) of the victim drug, where θ represents the EC50 or Emax and the shifts are applied via the insertion of a GPDI term (Eq. (1)) [8]:

$$\theta \cdot \left(1 + \frac{\text{INT} \cdot C^{\text{H}_{\text{INT}}}}{\text{EC50}_{\text{INT}}^{\text{H}_{\text{INT}}} + C^{\text{H}_{\text{INT}}}} \right) \quad (1)$$

The INT parameter describes the fractional change of the pharmacodynamic parameter, EC50_{INT} parameterizes the interaction potency and H_{INT} the sigmoidicity of the interaction. These parameters are directional as indicated by subscript letters in Eqs. (3)-(6) (e.g. $_{AB}$ indicates A as victim and B as perpetrator drug) and enable the description of the direction of the interaction [8]. When the GPDI term is applied on both combination partners, interactions become bidirectional and both drugs can be perpetrator and victim at the same time.

In this study, an implementation of the GPDI model in Bliss Independence [9] was used for design optimization and evaluation. The GPDI model for Bliss Independence is derived as follows: A competitive interaction type for two drugs A and B can be described as shift on EC50 (Eqs. (2)-(3)) with

$$E_A = \frac{\text{Emax}_A \cdot C_A^{\text{H}_A}}{\left(\text{EC50}_A \cdot \left(1 + \frac{\text{INT}_{AB} \cdot C_B^{\text{H}_{\text{INT},AB}}}{\text{EC50}_{\text{INT},AB}^{\text{H}_{\text{INT},AB}} + C_B^{\text{H}_{\text{INT},AB}}} \right) \right)^{\text{H}_A} + C_A^{\text{H}_A}} \quad (2)$$

and

$$E_B = \frac{\text{Emax}_B \cdot C_B^{\text{H}_B}}{\left(\text{EC50}_B \cdot \left(1 + \frac{\text{INT}_{BA} \cdot C_A^{\text{H}_{\text{INT},BA}}}{\text{EC50}_{\text{INT},BA}^{\text{H}_{\text{INT},BA}} + C_A^{\text{H}_{\text{INT},BA}}} \right) \right)^{\text{H}_B} + C_B^{\text{H}_B}} \quad (3)$$

An allosteric interaction type can be described as shift on Emax (Eqs. (4)-(5)) with

$$E_A = \frac{\text{Emax}_A \cdot \left(1 + \frac{\text{INT}_{AB} \cdot C_B^{\text{H}_{\text{INT},AB}}}{\text{EC50}_{\text{INT},AB}^{\text{H}_{\text{INT},AB}} + C_B^{\text{H}_{\text{INT},AB}}} \right) \cdot C_A^{\text{H}_A}}{\text{EC50}_A^{\text{H}_A} + C_A^{\text{H}_A}} \quad (4)$$

and

$$E_B = \frac{\text{Emax}_B \cdot \left(1 + \frac{\text{INT}_{BA} \cdot C_A^{\text{H}_{\text{INT},BA}}}{\text{EC50}_{\text{INT},BA}^{\text{H}_{\text{INT},BA}} + C_A^{\text{H}_{\text{INT},BA}}} \right) \cdot C_B^{\text{H}_B}}{\text{EC50}_B^{\text{H}_B} + C_B^{\text{H}_B}} \quad (5)$$

in which E_A and E_B describe the effect of the single drugs A and B, Emax_A and Emax_B display the maximum possible mono drug effects for drugs A and B, C_A and C_B each drug concentration and H_A and H_B are pharmacodynamic sigmoidicity parameters.

The polarity of each INT parameter defines the interaction type. If $\text{INT} = 0$, the GPDI term becomes 1 and no interaction is present. For drug interactions on EC50, $-1 < \text{INT} < 0$ describes a synergistic interaction as the EC50 is decreased and $\text{INT} > 0$ an antagonistic interaction as the EC50 is elevated. If both INT parameters have the same polarity the occurring interaction is bidirectionally synergistic or antagonistic and in opposite, the interaction becomes asymmetric when the polarity of both INT parameters is reversed. The polarity of INT is opposite, when the interaction is implemented on Emax (i.e. $\text{INT} > 0$ describes a synergistic interaction as Emax increases). For simplification, as in the study by Chen *et al.* [5], in the optimization and SSE study the interaction potency was fixed to the drug potency ($\text{EC50}_{\text{INT}} = \text{EC50}$) and the interaction sigmoidicity (H_{INT}) was set to 1.

The combinational drug effects were calculated using Bliss Independence with single drug effects normalized to 1 for calculation of the probabilistic Bliss Independence term and then scaled back to the effect scale (Eqs. (6)-(7)):

$$E_{\text{max}} = \max(E_{\text{max},A}, E_{\text{max},B}) \quad (6)$$

$$E_{\text{comb}} = \left(\frac{E_A}{E_{\text{max}}} + \frac{E_B}{E_{\text{max}}} - \frac{E_A}{E_{\text{max}}} \cdot \frac{E_B}{E_{\text{max}}} \right) \cdot E_{\text{max}} \quad (7)$$

using the terms for E_A and E_B containing the GPDI terms as defined above (Eq. (2)-(5)).

Reference Checkerboard Designs and Novel Design Candidates

Starting point for the development of new checkerboard designs were layouts proposed by Chen *et al.* [5]. In their study, two conventional designs build on standard drug concentrations were compared to a novel, optimized design based on drug potency values. The following three designs were used as reference designs in this study:

- i) The conventional rich design consisted of ten-by-ten drug concentrations (i.e. 100 testing scenarios) including one experiment without treatment (natural growth),

nine mono testing scenarios for each drug and 81 drug combination scenarios. The drug concentrations tiers were set as two-fold increments ranging from 0.25 to 64 $\mu\text{g}/\text{mL}$ (Fig. 2a).

- ii) The conventional sparse design was reduced to four-by-four drug concentrations (i.e. 16 testing scenarios) including one scenario without treatment, three mono testing scenarios for each drug and 9 combination scenarios. The drug concentration tiers in this sparse design were set as eight-fold increments ranging from 1 to 64 $\mu\text{g}/\text{mL}$ (Fig. 2b).
- iii) The optimized EC-4 \times 4-design by Chen *et al.* [5] also covered 16 testing scenarios, but instead of standard eight-fold concentrations the concentrations depended on drug potency values (EC20, EC50, EC80) (Fig. 2c).

The following two optimized rhombic designs which were newly proposed in this study also relied on drug potency values and covered two-by-two combination scenarios, but with no horizontal rectangular shape (Fig. 3):

- i) In the free rhombic design, all combination scenarios were independent from each other and the design, i.e. the length and angles of the shape of the experimental layout were solely driven by the optimization studies.
- ii) The fixed rhombic design was a simplification of the free rhombic design. In this design a middle EC of one drug is used in two combination scenarios while an upper and lower concentration are tested solely in one combination scenario. This simplification was designed to have a more practical *in vitro* application as illustrated on Fig. 3.

The newly developed rhombic checkerboard designs also included one scenario without treatment (natural growth) and mono testing scenarios with two-fold concentrations ranging

from 0.5 \cdot EC50 to 2 \cdot EC50. The mono testing concentrations scenarios were no component of the optimization studies.

All checkerboard concentrations (C) based on drug potency values (ECXX) were calculated based on a sigmoidal Emax model, with ECXX describing the decimal of the maximal effect (e.g. 0.2 for EC20) (Eq. (8)):

$$C = \sqrt[H]{\frac{ECXX \cdot E_{\max} \cdot EC50^H}{E_{\max} - ECXX \cdot E_{\max}}} \quad (8)$$

Development of the Optimized Rhombic Designs

The rhombic checkerboard designs were developed using the R software (version 3.6.2)[10]. Minimizations were performed using 'optim' from the R package stats (version 3.6.3)[10].

For design development, 1000 parameter sets of two random drugs A and B were simulated to mimic typical antibacterial drugs (Fig. 1). Additionally, to simulate different types of drug interactions for each of those drug pairs three sets of interaction parameters describing a synergistic, antagonistic and asymmetric interaction were sampled and applied as interactions on EC50 and Emax. The drugs Emax values (log10 CFU/mL) were sampled between 5 and 10, the EC50 values ($\mu\text{g}/\text{mL}$) between 2 and 3 and H between 1 and 3. The INT parameters were sampled between -0.9 and 4.

For the design development, the inverse determinant of expected Fisher information matrix (FIM) was calculated and used as objective function value (OFV) (Eqs. (9)-(10)):

$$FIM = \frac{1}{\sigma^2} (J^T \cdot J) \quad (9)$$

$$OFV = \frac{1}{\det(FIM)} \quad (10)$$

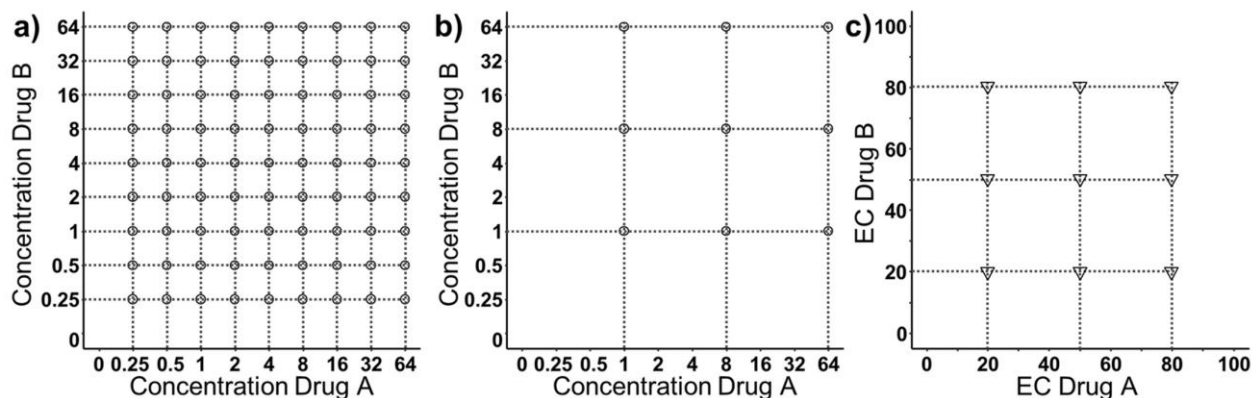
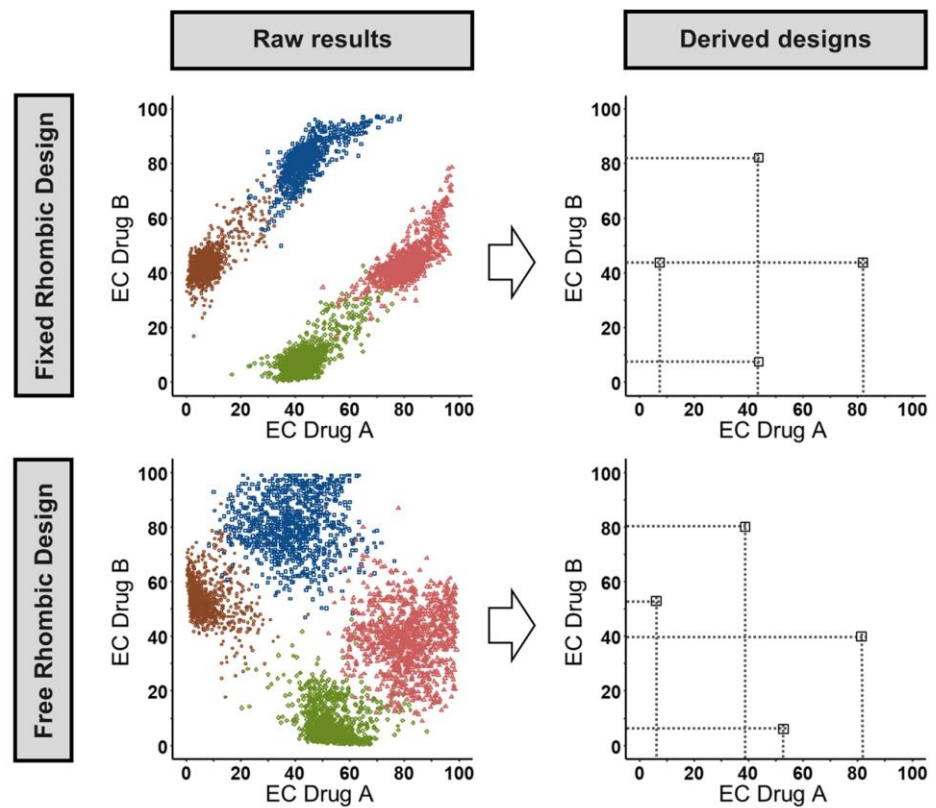


Fig. 2 Overview of the literature-based reference designs: Design (a) is the conventional rich design, design (b) is the conventional sparse design, design (c) is the EC-4 \times 4-design earlier proposed by Chen *et al.* [5], based on effective concentrations EC20, EC50 and EC80. For simplification, only the combination scenarios are shown.

Fig. 3 Development of the optimized rhombic designs. The median of the raw results of the optimization of 1000 simulated drug concentrations (left) was considered to be the optimal fixed or free rhombic checkerboard design (right). For simplification, only the combination scenarios are shown, as the monotherapy scenarios were not included in the optimization.



with J being the Jacobian (matrix of first-order derivatives of the offered combination scenarios with respect to the model parameters) and σ^2 the additive residual variance (fixed to a constant as it does not influence the minimization). For each parameter set the drug concentrations for the adaptive designs and their static effect sizes based on the GPDI model outlined above were calculated.

The OFV was calculated separately for each parameter set of the two drugs A and B. For each parameter set interactions on EC50 or Emax including the three differently sampled interaction types (synergism, antagonism, asymmetric) were considered in the OFV as weighed sum [11] to simultaneously optimize a design for different conceivable drug interactions. All modes of interactions and interaction types were weighted same, given that each scenario shares the exact same number of parameters and data points.

Minimization of the OFV was then performed with EC-values forming the combination scenarios as design variables using Nelder-Mead [12] algorithm pre-minimizing and L-BFGS-B [13] algorithm for a final minimization.

Finally, the medians of the ECs of all 1000 simulated parameter sets were considered to be the optimal design (Fig. 1). Optimization runs converging in local minima with implausible results (e.g. estimates with boundary problems) after application of 1000 retries with different sets of initials were excluded from data analysis.

Design Evaluation in Stochastic Simulation and Estimation

The optimized designs were subsequently evaluated in stochastic simulation and estimation (SSE) studies. The SSE were performed with the R software (version 3.6.3)[10]. Differential equations were solved using the 'deSolve' package (version 1.28)[14]. To improve performance, differential equations were encoded in C, compiled as shared objects (.so) and linked to the 'deSolve' interface. Estimation of parameters was performed using 'optim' from the R package stats (version 3.6.3) [10].

For the SSE, a realistic time-kill experiment mimicking scenario was chosen: 1000 hypothetical drug combinations were randomly sampled and the effect on colony forming units (CFU) in an ordinary differential equation system (Eq. (11)) with simultaneous growth with a first order growth rate k_G and killing effect rate E was simulated.

$$\frac{dCFU}{dt} = k_G \cdot CFU - E \cdot CFU \quad (11)$$

As initial condition a typical inoculum of $5 \cdot 10^5$ CFU/mL was assumed and the growth rate (k_G) was set to 2.08 h^{-1} , which corresponds to a bacterial doubling time of 20 min,

typical for *E. coli* [15]. The addition of drug was simulated at $t=0$ h and CFU were read after 4 and 24 h.

In all simulations, the EC50 of both interacting drugs was sampled between 0.1 and 60 $\mu\text{g}/\text{mL}$, the sigmoidicity parameters H_A and H_B were sampled between 1 and 3 and the Emax of both drugs were sampled conservatively between 1 and 1.5 h^{-1} to prevent the termination of runs due to excessive killing, which can lead to very small CFU counts challenging the tolerance of differential equation solver ($< 1e-7$ CFU/mL). To mimic common drug interactions, the interaction parameters INT were sampled from -0.9 to -0.5 and 0.5 to 4, corresponding to the additivity margins evaluated for the GPDI model [8]. In a second approach strong mono-directional antagonistic interactions were simulated to imitate a drug combination in which one drug fully suppresses the effect of the companion drug (Supplement Text 1). Additionally, the type of interaction (EC50 or Emax) was randomly sampled.

In a first SSE (Fig. 1), a determination of the mono drug pharmacodynamics before simulating the checkerboard experiments was simulated to challenge the robustness of the adaptive EC-based designs being dependent on the estimated EC50. This was done as the 'true' EC50 is usually unknown and the EC50 is also determined with uncertainty, which might impact the calculation of the concentrations in the design. This EC50 determination was based on the ODE system as outlined above and included a growth scenario and three concentration scenarios based on standard two-fold concentration scenarios around the EC50. The EC50s were estimated using a sigmoidal Emax-model (Eq. (11)). The model described the effect (E) as a function of the drug concentration (C) with the maximum effect (Emax), drug potency (EC50) and sigmoidicity of the drug effect (H) as parameters:

$$E = \frac{E_{\text{max}} \cdot C^H}{EC50^H + C^H} \quad (12)$$

The estimated EC50s were then used to calculate the final concentrations for the adaptive drug potency based experimental designs used for the interaction estimation. Therefore, the EC-4 \times 4 and rhombic checkerboard design concentrations were calculated individually for all simulated drug combinations whereas the conventional reference designs always covered the same standard concentrations as outlined above.

In a second SSE (Fig. 1) the designs were then compared with respect to the abilities to identify drug interactions. The ODE system outlined above was used to simulate dynamic checkerboards with combined effects based on the GPDI model. For interaction estimation the mono drug

pharmacodynamic parameters were provided and the interaction parameters were first assessed in a pre-evaluation using the Nelder-Mead algorithm with different polarities of the INT parameters as initial values. The OFV, that was minimized, was calculated using the extended least squares criterion [16].

The Akaike information criterion (AIC) for a potential Emax or EC50 interaction was calculated and the difference between the best fitting EC50 model and the best fitting Emax model was computed and used as decision criteria to identify the correct interaction [17]. To evaluate the ability of the different experimental designs to discriminate between EC50 and Emax interactions the minimum AIC difference for 95% of the estimations was calculated. A higher AIC difference was interpreted as a surrogate for a more distinct discrimination of the experimental design between allosteric and competitive interacting drugs.

After estimation of INT parameters, the Hessian was calculated within the 'optim' function. The standard errors of the estimates (SE's) were calculated as square root of the diagonal values on the inverse Hessian matrix evaluated at the OFV minimum. 95% confidence intervals (CI) of the INT parameter estimates were calculated as INT-parameter $\pm 1.96 \cdot \text{SE}$. Relative bias (rBias) (Eq. (13)) and relative imprecision (rRMSE) (Eq. (14)) were calculated as follows:

$$\text{rBias} = 100\% \cdot \frac{1}{N} \cdot \sum_i \frac{\text{estimation}_i - \text{true}_i}{\text{true}_i} \quad (13)$$

$$\text{rRMSE} = 100\% \cdot \sqrt{\frac{1}{N} \cdot \sum_i \frac{(\text{estimation}_i - \text{true}_i)^2}{\text{true}_i^2}} \quad (14)$$

with estimation_i referring to the i^{th} estimated INT parameters and true_i being the i^{th} true parameters used for simulations. N represents the number of true parameter-sets.

To evaluate the value of the experimental designs in a qualitative interaction screening the misclassification rate (MCR) (Eq. (15)) was calculated as a metric for a false interaction identification neglecting the absolute value of the INT parameter but assessing solely the polarity of the INT parameters.

$$\text{MCR} = 100\% - 100\% \cdot \frac{\text{correctly classified interaction}}{N} \quad (15)$$

An interaction was rated as correctly classified, when the polarity of both INT parameters including the 95% CI matched the underlying true value that was used for simulation. Additionally, the MCR for the identification of the correct mechanism of interaction (i.e. EC50 or Emax interaction) was calculated.

Results

Development of the Optimized Rhombic Designs

The reference designs and newly proposed rhombic designs are visualized on Figs. 2 and 3 respectively. The corresponding EC-values forming the rhombic designs can be obtained from Table I. Minimization problems within the optimization did not occur for the fixed rhombic design. For the free rhombic design 2% of the minimizations converged in local minima with boundary problems and were removed. Conventional checkerboard designs as the conventional rich and conventional sparse reference design do have a symmetric rectangular layout just as the EC-4 × 4-design proposed by Chen *et al.* as a rationally derived experimental design. In opposite to these designs, the optimization of the free design formed a rhombic design with no classic rectangular shape. The final free rhombic design is nearly mirror symmetric to the diagonal of the checkerboard. In comparison, the fixed rhombic design is forced to be mirror symmetric to be more practicable for application in *in vitro* studies.

Table I Design Variables Corresponding to the Developed Rhombic Checkerboard Designs (Fig. 2)

Free rhombic design		Fixed rhombic design	
EC39:EC81		EC44:EC82	
EC06:EC53	EC81:EC39	EC08:EC44	EC82:EC44
EC52:EC08		EC44:EC08	

Results are presented as ECXX Drug A:ECXX Drug B

In none of the developed designs the optimization led to combinations scenarios formed out of equal EC-values, as e.g. EC20:EC20, EC50:EC50 and EC80:EC80 in the EC-4 × 4-design.

Design Evaluation in Stochastic Simulation and Estimation

The estimation of the EC50 resulted in unbiased estimates with a mean relative imprecision of 2.10%. The accuracy and precision metrics of the different experimental designs estimating the interaction parameters are displayed on Fig. 4. The misclassification rates of all designs are illustrated on Fig. 5. The AIC differences between an EC50 or Emax model, as metric for the discrimination between allosteric and competitive interactions are shown in Table II. All designs led to small relative bias (rBias) (<2.06%) (Fig. 4), indicating that all designs were able to support an accurate estimation of the interaction parameters. Comparing the relative imprecision (rRMSE) of the different designs, the conventional rich design with its 81 combination scenarios and the EC-4 × 4 design with its 9 combination scenarios allowed estimation of the INT-parameters most precisely (rRMSE rich design: INT_{AB}: 16.54%, INT_{BA}: 13.91%; rRMSE EC-4 × 4-design: INT_{AB}: 14.19%, INT_{BA}: 14.14%). The conventional sparse design, which is like the EC-4 × 4-design a reduced design by a factor of nine (nine combination scenarios) was least precise (INT_{AB}: 25.16%, INT_{BA}: 24.78%).

The further reduced rhombic designs with only four combination scenarios, enabled a precision of the estimates between the EC-4 × 4-design and the conventional sparse design (Fig. 4).

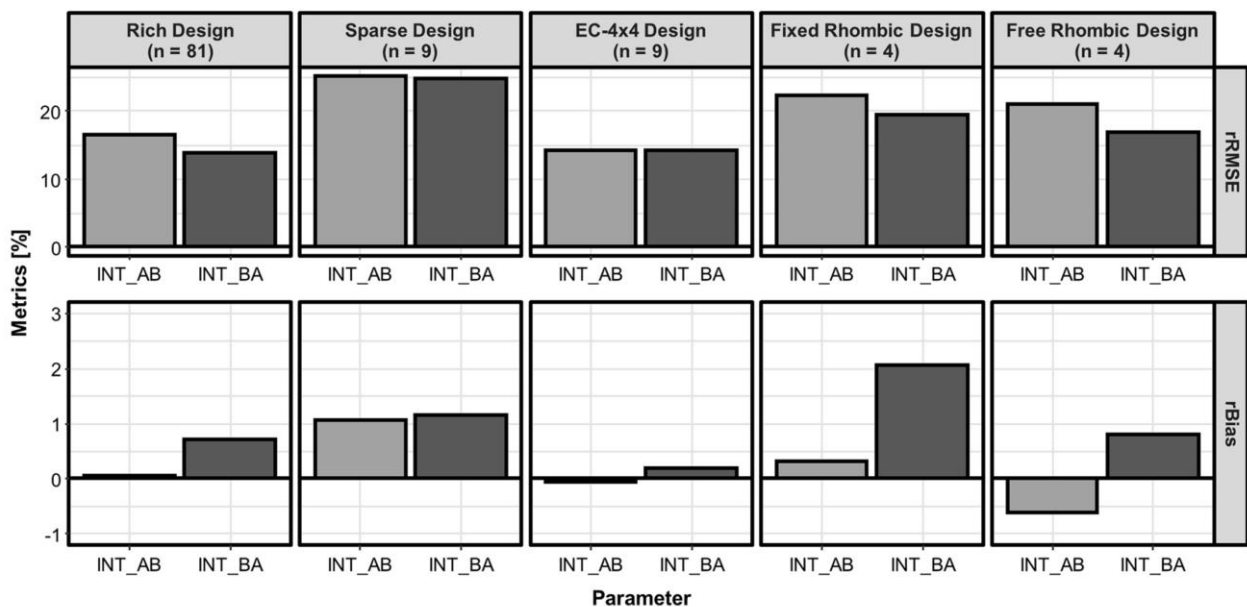


Fig. 4 The relative root mean square error (rRMSE) and relative bias (rBias) for the interaction parameters (INT_{AB}, INT_{BA}) estimated by the different checkerboard design in the SSE study. n represents the number of combination scenarios included in the respective experimental design.

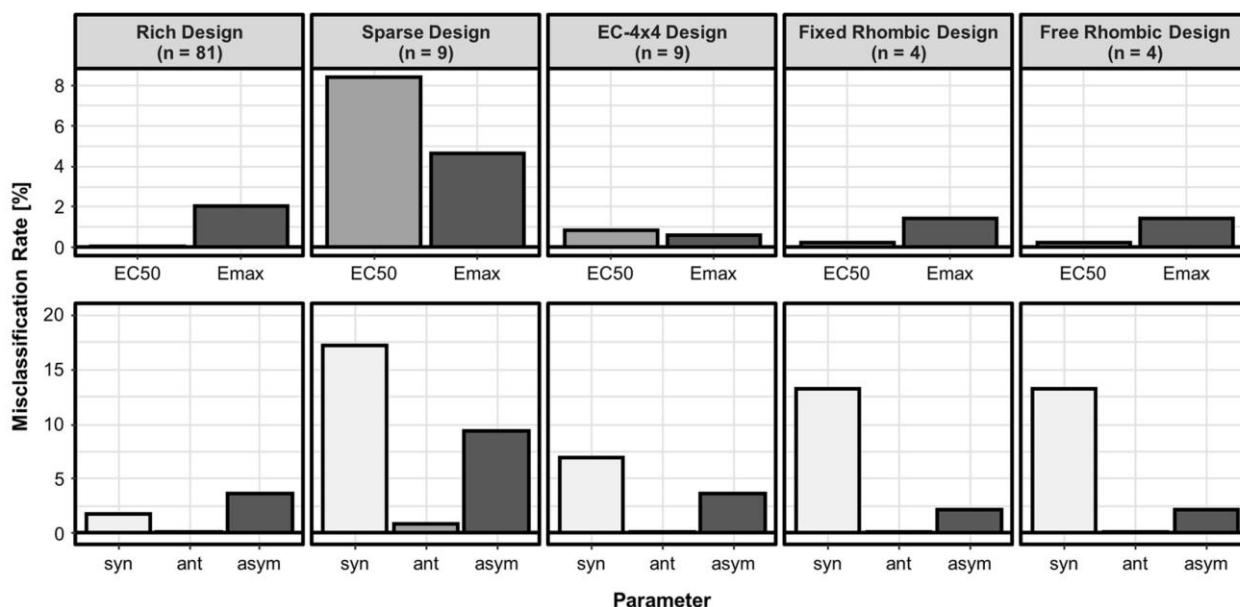


Fig. 5 Misclassification rates of the different checkerboard designs in the SSE study. Classification rates for discriminating competitive (EC50) or allosteric (Emax) interactions were calculated as well as for identifying the correct type of the interaction (syn: synergy, ant: antagonism, asym: asymmetry). n represents the number of combination scenarios included in the respective experimental design.

Table II SSE Statistics on the Ability of the Different Experimental Designs to Discriminate Between EC50 and Emax Interactions

	Reference designs			Rhombic designs	
	conventional		EC 4×4	fixed	free
	rich	sparse			
Combination scenarios	81	9	9	4	4
Min. AIC ^a difference for interaction discrimination (EC50, Emax) in ≥ 95% of the simulations	47.83	0.81	15.24	9.22	5.52

^aAIC, Akaike Information criterion

The overall lowest misclassification rates were displayed by the conventional rich design. The EC-4×4-design and the rhombic designs led to lower misclassification rates than the conventional sparse design (Fig. 5). The free rhombic design overall misclassified less interactions than the fixed rhombic design. In all designs synergistic interactions were misclassified most often (Fig. 5).

When considering strong antagonistic monodirectional drug interactions leading to full suppression of the effect of the victim drug, the conventional designs relying on standard concentrations showed advantages against all adaptive designs with effective concentrations since the effective concentrations are less informative in such extreme cases (Supplement Text 2, Supplement Fig. 1).

The AIC difference between an interaction on Emax and EC50 for 95% of the estimations as marker for the distinctness of the discrimination between EC50 and Emax interactions was highest for the conventional rich design (47.83) and

for the EC-4×4-design (15.24). Again, the rhombic designs were inferior with regard to the distinctness of the interaction discrimination than the richer EC-4×4 design and the conventional rich design but superior to the conventional reduced design (Table II).

Discussion

The optimized rhombic designs proposed in this study include solely four scenarios required for combination testing and present universal applicable designs due to their reference on effective concentrations. With their rhombic shaped arrangement of the combination scenarios rather than a conventional rectangular one, they suggest that the combinations of similar effective drug concentrations (i.e. EC50-EC50 combination) are less informative than off-diagonal concentration combinations.

These proposed designs were included in SSE studies and were compared to reference designs. In this comparison, it was considered that a preliminary EC50 determination with additional uncertainty had to be performed for the EC-based designs. The herein simulated EC50 determination led to very precise and unbiased estimates of the drug potencies and therefore had limited impact on the EC-based design in this simulated setting. Also, the other parameters of the drugs were considered to be known and fixed to the true values, when estimating the interactions. This influence will be more relevant, when transferring the optimal design in application areas, where high-quality information on the pharmacodynamics of the drugs is not available.

The substantial reduction in tested combination scenarios in the here newly proposed rhombic designs is obviously linked to a loss of information. Despite their very reduced layout, the optimized designs based on effective concentrations were still superior regarding accuracy, precision and misclassification rates compared to the conventional sparse design and they could compete with the reference designs in case of classification of interaction. Therefore, this reduction could be very useful in early phases of interaction screening to enable a higher throughput when elucidating drug interactions. The simulation studies mimicked modern, so called 'dynamic' checkerboard experiments with readout of viable bacteria, instead of turbidity. Therefore, the designs enable a wider spectrum of interaction analysis. Moreover, as the designs are based on the GPDI model, they are designed for the identification of directional interactions and can identify perpetrator and victim drugs and discriminate interactions on EC50 and Emax. In conventional checkerboards with turbidity as endpoint, single concentration testing as performed in multiple-combination bactericidal tests, time-kill assays or Etest [2], the generation of information about the combined pharmacodynamic effect surface cannot be achieved. Therefore, the workload reduction especially in dynamic checkerboards is effective and enables a more straightforward understanding of drug interactions to a fuller extent, even though the optimized designs require prior knowledge regarding the drug-response relation to determine the by design needed effective concentrations. This requires solely active drugs and therefore the designs based on effective concentrations can have limited applicability for detection of the potentiation of a drug by an inactive combination partner or coalism of two inactive drugs. Nevertheless, it could be encouraged to utilize the power of experimental design optimization techniques to support rational approaches combination designs beyond antibiotic drugs.

In opposite to the optimized design proposed by Chen *et al.* [5], which was rationally developed and

evaluated with focus on EC50 interactions, the designs in this study were developed with an D-optimal inspired approach and considered interactions on Emax and EC50. Additionally, the designs were all also evaluated extensively in Bliss Independence using the GPDI model, allowing a wide variability of possible interactions on EC50 and Emax. Thus, all rhombic designs are associated with an enormous improvement in gain of information on drug interactions *versus* a reduction of workload to enable a high throughput as compared to conventional approaches. Moreover, through the usage of drug specific EC-values, testing concentrations are defined rationally and the designs allow more targeted studies of drug interactions. This can make interaction testing more efficient, even though the designs are inferior to conventional designs, when very strong drug interactions are present, which are not covered in the range of the effective concentrations for the respective design. In these cases, unspecific standard concentrations can initially be beneficial through their wider concentration range and additional testing for the adaptive effective concentration-based designs is required to enable a reliable identification of the drug interactions (Supplement Text 3).

We acknowledge the following limitations of our study: D-optimal design strategies are sensitive to underlying prior information and the developed designs suffer if the final model differs clearly from the prior model [18]. However, the chosen GPDI model is already compared and validated against different interaction models. It showed to be superior to an empiric Bliss Independence interaction model and is universally applicable [8]. Furthermore, it is able to infer about mechanistic information in the underlying interaction [8]. Beside the underlying model the optimality criterion can have an influence on the identified design candidates [19, 20]. As this study was inspired by the traditional D-optimality criterion alternative approaches like A- or E-optimality might result in slightly different designs. Nevertheless, the SSE evaluation confirmed the capabilities of the designs derived with the D-optimal inspired method in the identification of pharmacodynamic drug interactions.

The chosen optimization and evaluation settings are focused on antibiotics that may limit the direct transfer of the experimental designs, but does not exclude it. For simplification, in our design development and in the SSE studies no simultaneous interactions on EC50 and Emax were considered. In addition, base of the SSE studies was a simplified one compartment model to describe the bacterial growth. This means, that development of adaptive resistance or tolerances were quantified as interactions and not in a mechanistic fashion. Hence, further research is required, if the designs shall be used within more complex mechanistic models.

Conclusion

In this study rhombic checkerboard designs based on D-optimized effective concentrations were proposed. For the commonly used additivity criterion on pharmacodynamic interaction modelling, Bliss Independence, a fixed rhombic design with the combination scenarios EC08/EC44, EC44/EC08, EC44/EC82, EC82/EC44 is the simplest of the developed designs due to the fixed middle concentration and enables the determination of synergistic, antagonistic or asymmetric drug interactions with a reduced workload compared to conventional checkerboard designs. The new proposed designs, which reduce combination testing by 95% compared to conventional rich designs and by 55% compared to sparser design layouts, are inferior with regard to accuracy and precision to the conventional rich design and an earlier proposed EC-based design, due to a loss of information during reduction, but can be beneficially compared to a conventional sparse design in case of classification of an interaction. Thus, the present study showed that checkerboard designs based on interaction models with optimized drug specific effective concentrations are superior to conventional designs with standard concentrations and are very attractive to enable higher throughput with maintained or even increased quality of results. Additionally, a model-based evaluation of the experimental data as suggested in this study can contribute to a deeper elucidation of drug interactions. Beside the optimization of checkerboard designs, the benefit of powerful optimization strategies of experimental designs to economize and improve experimental setups could also be used on various experimental settings. The herein developed designs will be used and evaluated in further *in vitro* experiments to examine drug interactions.

Supplementary Information The online version contains supplementary material available at <https://doi.org/10.1007/s11095-022-03396-7>.

Author Contributions SGW and NK planned the study; NK and RA conducted the research; NK wrote the original draft; NK, RA, NG, WC and SGW wrote, reviewed, edited and approved the final manuscript.

Funding Open Access funding enabled and organized by Projekt DEAL. This project resulted from a German–French research cooperation called ‘CO-PROTECT’ and was supported by a grant from the Federal Ministry of Education and Research (BMBF), Germany, grant agreement number 16GW0249K, and by a grant from the National Agency of Research (ANR), France, grant agreement number R19094GG.

Data Availability The datasets generated and analyzed during the current study are available from the corresponding author on reasonable request.

Declarations

Conflict of Interest Niklas Kroemer, Romain Aubry, Nicolas Grégoire, William Couet and Sebastian G. Wicha declare that they have no conflict of interest.

Open Access This article is licensed under a Creative Commons Attribution 4.0 International License, which permits use, sharing, adaptation, distribution and reproduction in any medium or format, as long as you give appropriate credit to the original author(s) and the source, provide a link to the Creative Commons licence, and indicate if changes were made. The images or other third party material in this article are included in the article's Creative Commons licence, unless indicated otherwise in a credit line to the material. If material is not included in the article's Creative Commons licence and your intended use is not permitted by statutory regulation or exceeds the permitted use, you will need to obtain permission directly from the copyright holder. To view a copy of this licence, visit <http://creativecommons.org/licenses/by/4.0/>.

References

1. Tyers M, Wright GD. Drug combinations: a strategy to extend the life of antibiotics in the 21st century. *Nat Rev Microbiol.* 2019;17(3):141–55.
2. Doern CD. When does 2 plus 2 equal 5? A review of antimicrobial synergy testing. *J Clin Microbiol.* 2014;52(12):4124–8.
3. Orhan G, Bayram A, Zer Y, Balci I. Synergy tests by E test and checkerboard methods of antimicrobial combinations against *Brucella melitensis*. *J Clin Microbiol.* 2005;43(1):140–3.
4. Wicha SG, Kees MG, Kuss J, Kloft C. Pharmacodynamic and response surface analysis of linezolid or vancomycin combined with meropenem against *Staphylococcus aureus*. *Pharm Res.* 2015;32(7):2410–8.
5. Chen C, Wicha SG, Nordgren R, Simonsson USH. Comparisons of analysis methods for assessment of pharmacodynamic interactions including design recommendations. *AAPS J.* 2018;20(4):77.
6. Atkinson AC, Donev AN. Optimum experimental designs. Oxford: Oxford University Press; 1992.
7. Retout S, Duffull S, Mentré F. Development and implementation of the population Fisher information matrix for the evaluation of population pharmacokinetic designs. *Comput Methods Programs Biomed.* 2001;65(2):141–51.
8. Wicha SG, Chen C, Clewe O, Simonsson USH. A general pharmacodynamic interaction model identifies perpetrators and victims in drug interactions. *Nat Commun.* 2017;8(1):2129.
9. Bliss CI. The toxicity of poisons applied jointly. *Ann Appl Biol.* 1939;26(3):585–615.
10. R Core Team. R: A language and environment for statistical computing. R Foundation for Statistical Computing. Vienna: R Foundation for Statistical Computing; 2020. p. <https://www.R-project.org>.
11. Fishburn PC. Letter to the Editor—Additive utilities with incomplete product sets: Application to priorities and assignments. *Oper Res.* 1967;15(3):537–42.
12. Nelder JA, Mead R. A simplex method for function minimization. *Comput J.* 1965;7(4):308–13.
13. Byrd RH, Lu P, Nocedal J, Zhu C. A limited memory algorithm for bound constrained optimization. *SIAM J Sci Comput.* 1995;16(5):1190–208.
14. Soetaert K, Petzoldt T, Setzer RW. Solving differential equations in R: Package deSolve. *J Stat Softw.* 2010;33(9):1–25.
15. Gibson B, Wilson DJ, Feil E, Eyre-Walker A. The distribution of bacterial doubling times in the wild. *Proc R Soc B Biol Sci.* 2018;285(1880):20180789.

Pharmaceutical Research

16. Spilker ME, Vicini P. An evaluation of extended vs weighted least squares for parameter estimation in physiological modeling. *J Biomed Inform.* 2001;34(5):348–64.
17. Akaike H. A new look at the statistical model identification. *IEEE Trans Automat Contr.* 1974;19(6):716–23.
18. Seurat J, Nguyen TT, Mentré F. Robust designs accounting for model uncertainty in longitudinal studies with binary outcomes. *Stat Methods Med Res.* 2020;29(3):934–52.
19. Loingeville F, Nguyen TT, Riviere MK, Mentré F. Robust designs in longitudinal studies accounting for parameter and model uncertainties—application to count data. *J Biopharm Stat.* 2020;30(1):31–45.
20. Jones B, Allen-Moyer K, Goos P. A-optimal versus D-optimal design of screening experiments. *J Qual Technol.* 2021;53(4):369–82.

Publisher's Note Springer Nature remains neutral with regard to jurisdictional claims in published maps and institutional affiliations.

3.2 Publication II

Evaluation of *in vitro* pharmacodynamic drug interactions of ceftazidime/avibactam and fosfomycin in *Escherichia coli*

Niklas Kroemer, Miklas Martens, Jean-Winoc Decousser, Nicolas Grégoire,
Patrice Nordmann, Sebastian G. Wicha

Journal of Antimicrobial Chemotherapy (2023)

Impact Factor: 5.2 (2022)

Synopsis

Ceftazidime/avibactam and fosfomycin are known to interact synergistically against some *K. pneumoniae* as well as *P. aeruginosa* strains, but a systematic evaluation in other *Enterobacteriaceae* such as *E. coli* was lacking.[28] Important features of a meaningful *in vitro* study to gather insights for a clinical translation of the drug combinations are the following: I) generation of detailed mechanistic and quantitative understanding of bacterial dynamics, drug effects and interactions and II) the inclusion of various well-defined bacterial strains expressing clinically relevant resistance mechanisms.[4] Therefore, the study conducted in Publication II aimed for a systematic analysis of the drug interactions of ceftazidime/avibactam and fosfomycin in eight isogenic and six clinical *E. coli* strains expressing common extended spectrum beta-lactamases or carbapenemases. Firstly, an interaction screening utilising the optimal experimental design developed in Publication I (see 3.1) was performed and the pharmacodynamic drug interactions were assessed in exposure-response-surface analyses. Secondly, the identified interactions were corroborated in three clinical *E. coli* isolates in detailed static time kill experiments and evaluated by means of semi-mechanistic modelling.

The screening identified synergies for six out of eight isogenic strains and four out of six clinical isolates. Significant reductions of the EC50 with variable directionality were identified as mechanisms of the interactions.

The static time kill experiments confirmed the identified interactions. Subsequent PK/PD modelling elucidated enhanced killing effects with EC50 reductions up to 97% as mechanism of the increased antibacterial effect in combination. However, a correlation of the genetic background of the individual strains and the manifestation of the drug interactions could not be identified.

The broad synergistic interactions of ceftazidime/avibactam and fosfomycin against *E. coli* verified the potential for a clinical application of the drug combination with regard to dose reductions or re-sensitisation of resistant bacteria.

Evaluation of *in vitro* pharmacodynamic drug interactions of ceftazidime/avibactam and fosfomycin in *Escherichia coli*

Niklas Kroemer ¹, Miklas Martens¹, Jean-Winoc Decusser², Nicolas Grégoire^{3,4,5}, Patrice Nordmann⁶ and Sebastian G. Wicha^{1*}

¹Department of Clinical Pharmacy, Institute of Pharmacy, University of Hamburg, Hamburg, Germany; ²Dynamic Team—EA 7380, Faculté de santé, Université Paris-Est-Créteil Val-De-Marne, Créteil, France; ³Inserm U1070, Pharmacologie des Anti-infectieux et Antibiorésistance, Poitiers, France; ⁴Université de Poitiers, UFR de Médecine Pharmacie, Poitiers, France; ⁵CHU de Poitiers, Laboratoire de Toxicologie-Pharmacologie, Poitiers, France; ⁶Medical and Molecular Microbiology, University of Fribourg, Fribourg, Switzerland

*Corresponding author. E-mail: Sebastian.Wicha@uni-hamburg.de

Received 24 March 2023; accepted 31 July 2023

Background: Combination therapy can increase efficacy of antibiotics and prevent emergence of resistance. Ceftazidime/avibactam and fosfomycin may be empirically combined for this purpose, but a systematic and quantitative evaluation of this combination is needed.

Objectives: In this study, a systematic analysis of the pharmacodynamic interactions of ceftazidime/avibactam and fosfomycin in clinical and isogenic *Escherichia coli* strains carrying genes coding for several carbapenemases or ESBLs was performed and pharmacodynamic interactions were quantified by modelling and simulations.

Methods: Pharmacodynamic interactions were evaluated in ‘dynamic’ checkerboard experiments with quantification of viable bacteria in eight isogenic and six clinical *E. coli* strains. Additionally, supplemental time–kill experiments were performed and genomic analyses were conducted on representative fosfomycin-resistant subpopulations. Models were fitted to all data using R and NONMEM®.

Results: Synergistic drug interactions were identified for 67% of the clinical and 75% of the isogenic isolates with a mean EC₅₀ reduction of >50%. Time–kill experiments confirmed the interactions and modelling quantified EC₅₀ reductions up to 97% in combination and synergy prevented regrowth of bacteria by enhanced killing effects. In 9 out of 12 fosfomycin-resistant mutants, genomic analyses identified previously reported mutations.

Conclusions: The broad synergistic *in vitro* activity of ceftazidime/avibactam and fosfomycin confirms the potential of the application of this drug combination in clinics. The substantial reduction of the EC₅₀ in combination may allow use of lower doses or treatment of organisms with higher MIC values and encourage further research translating these findings into the clinical setting.

Introduction

Infections with carbapenemase or ESBL-producing Enterobacterales represent a major healthcare threat.^{1,2} Rational combinations of antibiotics can extend the shelf-life of drugs by preventing the emergence of resistance and achieve high efficacy.³ Ceftazidime/avibactam represents a novel β-lactam/β-lactamase inhibitor combination for which benefits in treatment outcome are reported when used in combination.⁴ The fixed combination is currently approved against complicated intra-abdominal infections, urinary tract infections and hospital-acquired pneumonia, including ventilator-associated pneumonia. An empirically frequently used combination partner is fosfomycin, which is indicated for the same infections, when given IV, but not recommended to

be used alone.⁵ In particular, efficacy of the combination of extended-spectrum cephalosporins and fosfomycin has been extensively shown for the treatment of MRSA infections.⁶ Additionally, combinations with ceftazidime/avibactam have been evaluated *in vitro* to have potential against MDR *Klebsiella pneumoniae* or *Pseudomonas aeruginosa*, but the effects are dependent on underlying resistance enzymes.^{7,8}

Hence, this study provides a detailed *in vitro* analysis of the pharmacodynamic (PD) drug interactions of ceftazidime/avibactam and fosfomycin in 14 isogenic and clinical *Escherichia coli* strains carrying genes coding for specific carbapenemases or ESBLs. To elucidate the drug interactions, ‘dynamic’ checkerboard experiments with quantification of viable bacteria beyond turbidity as surrogate for bacterial growth were conducted.⁹

Kroemer et al.

Additionally, detailed time–kill experiments with selected strains were performed. All quantitative data were evaluated by modelling and simulations using different implementations of the general PD interaction (GPDl) model to characterize and quantify the PD drug interactions.¹⁰ Ultimately, selected resistance development was elucidated on a genetic level.

Materials and methods

Bacterial strains, antimicrobials and media

Eight isogenic *E. coli* CFT073 strains carrying the cloning vector pACYC184 plasmid with selected genes coding for different carbapenemases or ESBLs and six clinical *E. coli* strains where previous WGS identified ESBL genes were investigated (Table 1). Those resistance markers were chosen according to their extended distribution in Enterobacteriales worldwide and in particular in Europe.

Ceftazidime, avibactam, fosfomycin and glucose-6-phosphate (all Sigma–Aldrich, USA) stocks were prepared in sterile 0.9% NaCl solution, stored at –80°C and used timely. Growth medium and agar plates containing ceftazidime were supplemented with a fixed concentration of 4 mg/L avibactam corresponding to the EUCAST guidelines, as well as 25 mg/L glucose-6-phosphate added to fosfomycin.

Bacteria were grown on Columbia agar (Carl Roth, Germany). Depending on the cloning the isogenic strains were grown selectively on agar containing 10 mg/L tetracycline (Chemodex, Switzerland) or 25 mg/L chloramphenicol (Sigma–Aldrich, USA). Agar plates containing

5× MIC concentrations were used to survey phenotypic resistance development. The experiments were conducted in CAMHB (Millipore, USA). Stability of the drugs was assumed over the short time course of the experiments.

Susceptibility testing

The MICs of ceftazidime, ceftazidime/avibactam and fosfomycin were determined in triplicate after 24 h by microdilution, according to the CLSI guideline, and the modal value was reported.¹¹ The avibactam concentration was kept constant at 4 mg/L for determination of the ceftazidime/avibactam MICs.

PD interaction screening

In a first step, PD drug parameters including the EC_{50-24h} were determined in triplicate using the same concentration levels as in the MIC experiment, but with an elevated inoculum of 10⁶ cfu/mL and 2 h of preincubation phase at 37°C ambient air before addition of the drugs. For the determination of the ceftazidime/avibactam EC_{50-24h}, as well as for the successive chequerboard experiments, the avibactam concentration was kept constant at 4 mg/L. After 24 h of incubation, samples were taken from a drug-free well, two visual turbid wells and two visual clear wells, serially diluted and plated on agar plates. Manual counting of the bacteria was performed after 24 h and the cfu/mL were calculated. A description of the estimation of the EC_{50-24h} using a sigmoidal E_{max} model is given in Supplementary Text S1 (available as [Supplementary data](#) at JAC Online).

Table 1. Overview of the different included strains in the screening experiments with their respective MIC, EC_{50-24h} and the determined PD drug interactions including the calculated interaction shift at EC_{50-24h} of the perpetrator with their CIs

Strain information		MIC (mg/L)					EC _{50-24h} (mg/L)	PD drug interaction	
Name	Genetic background	CAZ	CZA	FOF	CZA	FOF	Type	Direction (victim/perpetrator)	Interaction shift at EC _{50-24h} (95% CI)
<i>E. coli</i> WT	Isogenic: empty plasmid	0.125	0.125	4	0.11	38.58	Synergy	FOF/CZA	–0.61 (–0.42 to –0.80)
<i>E. coli</i> CTX-M-1	Isogenic	0.5	0.125	8	0.11	3.53	Synergy	CZA/FOF	–0.70 (–0.60 to –0.80)
<i>E. coli</i> CTX-M-3	Isogenic	0.5	0.125	8	0.09	20.07	Synergy	FOF/CZA	–0.60 (–0.41 to –0.79)
<i>E. coli</i> CTX-M-9	Isogenic	0.25	0.125	4	0.14	15.39	Synergy	FOF/CZA	–0.93 (–0.82 to –1.00)
<i>E. coli</i> CTX-M-15	Isogenic	2	0.125	16	0.12	20.91	Bliss	—	0
<i>E. coli</i> OXA-48	Isogenic	0.125	0.125	8	0.13	41.50	Synergy	FOF/CZA	–0.55 (–0.39 to –0.72)
<i>E. coli</i> OXA-181	Isogenic	0.125	0.125	8	0.15	17.88	Bliss	—	0
<i>E. coli</i> KPC-3	Isogenic	256	1	4	2.58	39.75	Synergy	CZA/FOF	–0.24 (–0.18 to –0.29)
<i>E. coli</i> YAL_AMA	Clinical: bla _{OXA-244} , bla _{CTX-M-15}	16	0.125	16	0.09	4.08	Synergy	FOF/CZA	–0.42 (–0.15 to –0.69)
<i>E. coli</i> JUM_JEA	Clinical: bla _{OXA-48} , bla _{CTX-M-15}	16	0.06	4	0.04	4.02	Synergy	CZA/FOF	–0.16 (–0.04 to –0.27)
<i>E. coli</i> MER_MIL	Clinical: bla _{OXA-48} , bla _{TEM-1B}	0.25	0.25	8	0.14	7.10	Synergy	FOF/CZA	–0.16 (–0.02 to –0.30)
<i>E. coli</i> OLA_HAM	Clinical: bla _{OXA-244} , bla _{CTX-M-15}	32	0.5	4	0.28	35.96	Bliss	—	0
<i>E. coli</i> N1067	Clinical: bla _{OXA-181}	8	0.5	4	0.19	11.90	Bliss	—	0
<i>E. coli</i> N790	Clinical: bla _{OXA-244}	0.125	0.125	32	0.09	31.98	Synergy	CZA/FOF	–0.80 (–0.61 to –1.00)

The avibactam concentration was 4 mg/L in all experimental scenarios. CAZ, ceftazidime; CZA, ceftazidime/avibactam; FOF, fosfomycin.

Ceftazidime/avibactam and fosfomycin interactions in *E. coli*

In a second step, to identify PD drug interactions of ceftazidime/avibactam and fosfomycin, 'dynamic' chequerboards with an optimized fixed rhombic design consisting of four combination scenarios based on effective concentrations as previously described was utilized.^{9,12} In brief, an experimental design was used where highly informative concentrations of the antibiotics were calculated based on the determined EC_{50-24h} and comprised drug combinations at (ceftazidime/avibactam and fosfomycin, respectively): $EC_{08}+EC_{44}$, $EC_{44}+EC_{08}$, $EC_{44}+EC_{82}$, $EC_{82}+EC_{44}$. Additionally to these four highly informative combination scenarios, two scenarios at EC_{44-24h} were included. The chequerboard experiments were inoculated with 10^6 cfu/mL and after 2 h of preincubation phase at 37°C ambient air antibiotics were added. The total cfu count was quantified after 0, 24 and 48 h by serial dilution and plating on drug-free agar plates as described above. To monitor the emergence of resistant subpopulations, samples after 48 h were also plated on agar plates containing fosfomycin or ceftazidime/avibactam at $5\times$ MIC. Mutation frequencies were calculated afterwards by division of cfu/mL determined on drug-containing agar plates by cfu/mL determined on drug-free medium. Cfus on plates containing the antibiotics were read after 48 h. Additionally to the evaluation of the phenotypic resistance to ceftazidime/avibactam and fosfomycin, fosfomycin-resistant mutants of three selected clinical isolates were genomically analysed. The experiments were conducted as duplicates.

Time-kill experiments

For three selected clinical *E. coli* isolates, static time-kill experiments were performed in order to corroborate the interactions determined in the chequerboard experiments. Additionally, the emerged subpopulations resistant to fosfomycin during the chequerboard assays of those strains were analysed genomically. The time-kill experiments were inoculated with 10^6 cfu/mL and after 2 h of preincubation phase at 37°C ambient air the antibiotics were added. Samples were drawn at 0, 2, 4, 8, 24 and 30 h after addition of the drugs, serially diluted and plated on agar plates. After 24 h of incubation the colonies were counted manually and the cfu/mL counts were calculated.

Each time-kill curve was performed at least in duplicate. Time-kill experiments with concentrations reaching effect sizes ranging from full eradication after 30 h to small effects with regrowth were performed for ceftazidime/avibactam and fosfomycin alone and in combination. The investigated concentrations in all experiments were based on 2-fold increments and titrated down until regrowth was observed. Corresponding to the EUCAST recommendation for susceptibility testing, the avibactam concentration was kept constant at 4 mg/L. At that concentration a neglectable antibacterial effect of avibactam by its own and a full suppression of the β -lactamases was assumed.

Genomic analysis

The genomes of the six clinical strains were sequenced using Illumina sequencing technology, as previously described.¹³ Genomes were assembled with Shovill v1.0.4 (<https://github.com/tseemann/shovill>). The resistome was identified using the ResFinder database available on the Center for Genomic Epidemiology platform (<https://www.genomicepidemiology.org/>).

SNPs and small insertions and deletions (indels) were identified by comparing the genome of resistant mutants with the original strains using breseq software.¹⁴ The contribution of mutated genes to the fosfomycin resistance was tested against previously published studies.

Pharmacometric modelling*PD interaction screening*

To identify the drug interactions in the PD interaction screening pharmacokinetic/pharmacodynamic (PK/PD) models were developed in R.¹⁵ Therefore, the cfu/mL data of the chequerboard experiments after 24 h

were combined with the EC_{50} experiment data and analysed jointly. Single-drug effects at 24 h, expressed as \log_{10} cfu/mL were modelled using an E_{max} model. Combined-drug effects were calculated as Bliss independence. Subsequently, the expected 'no interaction' surface assuming Bliss independence and interactions on drug potency (EC_{50}) were evaluated.¹⁶ PD interactions on EC_{50} were estimated using the GPDI term.¹⁰ The GPDI model is an interaction model that enables the directional description and quantification of drug interactions by identifying perpetrator and victims of a drug interaction. In the context of the GPDI model, a victim drug is a drug for which EC_{50} or maximum effect is altered concentration-dependently in the presence of a perpetrator drug. Thereby, not only monodirectional synergistic or antagonistic drug interactions, but also bidirectional interactions with one drug being perpetrator and victim at the same time can be described. The magnitude of a drug interaction can be directly interpreted by an interaction parameter characterizing an interaction shift. This interaction shift corresponds to a fractional change of a respective PD parameter as a result of a drug interaction (e.g. -0.5 corresponds to a 50% reduction). A specific description of the GPDI model and the model-based evaluation of the PD interactions is given in Text S2.

Time-kill experiments

Semi-mechanistic PK/PD models describing the data of the time-kill experiments were developed in NONMEM[®] 7.5.0 (ICON, Gaithersburg, MD, USA) using first-order conditional estimation with interaction (FOCE-I) separately for the three clinical *E. coli* strains for which kinetic time-kill data were produced. A detailed description of the model-building process is described in Text S3. In brief, the data from the EC_{50} determination, the chequerboard experiments and from the time-kill experiments were combined and in a first step the drug effects of ceftazidime/avibactam or fosfomycin without combination partner were described with sigmoidal maximum effect (E_{max}) or power effect models in a two-compartment base model with a susceptible and a resistant subpopulation (Figure 1). Like in the interaction screening, combined drug effects were calculated as Bliss independence. The drug interactions were modelled via the implementation of the GPDI model on the drug potencies or maximum drug effects on the two subpopulations with focus on the resistant bacteria. Monodirectional interactions as well as bidirectional interactions were considered. The model selection was based on Akaike information criterion (AIC), visual model fit, model stability and condition number.¹⁷ Biological variability was supported by an exponential interindividual variability on the inoculum of the resistant population. Parameter uncertainty was assessed using the sampling importance resampling (SIR) algorithm implemented by Perl-speaks-NONMEM (PsN) 5.0 (Uppsala University, Sweden) with the relative standard errors (RSEs) produced by the covariance step in NONMEM informing a proposal distribution.¹⁸

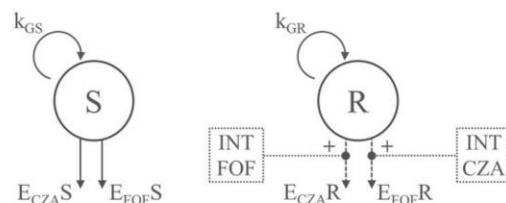


Figure 1. Scheme of the PD models for the time-kill experiments of the three clinical *E. coli* strains. CZA, ceftazidime/avibactam; FOF, fosfomycin; E, effect; S, susceptible subpopulation; R, resistant subpopulation; INT, drug interaction; k_{GS} , growth rate of S (mainly characterizing unexposed bacterial growth); k_{GR} , growth rate of R (mainly characterizing regrowth under drug exposure); $cfu = S + R$.

Results

Susceptibility testing

The MICs and EC₅₀s of ceftazidime/avibactam and fosfomycin for the isogenic and clinical strains are listed in Table 1. The isogenic strain carrying a gene coding for KPC-2 and four of six clinical isolates were resistant to ceftazidime alone. All strains were susceptible to ceftazidime/avibactam and fosfomycin according to the EUCAST breakpoint tables v. 13.0, i.e. ceftazidime: resistant (R) > 4 mg/L; ceftazidime/avibactam: R > 8 mg/L; fosfomycin IV: R > 32 mg/L.

PD interaction screening

The systematic screening identified strong synergistic *in vitro* PD interactions for ceftazidime/avibactam and fosfomycin (reduction of EC₅₀ between 15% and 93%) for most of the evaluated strains (Table 1). Synergies were identified for 75% of the isogenic and 67% of the clinical isolates. No interactions were identified for the remaining strains. No antagonistic drug interactions were identified. When observing synergy, fosfomycin was mostly the victim of the interaction, with ceftazidime/avibactam as perpetrator enhancing the potency of fosfomycin, but no clear correlation between the direction of the interaction and features of the strains could be identified (Text S4, Figure S1). Calculated response surfaces are illustrated in Figure 2. Those calculated response surfaces highlight the concentration ranges bidimensionally at which the synergistic drug interactions led to higher drug effects than expected Bliss independence (green areas). Additionally, the corresponding estimated drug concentration response surfaces are displayed in Figure S2.

The emergence of phenotypically resistant subpopulations was reduced in combination compared with the exposure to ceftazidime/avibactam or fosfomycin alone. The detailed ratios of phenotypically resistant bacteria after 48 h in the checkerboard experiments are reported in Table 2. In some cases, the numerical total bacterial count was resistant to 5× MIC and, therefore, a value limited to 1 was reported. Generally, the resistance development was reproducible in the duplicates of the experiments. However, the emergence of ceftazidime/avibactam-resistant bacteria was especially subject to high variability. In total, in six strains, emergence of a subpopulation resistant to ceftazidime/avibactam was observed when exposed to the drug alone. In all of those strains, the addition of fosfomycin at the inactive EC₀₈ inhibited the emergence of a resistant subpopulation. Higher emergence of resistance to fosfomycin was observed. In all strains, resistances emerged when fosfomycin was used as a single drug. The addition of ceftazidime/avibactam at the inactive EC₀₈ reduced the number of strains displaying emergence of resistance to fosfomycin by 60% to a total of six strains. In three clinical strains the emergence of resistance to fosfomycin could not be inhibited by the addition of ceftazidime/avibactam. Notably, in those three strains no ceftazidime/avibactam-resistant subpopulation emerged in the EC₄₄-ceftazidime/avibactam scenario but did when fosfomycin was added with EC₀₈.

Pharmacometric modelling

The time–kill curves were well described by a two-population model with a susceptible and a resistant bacterial subpopulation.

Thereby the bacterial dynamics in the experiments with ceftazidime/avibactam and fosfomycin, as well as their combination, were described with those joint two subpopulations (Figure 1). The estimated E_{max} values of ceftazidime/avibactam and fosfomycin in all strains exceeded the growth rates of both respective subpopulations and can thereby describe net bactericidal effects. The exploratory graphical analysis of the combinational drug effects and different tested implementations of the GPDI model suggested drug interactions on drug EC₅₀. The GPDI model identified monodirectional PD drug interactions with strain-dependent interaction directions (Table 3): while the EC₅₀ of fosfomycin was reduced at a maximum by 89% or 91%, for *E. coli* YAL-AMA or *E. coli* MER_MIL, respectively, for *E. coli* JUM-JEA the EC₅₀ of ceftazidime was reduced by 97%. Hence, the models confirmed the synergistic interactions and directionalities of the interactions, which were already determined in the checkerboard screening experiments.

Details of the PD modelling are described in Text S5. The model parameter estimates are displayed in Table 3. Visual predictive checks (VPCs) confirmed an adequate predictive performance of the models (Figures 3–5). The VPCs included additional simulations assuming no drug interactions (blue shaded areas in Figures 3–5). The calculated Bliss independence highlights the concentration ranges at which a drug interaction becomes apparent. For very low and high concentrations the bacterial dynamics of ‘no interaction’ and synergistic effects do overlap (e.g. Figure 3: ceftazidime/avibactam 0.06 mg/L–fosfomycin 0.125 mg/L and ceftazidime/avibactam 0.125 mg/L–fosfomycin 16 mg/L). At intermediate concentrations the synergistic drug interactions led to enhanced killing, which prevented regrowth of the bacteria. In these scenarios, regrowth would have been expected for Bliss independence drug effects (e.g. Figure 3: ceftazidime/avibactam 0.015 mg/L–fosfomycin 2 mg/L).

Genomic analysis

The resistome of the clinical strains is reported in Table 1. The genomic analysis of the fosfomycin-resistant mutants obtained from the selected clinical strains is reported in Table 4. All the genomic data are publicly available through BioProject PRJEB60842. In 9 out of 12 phenotypically fosfomycin-resistant mutants, the genomic analysis identified one or two mutations and/or deletions, which were previously reported as responsible for fosfomycin resistance.

Discussion

The systematic PD interaction screening of ceftazidime/avibactam and fosfomycin in 14 isogenic and clinical *E. coli* isolates carrying genes coding for ESBLs or carbapenemases identified mainly synergistic or no interactions. Those positive interactions between fosfomycin and ceftazidime/avibactam might have been possible due to the fact that *E. coli* does not naturally possess fosfomycin resistance genes, in contrast to other enterobacterial species, such as *Klebsiella* spp., and *Enterobacter* spp., and *P. aeruginosa*. While mainly additive and indifferent drug interactions of ceftazidime/avibactam and fosfomycin beside synergy have been assessed in *K. pneumoniae* or *P. aeruginosa* isolates, this study adds insights into this drug combination for different *E. coli* isolates.^{21–23} The broad appearance of synergistic drug

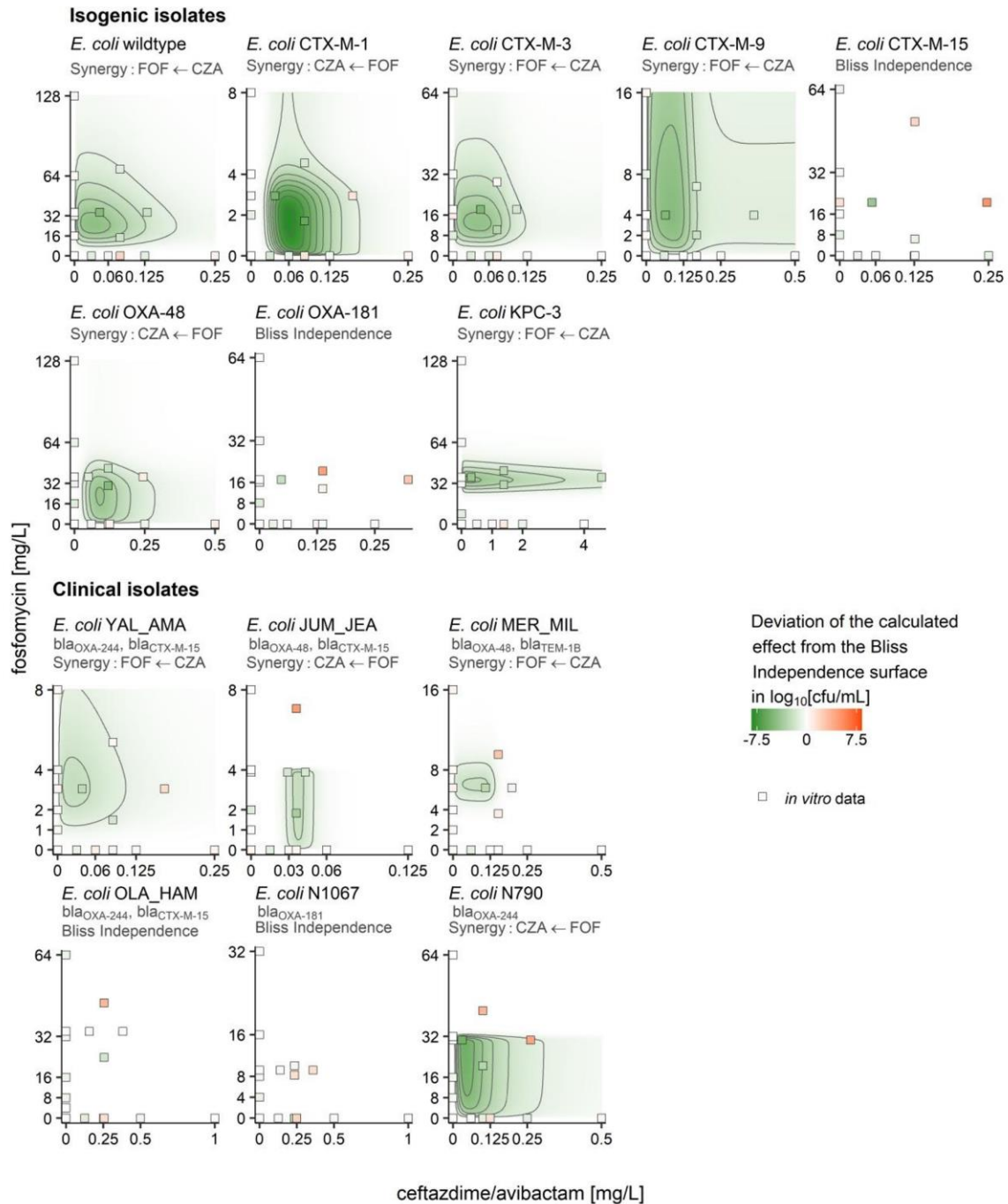
Ceftazidime/avibactam and fosfomycin interactions in *E. coli*

Figure 2. Deviation of the calculated effect from the expected Bliss independence surface. Directions of the interactions are illustrated by arrows (victim ← perpetrator). Green areas represent synergistic areas of effect and red areas antagonistic areas of effect. The squares correspond to obtained *in vitro* data filled with respective colour gradient as outlined above. The avibactam concentration as supplement for ceftazidime was fixed to 4 mg/L. CZA, ceftazidime/avibactam; FOF, fosfomycin. This figure appears in colour in the online version of JAC and in black and white in the print version of JAC.

interactions and diverse directions of the interactions in this screening do not allow clear conclusions to be drawn on an impact of the specific β -lactamase genotype on the type of

interaction or the direction of the interaction. In contrast, the results indicate wide beneficial effects of the combination of ceftazidime/avibactam and fosfomycin in susceptible *E. coli*

Kroemer et al.

Table 2. Overview on the emergence of resistant subpopulations and identified resistances in the chequerboard experiments

Strain	Emergence of resistant subpopulations against 5x MIC CZA		Emergence of resistant subpopulations against 5x MIC FOF	
	Mono drug exposure:	Combined exposure:	Mono drug exposure:	Combined exposure:
	EC ₄₄ CZA	EC ₄₄ CZA: EC ₀₈ FOF	EC ₄₄ FOF	EC ₄₄ FOF: EC ₀₈ CZA
<i>E. coli</i> WT	0 9.43 × 10 ⁻⁶	0 0	9.86 × 10 ⁻¹ 8.72 × 10 ⁻¹	0 0
<i>E. coli</i> CTX-M-1	0 5.75 × 10 ⁻⁵	0 0	2.95 × 10 ⁻² 7.72 × 10 ⁻²	0 1.50 × 10 ⁻¹
<i>E. coli</i> CTX-M-3	0 6.40 × 10 ⁻⁵	0 0	1.52 × 10 ⁻⁶ 5.58 × 10 ⁻⁶	1 0
<i>E. coli</i> CTX-M-9	0 0	0 0	1.89 × 10 ⁻¹ 2.55 × 10 ⁻¹	0 0
<i>E. coli</i> CTX-M-15	0 1.00 × 10 ⁻³	0 0	8.33 × 10 ⁻³ 3.66 × 10 ⁻³	0 0
<i>E. coli</i> OXA-48	0 1.36 × 10 ⁻⁴	0 0	1.64 × 10 ⁻¹ 7.78 × 10 ⁻²	0 1
<i>E. coli</i> OXA-181	0 0	0 0	5.59 × 10 ⁻³ 1.15 × 10 ⁻³	0 0
<i>E. coli</i> KPC-3	9.96 × 10 ⁻² 6.95 × 10 ⁻¹	0 0	1 1	0 0
<i>E. coli</i> YAL_AMA	0 0	0 0	1.10 × 10 ⁻⁵ 1.92 × 10 ⁻⁶	0 0
<i>bla</i> _{OXA-244} , <i>bla</i> _{CTX-M-15}				
<i>E. coli</i> JUM_JEA	0 0	1 0	1 8.03 × 10 ⁻¹	7.93 × 10 ⁻¹ 7.11 × 10 ⁻¹
<i>bla</i> _{OXA-48} , <i>bla</i> _{CTX-M-15}				
<i>E. coli</i> MER_MIL	0 0	0 0	4.87 × 10 ⁻⁶ 4.81 × 10 ⁻⁶	0 0
<i>bla</i> _{OXA-48} , <i>bla</i> _{TEM-1B}				
<i>E. coli</i> OLA-HAM	0 0	0 5.90 × 10 ⁻⁴	1 8.75 × 10 ⁻¹	1 1
<i>bla</i> _{OXA-244} , <i>bla</i> _{CTX-M-15}				
<i>E. coli</i> N1067	0 0	7.93 × 10 ⁻¹ 0	9.28 × 10 ⁻¹ 5.17 × 10 ⁻¹	0 1
<i>bla</i> _{OXA-181}				
<i>E. coli</i> N790	0 0	0 0	3.49 × 10 ⁻³ 1.17 × 10 ⁻⁴	0 0
<i>bla</i> _{OXA-244}				

Resistances are reported as two mutation frequencies (separated by |), accounting for variable emergence of resistance in the two chequerboard duplicates. '1' is reported when the resistant bacteria represent the whole bacterial population after 48 h in the chequerboard experiment. CZA, ceftazidime/avibactam; FOF, fosfomycin.

isolates already carrying genes coding for different β-lactamases. Nevertheless, in 60% of the strains, fosfomycin was identified as the victim of the interaction with amplified effects, when ceftazidime/avibactam was present.

The genomic analysis identified already published mutations/indels correlated to fosfomycin resistance among 9 out of 12 resistant mutants; the genes coding for the two transport uptake systems (*glpT* and *uhpT*) and the genes involved in their regulation (*uhpABC*, *cyaA*, *ptsI*).²⁰ Regarding the remaining mutants, the role of other mechanisms could be debated. For example, fosfomycin could act as substrate for some efflux pumps naturally present in *E. coli* belonging to the major facilitator (MFS) or the resistance-nodulation-cell division (RND) family (such as MdtB, MdtC, MdtG/YceE or Bcr).²⁴ To go further in this hypothesis, additional experiments testing gene expression should be implemented.

A hypothesis for the observed synergistic mode of action could be independent fosfomycin uptake into the bacteria in combination with ceftazidime/avibactam. The genomic analysis identified transporter-related mutations being responsible for fosfomycin resistance. Cell-wall damage mediated by ceftazidime/avibactam could bypass this mechanism of resistance and enable independent uptake of fosfomycin into the bacterial cell. This mechanism has been discussed earlier for combinations of fosfomycin with other drugs.²⁵

Usually many data are needed to gain appropriate information of the combined PD of antibiotics and to investigate the

nature of drug interactions.²⁶ In this study an adaptive *in vitro* 'dynamic' chequerboard design based on drug potencies was used as a very condensed tool to elucidate drug interactions.¹² Thus, the interaction testing was streamlined and rationalized and a comparable and systematic dataset for all tested strains was generated. The 'dynamic' chequerboard approach with a continuous quantification of cfu instead of reliance on categorical turbidity of the broth provided semi-mechanistic insights into the PD drug interactions, which were analysed using modelling and simulation techniques based on the GPDI model.⁹ Therefore, a multidimensional interpretation of PD interactions beyond a binary turbidity threshold was possible.²⁷ The identified interactions and interaction directions from the chequerboard screening were corroborated for selected strains in time-kill experiments and semi-mechanistic modelling and simulation confirmed the hypothesis of the prevention of the emergence of resistant bacterial subpopulations by enhanced killing effects. Modelling of the time-kill data quantified the synergistic drug interaction as up to a 10-fold increase of the potency of the drugs by the presence of the combination partner.

We acknowledge the following limitations of our study. The focus of the interaction testing was the characterization of the drug interaction of the fixed combination of ceftazidime/avibactam with fosfomycin. To reduce the complexity of the drug interactions and the PK/PD modelling, the avibactam concentration in the chequerboard and time-kill experiments was fixed to 4 mg/L,

Ceftazidime/avibactam and fosfomycin interactions in *E. coli***Table 3.** Model parameters for the time-kill PD model presented with 95% CIs determined by SIR

Parameter	Value (95% CI)		
	<i>E. coli</i> YAL_AMA <i>bla</i> _{OXA-244} , <i>bla</i> _{CTX-M-15}	<i>E. coli</i> JUM_JEA <i>bla</i> _{OXA-48} , <i>bla</i> _{CTX-M-15}	<i>E. coli</i> MER_MIL <i>bla</i> _{OXA-48} , <i>bla</i> _{TEM-1B}
Structural model parameters			
Inoculum susceptible bacteria (S) log ₁₀ cfu/mL	6.81 (6.68–6.95)	6.50 (6.29–6.71)	6.77 (6.63–6.91)
Inoculum resistant bacteria (R) (log ₁₀ cfu/mL)	2.83 (2.51–3.15)	2.00 (1.52–2.61)	2.59 (2.21–3.03)
Maximum bacterial capacity (log ₁₀ cfu/mL)	8.84 (8.64–9.07)	8.90 (8.61–9.23)	8.65 (8.43–8.90)
Growth rate (S) (h ⁻¹)	1.47 (1.11–1.94)	3.66 (2.39–5.14)	1.11 (0.71–1.68)
Growth rate (R) (h ⁻¹)	0.54 (0.43–0.67)	0.69 (0.55–0.86)	0.51 (0.45–0.58)
Mono drug PD parameters			
<i>E</i> _{max} of CAZ on (S) (h ⁻¹)	3.37 (2.72–4.23)	5.28 (3.89–7.15)	2.14 (1.70–2.70)
EC ₅₀ of CAZ on (S) (mg/L)	0.05 (0.04–0.07)	0.0099 (0.0058–0.02)	0.048 (0.038–0.056)
Hill factor of CAZ on (S)	1.48 (0.90–2.41)	0.84 (0.54–1.27)	4.60 (2.34–12.22)
<i>E</i> _{max} of CAZ on (R) (h ⁻¹)	0.74 (0.63–0.88)	0.74 (0.60–0.91)	0.65 (0.58–0.74)
EC ₅₀ of CAZ on (R) (mg/L)	0.08 (0.07–0.10)	0.05 (0.04–0.06)	0.0794 (0.0668–0.0930)
Hill factor of CAZ on (R)	3.45 (2.26–5.18)	2.36 (1.56–3.43)	4.02 (2.40–7.21)
Slope of FOF on (S) (L/mg × h ⁻¹) ^a	2.51 (2.17–2.93)	—	—
<i>E</i> _{max} of FOF on (S) (h ⁻¹) ^a	—	6.39 (5.10–7.97)	3.76 (3.27–4.46)
EC ₅₀ of FOF on (S) (mg/L) ^a	—	0.22 (0.11–0.49)	0.53 (0.38–0.78)
Hill factor of FOF on (S) ^a	0.32 (0.28–0.37)	0.70 (0.49–1.08)	1.00 (0.73–1.41)
<i>E</i> _{max} of FOF on (R) (h ⁻¹)	0.71 (0.60–0.86)	0.84 (0.69–1.00)	0.61 (0.54–0.68)
EC ₅₀ of FOF on (R) (mg/L)	5.07 (4.13–6.18)	4.11 (3.96–4.34)	8.38 (8.09–8.82)
Hill factor of FOF on (R)	2.57 (1.76–3.96)	20 ^b	20 ^b
Interaction model			
Direction of the interaction	CAZ affecting FOF-EC ₅₀ on (R)	FOF affecting CAZ-EC ₅₀ on (R)	CAZ affecting FOF-EC ₅₀ on (R)
Maximum interaction ^d	-0.89 (-0.91– -0.86)	-0.97 (-0.99– -0.95)	-0.91 (-0.98 to -0.82)
EC ₅₀ of the interaction (mg/L)	0.0011 (0.0004–0.0015)	0.51 (0.39–0.63)	0.0182 (0.0115–0.0245)
Hill factor of the interaction	5.28 (2.23–14.75)	2.99 (2.22–4.07)	1.98 (1.27–2.55)
Variability model			
Inter-experimental variability on the inoculum of resistant bacteria (R) (%CV) ^c	35 (31–44)	77 (56–104)	54 (43–69)
Additive residual variability σ on log scale (log ₁₀ cfu/mL)	1.63 (1.55–1.77)	1.95 (1.84–2.18)	1.59 (1.51–1.74)

CAZ, ceftazidime; FOF, fosfomycin. The avibactam concentration was 4 mg/L in all experimental scenarios.

^aFor *E. coli* YAL_AMA the FOF effect on (S) was described as a power function; for *E. coli* JUM_JEA and *E. coli* MER_MIL the FOF effect on (S) was described as a sigmoidal *E*_{max} model.

^bParameter was fixed to a constant.

^c%CV was calculated as follows: %CV = $\sqrt{\exp(\sigma^2) - 1} \times 100\%$.

^dThe in-combination altered drug EC_{50-GPDI} of the victim drug by the GPDI model can be derived as follows: EC_{50-GPDI} = EC₅₀ × (1 + (INT × C^{H-INT} / (EC_{50-INT} × H-INT + C^{H-INT}))). EC₅₀, EC₅₀ of the victim drug; INT, maximum interaction; C, concentration of the perpetrator drug; H-INT, Hill factor of the interaction; EC_{50-INT}, EC₅₀ of the interaction. For small EC_{50-INT} the term can collapse to: EC_{50-GPDI} = EC₅₀ × (1 + INT).

as recommended for susceptibility testing by EUCAST, and ceftazidime/avibactam was treated as one drug in the evaluation of the data. Kristoffersson *et al.*²⁸ and Sy *et al.*²⁹ developed detailed models on the PK and PD interaction of ceftazidime and avibactam. However, due to the fixed concentration, the effect of ceftazidime/avibactam could be modelled as one drug effect, simplifying the complex effects of avibactam, which naturally inhibits ceftazidime degradation by β-lactamases, has a drug effect on bacteria on its own, and enhances the ceftazidime effect.²⁸ Therefore, the developed models are well applicable for the confirmation of the synergy identified in the checkerboard screening.

However, their predictive performance of patient-like dosing regimens will need to be carefully evaluated in subsequent studies, e.g. by inclusion of hollow-fibre experiments.

For fosfomycin, microdilution is not the recommended method for susceptibility testing by EUCAST (breakpoint tables v. 13.0) due to high variability and less accurate results compared with agar dilution.³⁰ Yet, high variability in the results for fosfomycin for the MIC and EC_{50-24h} determination was observed and both susceptibility parameters cannot be compared directly, as for the EC_{50-24h} a higher inoculum and a preincubation was applied. This variability is also displayed by the variability of the MIC and

Kroemer et al.

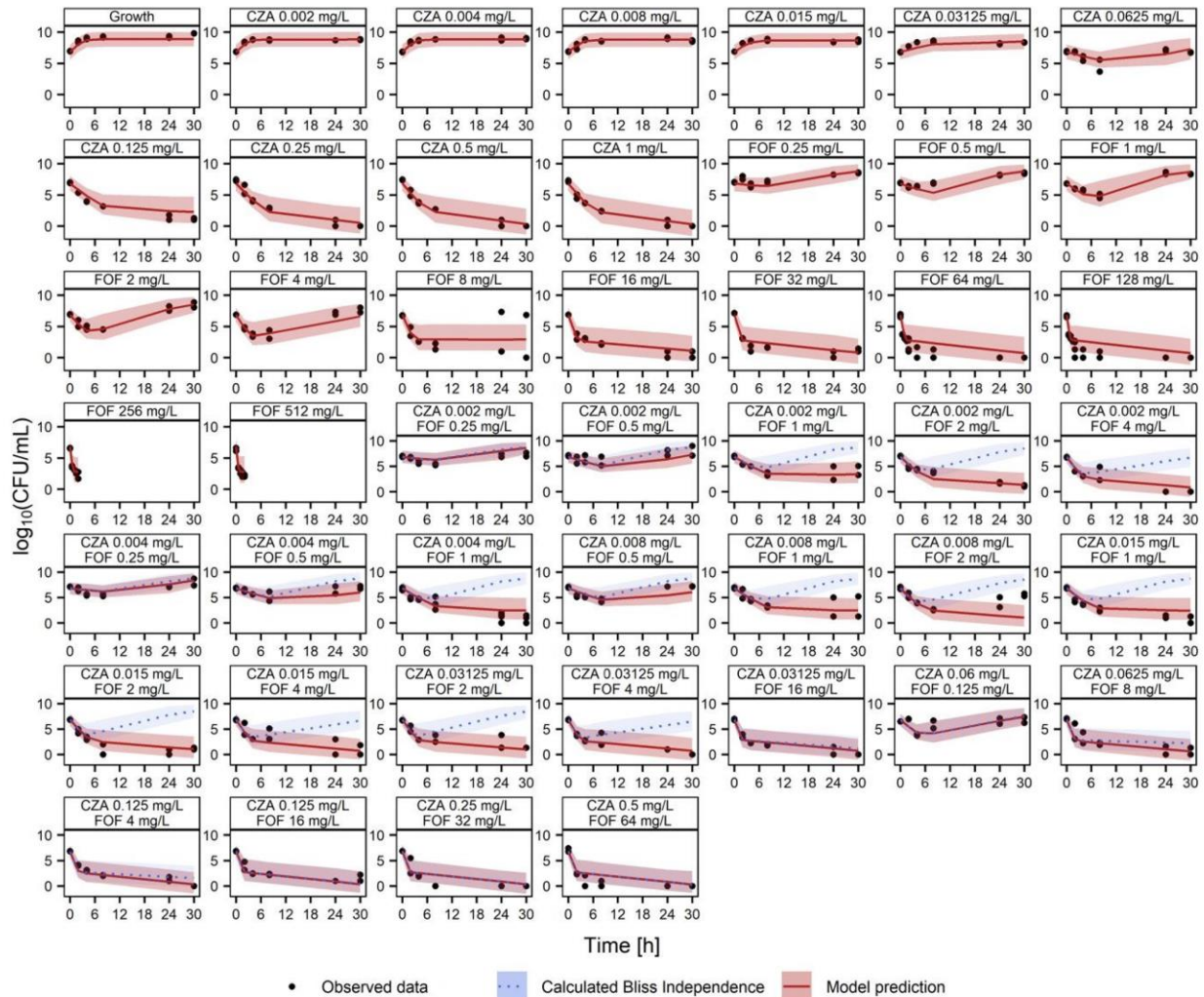


Figure 3. Stratified VPC on the PD model describing the bacterial count \log_{10} cfu/mL of *E. coli* YAL_AMA against ceftazidime/avibactam (CZA) and fosfomycin (FOF) ($MIC_{CZA} = 0.125$ mg/L; $MIC_{FOF} = 16$ mg/L). The avibactam concentration for ceftazidime was fixed to 4 mg/L. Dots: observations; solid line: median prediction; dotted line: expected Bliss independence; shaded areas: 90% prediction intervals. This figure appears in colour in the online version of JAC and in black and white in the print version of JAC.

EC_{50-24h} within the results for the isogenic strains, whereas a relationship between certain β -lactamases and decreased fosfomycin susceptibility cannot be ruled out.

For model-based interaction evaluation in the chequerboards some assumptions were made. Non-interaction drug effects were calculated as Bliss independence. This additivity criterion was chosen because it supports the calculation of combined effects of drugs with independent modes of action, which can be assumed for ceftazidime/avibactam and fosfomycin.

The sparse rhombic experimental layout is designed as a screening tool. Thereby it is able to identify the general fashion of a drug interaction, but the sparse data do not allow estimation of the interaction parameter and interaction potency in parallel.¹² A common simplification of the GPDI model would be the fixation of the potency of the interaction (EC_{50-INT}) to the drug's

EC_{50} . Due to the observed strong synergies this strategy was not sufficient and the potency of the interactions (EC_{50-INT}) had to be fixed to very small values to stabilize the estimation of the interactions. The focus was to rather correctly classify the interactions to synergy, Bliss independence or antagonism. This assumption led to a tendency of the models to underestimate the interaction effect sizes. Additionally, due to these assumptions and the design of the PK/PD models the interaction strengths besides the confirmation of type and direction of the interaction estimated for the chequerboard and time-kill experiments cannot be compared directly.

Overall, the evaluation of the drug interactions identified strong synergies across many different *E. coli* strains, but the screening experiments were only conducted in static PK conditions and *E. coli* isolates susceptible to ceftazidime/avibactam

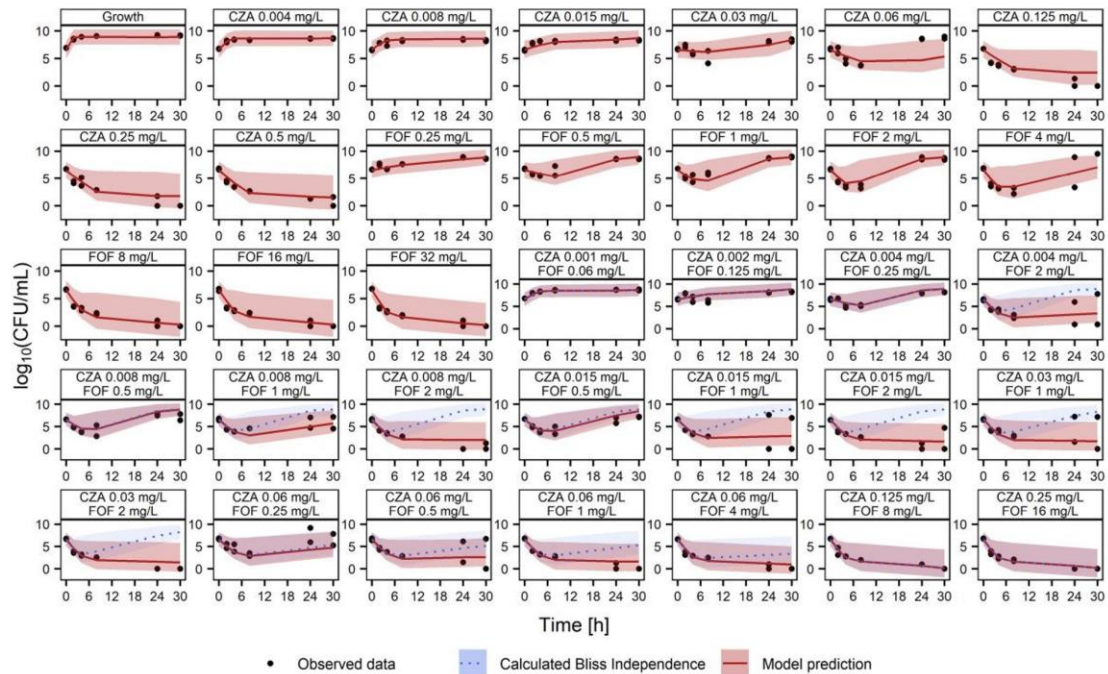
Ceftazidime/avibactam and fosfomycin interactions in *E. coli*

Figure 4. Stratified VPC on the PD model describing the bacterial count \log_{10} cfu/mL of *E. coli* JUM_JEA against ceftazidime/avibactam (CZA) and fosfomycin (FOF) ($MIC_{CZA}=0.06$ mg/L; $MIC_{FOF}=4$ mg/L). The avibactam concentration as supplement for ceftazidime was fixed to 4 mg/L. Dots: observations; solid line: median prediction; dotted line: expected Bliss independence; shaded areas: 90% prediction intervals. This figure appears in colour in the online version of JAC and in black and white in the print version of JAC.

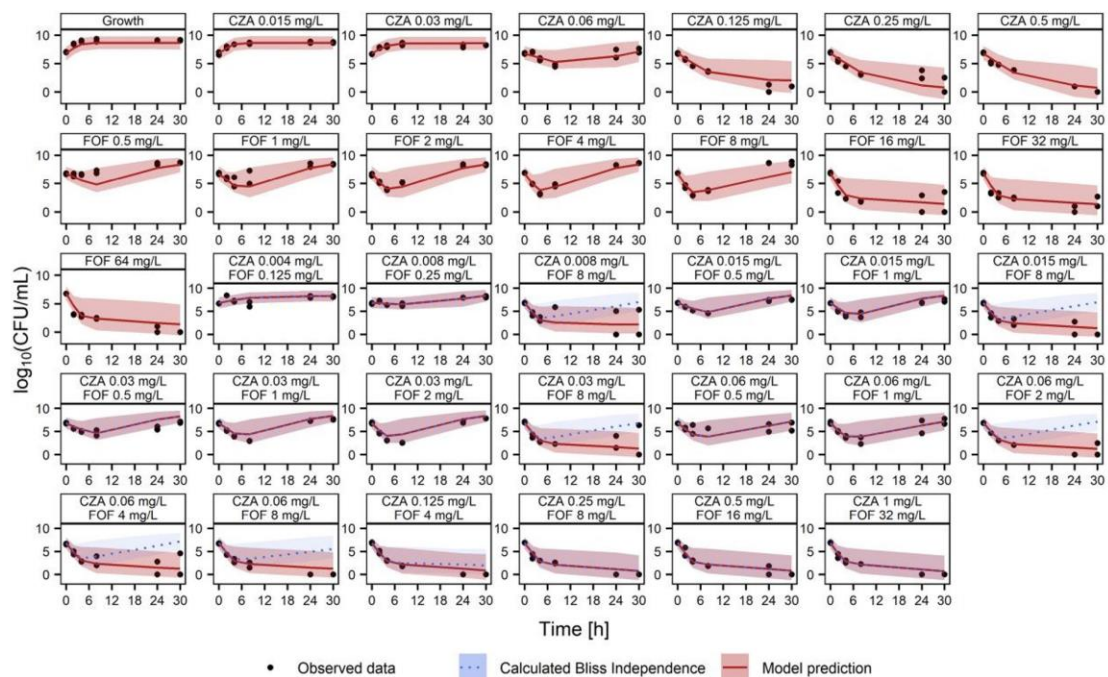


Figure 5. Stratified VPC on the PD model describing the bacterial count \log_{10} cfu/mL of *E. coli* MER_MIL against ceftazidime/avibactam (CZA) and fosfomycin (FOF) ($MIC_{CZA}=0.25$ mg/L; $MIC_{FOF}=8$ mg/L). The avibactam concentration as supplement for ceftazidime was fixed to 4 mg/L. Dots: observations; solid line: median prediction; dotted line: expected Bliss independence; shaded areas: 90% prediction intervals. This figure appears in colour in the online version of JAC and in black and white in the print version of JAC.

Kroemer *et al.***Table 4.** Overview on the identified mutations in selected clinical *E. coli* strains during the checkerboard experiments known to be responsible for fosfomycin resistance

Clinical strain name	Mutant name	Non-synonymous mutations/indels involved in fosfomycin resistance	Reference
<i>E. coli</i> JUM_JEA <i>bla</i> _{OXA-48} , <i>bla</i> _{CTX-M-15}	<i>E. coli</i> _JUM_JEA_clone_16	frameshift in the transcriptional regulatory protein UhpA	Takahata <i>et al.</i> ¹⁹
	<i>E. coli</i> _JUM_JEA_clone_18	premature stop codon (Y399X) in <i>uhpB</i>	Cattoir <i>et al.</i> ²⁰
	<i>E. coli</i> _JUM_JEA_clone_24	Δ76 bp deletion in hexose-6-phosphate:phosphate antiporter	Falagas <i>et al.</i> ⁷
	<i>E. coli</i> _JUM_JEA_clone_25	mutation in <i>uhpB</i>	Cattoir <i>et al.</i> ²⁰
	<i>E. coli</i> _JUM_JEA_clone_26	missense mutation in <i>glpT</i> Δ76 bp deletion in hexose-6-phosphate:phosphate antiporter	Cattoir <i>et al.</i> ²⁰
<i>E. coli</i> MER_MIL <i>bla</i> _{OXA-48} , <i>bla</i> _{TEM-1B}	<i>E. coli</i> _MER_MIL_clone_57	stop mutation in <i>uhpB</i>	Cattoir <i>et al.</i> ²⁰
	<i>E. coli</i> _MER_MIL_clone_62	disruptive in-frame deletion (<i>cyoA</i> —adenylate cyclase)	Falagas <i>et al.</i> ⁷
<i>E. coli</i> YAL_AMA <i>bla</i> _{OXA-244} , <i>bla</i> _{CTX-M-15}	<i>E. coli</i> _YAL_AMA_clone_89	Coding mutation in <i>ptsI</i> deletion in hexose-6-phosphate:phosphate antiporter	Falagas <i>et al.</i> ⁷
	<i>E. coli</i> _YAL_AMA_clone_94	deletion in <i>uhpT</i> frameshift in <i>ptsI</i>	Falagas <i>et al.</i> ⁷

and/or fosfomycin. A further evaluation of the identified synergy of ceftazidime/avibactam and fosfomycin in additional (double-) resistant strains is reasonable to evaluate the combination for potential resensitization and successful therapy of resistant pathogens against monotherapy. For a translation of the synergistic effects of ceftazidime/avibactam and fosfomycin into a clinical setting, dynamic hollow-fibre infection model studies could be utilized. Those studies mimicking human pharmacokinetics could add additional insights to simulate dosing regimens *in vitro* and develop a rationale for optimal application of the antibiotic combination therapy of ceftazidime/avibactam and fosfomycin. Additionally, dynamic experiments are needed to elucidate the impact of avibactam on the synergy of ceftazidime and fosfomycin. So far, clinical evidence on the translatability of the synergy into the clinics is lacking, but case reports indicate positive treatment outcomes of the combination therapy.³¹ In the clinical setting, broad synergistic drug interactions could be beneficial as in infections one defined strain can not always be identified.²⁶ Additionally, the observed suppression of development of resistances could contribute to expand the lifecycle of ceftazidime/avibactam as a therapeutic option until resistances are spread widely. With respect to fosfomycin, the strong synergistic effect sizes and reduced emergence of resistant subpopulations could enable a repurposing of this older drug, when resistances already occur. Generally, the observed strong synergistic effects could ensure sufficient therapeutic effect sizes at reduced target site concentrations or in critically ill patients with altered pharmacokinetics and reduced drug exposures. To ultimately utilize these benefits clinically, innovative combination dosing regimens with loading doses or reduced daily doses in order to decrease adverse effects could be conceivable.

Conclusions

The *in vitro* interaction screening coupled with GPDI model-based evaluation techniques identified synergistic interactions in 10 out of 14 evaluated clinical and isogenic *E. coli* strains. Ceftazidime/avibactam was mostly identified to enhance the fosfomycin potency and hence inhibit the regrowth compared with when fosfomycin would be used as single treatment. These *in vitro* results

confirm the potential for the clinical use of ceftazidime/avibactam and fosfomycin to increase efficacy and improve the treatment outcome.

Acknowledgements

Parts of the results were presented as poster presentations at the 31st European Congress of Clinical Microbiology and Infectious Diseases (ECCMID), virtual meeting (9–12 July 2021, abstract number 2117), Population Approach Group Europe (PAGE) meeting 2022, Ljubljana, Slovenia (28 June–1 July 2022, abstract number: 10127) and the 32nd International Congress of Antimicrobial Chemotherapy (ICC) 2022, Perth, Australia (27–30 November 2022, abstract number: 34).

Funding

This project resulted from a German-French research cooperation called ‘CO-PROTECT’ and was supported by a grant from the Federal Ministry of Education and Research (BMBF), Germany (grant agreement number 16GW0249K), and by a grant from the National Agency of Research (ANR), France (grant agreement number R19094GG).

Transparency declarations

None to declare.

Supplementary data

Figures S1 and S2 and Supplementary Texts S1–S5 are available as Supplementary data at JAC Online.

References

- Cassini A, Högberg LD, Plachouras D *et al.* Attributable deaths and disability-adjusted life-years caused by infections with antibiotic-resistant bacteria in the EU and the European economic area in 2015: a population-level modelling analysis. *Lancet Infect Dis* 2019; **19**: 56–66. [https://doi.org/10.1016/S1473-3099\(18\)30605-4](https://doi.org/10.1016/S1473-3099(18)30605-4)
- Tängdén T, Giske CG. Global dissemination of extensively drug-resistant carbapenemase-producing Enterobacteriaceae: clinical perspectives on

Ceftazidime/avibactam and fosfomycin interactions in *E. coli*

- detection, treatment and infection control. *J Intern Med* 2015; **277**: 501–12. <https://doi.org/10.1111/joim.12342>
- 3** Tyers M, Wright GD. Drug combinations: a strategy to extend the life of antibiotics in the 21st century. *Nat Rev Microbiol* 2019; **17**: 141–55. <https://doi.org/10.1038/s41579-018-0141-x>
- 4** Shields RK, Potoski BA, Haidar G *et al.* Clinical outcomes, drug toxicity, and emergence of ceftazidime-avibactam resistance among patients treated for carbapenem-resistant Enterobacteriaceae infections. *Clin Infect Dis* 2016; **63**: 1615–8. <https://doi.org/10.1093/cid/ciw636>
- 5** Bassetti M, Graziano E, Berruti M *et al.* The role of fosfomycin for multidrug-resistant gram-negative infections. *Curr Opin Infect Dis* 2019; **32**: 617–25. <https://doi.org/10.1097/QCO.0000000000000597>
- 6** Portier H, Kazmierczak A, Lucht F *et al.* Cefotaxime in combination with other antibiotics for the treatment of severe methicillin-resistant staphylococcal infections. *Infection* 1985; **13** Suppl 1: S123–8. <https://doi.org/10.1007/BF01644232>
- 7** Falagas ME, Vouloumanou EK, Samonis G *et al.* Fosfomycin. *Clin Microbiol Rev* 2016; **29**: 321–47. <https://doi.org/10.1128/CMR.00068-15>
- 8** Mikhail S, Singh NB, Kebriaei R *et al.* Evaluation of the synergy of ceftazidime-avibactam in combination with meropenem, amikacin, aztreonam, colistin, or fosfomycin against well-characterized multidrug-resistant *Klebsiella pneumoniae* and *Pseudomonas aeruginosa*. *Antimicrob Agents Chemother* 2019; **63**: 1–10. <https://doi.org/10.1128/AAC.00779-19>
- 9** Wicha SG, Kees MG, Kuss J *et al.* Pharmacodynamic and response surface analysis of linezolid or vancomycin combined with meropenem against *Staphylococcus aureus*. *Pharm Res* 2015; **32**: 2410–8. <https://doi.org/10.1007/s11095-015-1632-3>
- 10** Wicha SG, Chen C, Clewe O *et al.* A general pharmacodynamic interaction model identifies perpetrators and victims in drug interactions. *Nat Commun* 2017; **8**: 2129. <https://doi.org/10.1038/s41467-017-01929-y>
- 11** CLSI. *Methods for Dilution Antimicrobial Susceptibility Tests for Bacteria That Grow Aerobically; Approved Standard—Ninth Edition: M07*. 2012.
- 12** Kroemer N, Aubry R, Couet W *et al.* Optimized rhombic experimental dynamic checkerboard designs to elucidate pharmacodynamic drug interactions of antibiotics. *Pharm Res* 2022; **39**: 3267–77. <https://doi.org/10.1007/s11095-022-03396-7>
- 13** Bourrel AS, Poirel L, Royer G *et al.* Colistin resistance in Parisian inpatient faecal *Escherichia coli* as the result of two distinct evolutionary pathways. *J Antimicrob Chemother* 2019; **74**: 1521–30. <https://doi.org/10.1093/jac/dkz090>
- 14** Deatherage DE, Barrick JE. Identification of mutations in laboratory-evolved microbes from next-generation sequencing data using breseq. In: Sun L, Shou W, eds. *Engineering and Analyzing Multicellular Systems*. Vol. 1151. Methods in Molecular Biology. Springer, 2014; 165–88. https://link.springer.com/10.1007/978-1-4939-0554-6_12.
- 15** R Core Team. R: A Language and Environment for Statistical Computing. 2021.
- 16** Bliss CI. The toxicity of poisons applied jointly. *Ann Appl Biol* 1939; **26**: 585–615. <https://doi.org/10.1111/j.1744-7348.1939.tb06990.x>
- 17** Akaike H. A new look at the statistical model identification. *IEEE Trans Autom Control* 1974; **19**: 716–23. <https://doi.org/10.1109/TAC.1974.1100705>
- 18** Dosne AG, Bergstrand M, Harling K *et al.* Improving the estimation of parameter uncertainty distributions in nonlinear mixed effects models using sampling importance resampling. *J Pharmacokinetic Pharmacodyn* 2016; **43**: 583–96. <https://doi.org/10.1007/s10928-016-9487-8>
- 19** Takahata S, Ida T, Hiraishi T *et al.* Molecular mechanisms of fosfomycin resistance in clinical isolates of *Escherichia coli*. *Int J Antimicrob Agents* 2010; **35**: 333–7. <https://doi.org/10.1016/j.ijantimicag.2009.11.011>
- 20** Cattoir V, Pourbaix A, Magnan M *et al.* Novel chromosomal mutations responsible for fosfomycin resistance in *Escherichia coli*. *Front Microbiol* 2020; **11**: 575031. <https://doi.org/10.3389/fmicb.2020.575031>
- 21** Kastoris AC, Rafailidis PI, Vouloumanou EK *et al.* Synergy of fosfomycin with other antibiotics for Gram-positive and Gram-negative bacteria. *Eur J Clin Pharmacol* 2010; **66**: 359–68. <https://doi.org/10.1007/s00228-010-0794-5>
- 22** Avery LM, Sutherland CA, Nicolau DP. *In vitro* investigation of synergy among fosfomycin and parenteral antimicrobials against carbapenemase-producing Enterobacteriaceae. *Diagn Microbiol Infect Dis* 2019; **95**: 216–20. <https://doi.org/10.1016/j.diagmicrobio.2019.05.014>
- 23** Romanelli F, De Robertis A, Carone G *et al.* *In vitro* activity of ceftazidime/avibactam alone and in combination with fosfomycin and carbapenems against KPC-producing *Klebsiella pneumoniae*. *New Microbiol* 2020; **43**: 136–8.
- 24** Li X-Z, Plésiat P, Nikaido H. The challenge of efflux-mediated antibiotic resistance in Gram-negative bacteria. *Clin Microbiol Rev* 2015; **28**: 337–418. <https://doi.org/10.1128/CMR.00117-14>
- 25** Dijkmans AC, Zacarias NVO, Burggraaf J *et al.* Fosfomycin: pharmacological, clinical and future perspectives. *Antibiotics* 2017; **6**: 24. <https://doi.org/10.3390/antibiotics6040024>
- 26** Couet W. Pharmacokinetics/pharmacodynamics characterization of combined antimicrobial agents: a real challenge and an urgent need. *Clin Microbiol Infect* 2018; **24**: 687–8. <https://doi.org/10.1016/j.cmi.2018.03.047>
- 27** Odds FC. Synergy, antagonism, and what the checkerboard puts between them. *J Antimicrob Chemother* 2003; **52**: 1. <https://doi.org/10.1093/jac/dkg301>
- 28** Kristoffersson AN, Bissantz C, Okujava R *et al.* A novel mechanism-based pharmacokinetic-pharmacodynamic (PKPD) model describing ceftazidime/avibactam efficacy against β -lactamase-producing Gram-negative bacteria. *J Antimicrob Chemother* 2020; **75**: 400–8. <https://doi.org/10.1093/jac/dkz440>
- 29** Sy SKB, Zhuang L, Xia H *et al.* A mathematical model-based analysis of the time-kill kinetics of ceftazidime/avibactam against *Pseudomonas aeruginosa*. *J Antimicrob Chemother* 2018; **73**: 1295–304. <https://doi.org/10.1093/jac/dkx537>
- 30** Mojica MF, De La Cadena E, Hernández-Gómez C *et al.* Performance of disk diffusion and broth microdilution for fosfomycin susceptibility testing of multidrug-resistant clinical isolates of Enterobacteriales and *Pseudomonas aeruginosa*. *J Glob Antimicrob Resist* 2020; **21**: 391–5. <https://doi.org/10.1016/j.jgar.2020.01.003>
- 31** Gatti M, Giannella M, Rinaldi M *et al.* Pharmacokinetic/pharmacodynamic analysis of continuous-infusion fosfomycin in combination with extended-infusion cefiderocol or continuous-infusion ceftazidime-avibactam in a case series of difficult-to-treat resistant *Pseudomonas aeruginosa* bloodstream infections and/or hospital-acquired pneumonia. *Antibiot Basel Switz* 2022; **11**: 1739. <https://doi.org/10.3390/antibiotics11121739>

3.3 Publication III

**Pharmacokinetic/pharmacodynamic analysis of
ceftazidime/avibactam and fosfomycin combinations in an
in vitro hollow fiber infection model against multidrug-resistant
*Escherichia coli***

Niklas Kroemer, Lisa F. Amann, Aneeq Farooq, Christoph Pfaffendorf,
Miklas Martens, Jean-Winoc Decousser, Nicolas Grégoire,
Patrice Nordmann, Sebastian G. Wicha

Microbiology Spectrum (2024)

Impact Factor: 3.7 (2022)

Synopsis

The screening performed in Publication II (see 3.2) identified synergistic interactions of ceftazidime/avibactam and fosfomycin in a variety of isogenic and clinical *E. coli* strains. However, the evaluation came along with some limitations with regard to the direct translation of the findings into the clinical setting. In essence, the applied assays were conducted with static standard concentrations. Additionally, independent bactericidal effects of avibactam alone and the potentiation of ceftazidime mediated by avibactam was neglected. Hence, the study conducted in Publication III aimed to develop a clinical perspective of the synergy by translation of the observed interactions from static into dynamic pharmacokinetic conditions. Firstly, static time kill experiments were conducted to update the semi-mechanistic time kill model developed for Publication II with the interaction of ceftazidime and avibactam. Secondly, dynamic Hollow Fiber experiments mimicked mono and combination therapies of clinical and subtherapeutic doses to fully elucidate the synergistic drug interactions of ceftazidime, avibactam and fosfomycin. The data on the bacterial dynamics were used to expand the PK/PD model by description of the emergence of phenotypically resistant subpopulations. Simulations revealed the full potential of the synergy to allow for clinical dose reductions. In particular, a combination of simulated doses of 0.5 g q8h fosfomycin and 0.25/0.06 g q8h ceftazidime/avibactam led to the same outcome as a respective monotherapy of 6 g q8h fosfomycin or 1.5/0.375 g q8h ceftazidime/avibactam representing the possibility of twelve-fold and six-fold dose reductions for fosfomycin and ceftazidime/avibactam, respectively.

Thus, the study confirmed the clinical potential of the combination therapy and encourages to additionally optimise combined dosing regimens and include resistant strains to proof the hypothesis for the potential of re-sensitisation.



Antimicrobial Chemotherapy | Research Article

Pharmacokinetic/pharmacodynamic analysis of ceftazidime/avibactam and fosfomycin combinations in an *in vitro* hollow fiber infection model against multidrug-resistant *Escherichia coli*

Niklas Kroemer,¹ Lisa F. Amann,¹ Aneeq Farooq,¹ Christoph Pfaffendorf,¹ Miklas Martens,¹ Jean-Winoc Decousser,² Nicolas Grégoire,^{3,4,5} Patrice Nordmann,⁶ Sebastian G. Wicha¹

AUTHOR AFFILIATIONS See affiliation list on p. 11.

ABSTRACT Rational combination therapy offers a valuable option to increase efficacy and prevent emergence of resistance. Therefore, this study provides a translational pharmacokinetic/pharmacodynamic analysis of the synergy of /avibactam and fosfomycin in a clinical *Escherichia coli* strain expressing extended spectrum beta-lactamase (CTX-M-15 and TEM-4) and carbapenemase (OXA-244) genes. Detailed static time-kill experiments primed dynamic hollow fiber studies mimicking mono- and combination therapies with doses of ceftazidime/avibactam ranging from 0.06/0.015 to 2/0.5 g every 8 h (q8h) and doses of fosfomycin ranging from 0.125 to 6 g q8h. The drug effects and interactions were quantitatively evaluated by pharmacokinetic/pharmacodynamic modeling using semi-mechanistic and subpopulation synergy. A pharmacokinetic/pharmacodynamic model describing the effects of ceftazidime, avibactam, and fosfomycin and their synergy was developed from the static time-kill experiments and hollow fiber studies. Simulations revealed that combined doses as low as 0.5-g q8h fosfomycin and 0.25-/0.06-g q8h ceftazidime/avibactam lead to suppression of the bacterial count. Conversely, in monotherapy, substantially higher doses by a factor of 12 for fosfomycin (6 g q8h) or by a factor of 6 for ceftazidime/avibactam (1.5/0.375 g q8h) were needed to achieve a comparable killing over 72 h. The combination of ceftazidime/avibactam and fosfomycin was therefore shown to be highly synergistic and suppressed the emergence of resistances. Clinical evaluations of potential dose reductions or the possibility to treat strains with high-level resistance with this combination are warranted.

IMPORTANCE Mechanistic understanding of pharmacodynamic interactions is key for the development of rational antibiotic combination therapies to increase efficacy and suppress the development of resistances. Potent tools to provide those insights into pharmacodynamic drug interactions are semi-mechanistic modeling and simulation techniques. This study uses those techniques to provide a detailed understanding with regard to the direction and strength of the synergy of ceftazidime-avibactam and ceftazidime-fosfomycin in a clinical *Escherichia coli* isolate expressing extended spectrum beta-lactamase (CTX-M-15 and TEM-4) and carbapenemase (OXA-244) genes. Enhanced killing effects in combination were identified as a driver of the synergy and were translated from static time-kill experiments into the dynamic hollow fiber infection model. These findings in combination with a suppression of the emergence of resistance in combination emphasize a potential clinical benefit with regard to increased efficacy or to allow for dose reductions with maintained effect sizes to avoid toxicity.

KEYWORDS PK/PD, drug interactions, ceftazidime/avibactam, fosfomycin, synergy, hollow fiber infection model, *Escherichia coli*

Editor Tomefa E. Asempa, Hartford Hospital, Hartford, Connecticut, USA

Address correspondence to Sebastian G. Wicha, Sebastian.wicha@uni-hamburg.de.

The authors declare no conflict of interest.

See the funding table on p. 11.

Received 24 October 2023

Accepted 10 November 2023

Published 8 December 2023

Copyright © 2023 Kroemer et al. This is an open-access article distributed under the terms of the [Creative Commons Attribution 4.0 International license](https://creativecommons.org/licenses/by/4.0/).

The emergence of carbapenemase- and extended spectrum beta-lactamase (ESBL)-producing *Escherichia coli* and Enterobacterales, in general, is a threat to global health (1, 2). Besides the development of new antibiotics, rational combination therapy using marketed antibiotics is an option to increase efficacy due to synergistic interactions or to suppress the development of resistance and prolong the lifecycle of new agents (2).

A frequently evaluated drug for this purpose is fosfomycin (FOF) that has shown its synergistic potential in combination with other cell wall-interfering agents (3–5). Also, ceftazidime/avibactam (CZA) has already shown synergy for treating various multidrug-resistant Enterobacterales and *Pseudomonas aeruginosa* strains (6–8). Additionally, the common indications of CZA and FOF such as complicated intra-abdominal infections or urinary tract infections and hospital-acquired pneumonia, including ventilator-associated pneumonia, offer their use in combination. However, an evaluation on the clinical relevance of their drug interaction is lacking, and it remains unclear if the synergy could be exploited for dose reductions.

Pharmacokinetic/pharmacodynamic (PKPD) modeling is a state-of-the-art technique to translate the results from preclinical studies into the clinical setting (9, 10). With regard to drug combinations, PKPD models provide a semi-mechanistic understanding and quantification of drug interactions.

Hence, in this study, detailed static time-kill experiments were performed to elucidate the drug interactions of ceftazidime, avibactam, and FOF and evaluated by semi-mechanistic PKPD modeling. The model was then used to transfer the drug interactions into conceptual dynamic hollow fiber infection model (HFIM) experiments mimicking clinically achievable pharmacokinetics. Simulations were subsequently used to evaluate the potential for dose reductions in a combination therapy.

RESULTS

Bacterial isolate and susceptibility

The MICs against ceftazidime, CZA, and FOF of the clinical *E. coli* used in this study were 16, 0.125, and 16/0.5 mg/L (microdilution/agar dilution), respectively, and, therefore, classified as susceptible to CZA and FOF and resistant to ceftazidime alone according to the European Committee on Antimicrobial Susceptibility Testing (EUCAST) (11). Sequencing identified genes coding for CTX-M-15, TEM-4, and OXA-244 (OXA-48-like).

Static time-kill experiments

Strong synergistic drug interactions were observed in the static time-kill experiments leading to enhanced killing effects in combination. In detail, concentrations of 128-mg/L ceftazidime or 16-mg/L FOF alone were required to achieve reproducible suppression of bacterial growth over 30 h, and no evaluated concentration of avibactam alone led to killing effects (Fig. 1). In contrast, combinations of 0.125-/4-mg/L CZA were efficacious. In combination with 2-mg/L FOF, even lower concentrations of CZA (0.002/4 mg/L) were sufficient to suppress the bacterial growth over 30 h.

Dynamic HFIM

In the HFIM experiments, doses ranging from 6- to 0.125-g every 8 h (q8h) FOF and 2-/0.5- to 0.06-/0.015-g q8h CZA were mimicked. A dose of 1-g q8h FOF was the highest exposure tested not being able to reduce the bacterial count to or below the lower limit of quantification and prevent regrowth. Utilizing CZA in monotherapy, simulated doses of 0.5/0.125 g q8h displayed the highest exposure not suppressing regrowth. In combination, quarters of those doses (CZA 0.125/0.03 g q8h and FOF 0.25 g q8h) still achieved killing effects (Fig. 2). Below a certain exposure, a rapid emergence of 3× MIC FOF-resistant bacteria was observed within the first 12 h of experiment. On opposite, phenotypic resistance against 3× MIC CZA emerged later between 24 and 48 h.

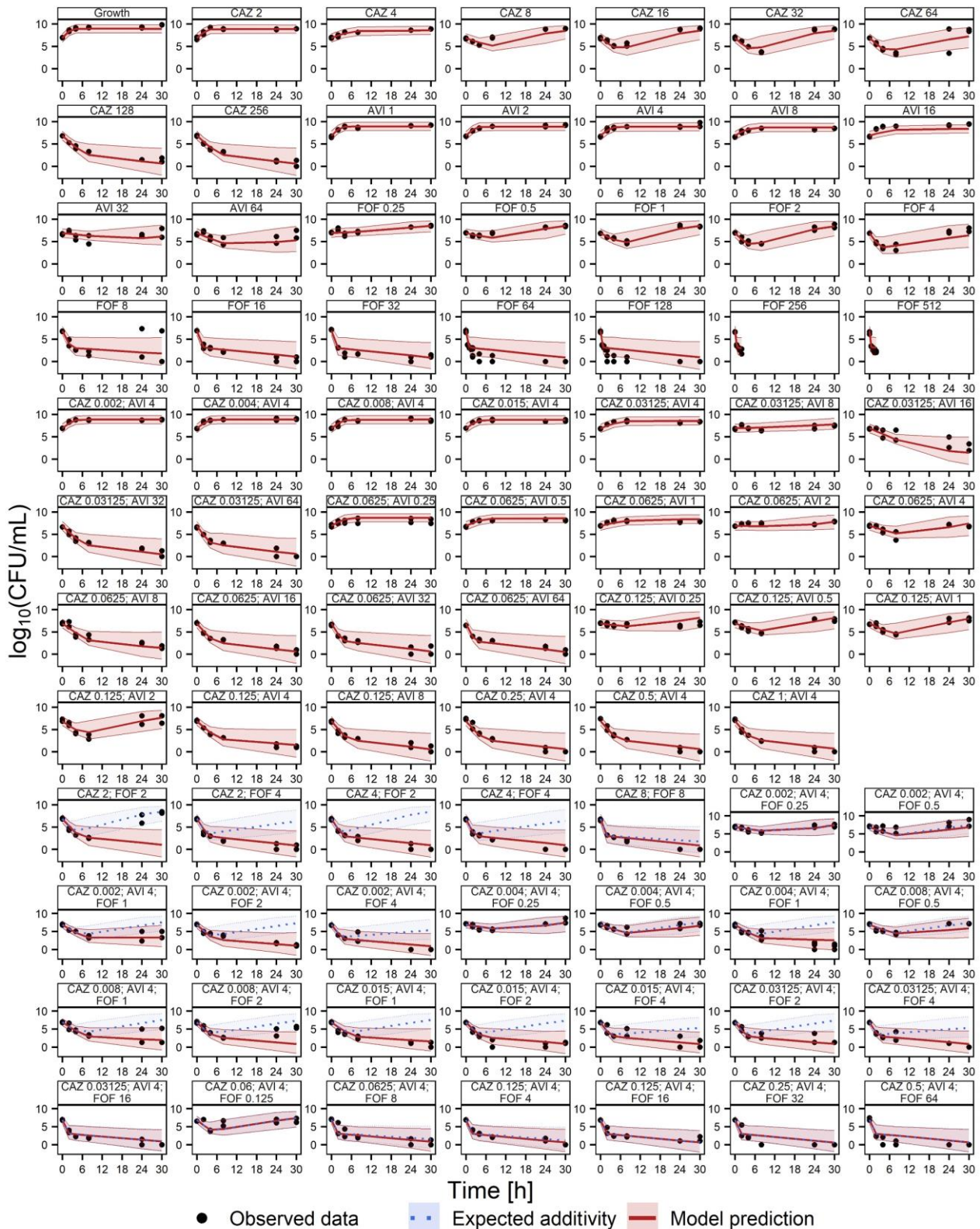


FIG 1 Stratified VPC ($n = 1,000$) on the static pharmacodynamic time-kill experiment model describing the bacterial count in \log_{10} (CFU/mL) of the clinical *E. coli* isolate against ceftazidime (CAZ), avibactam (AVI), and FOF. Respective concentrations of the scenarios are given in milligrams per liter. Dots, observations; solid line, median prediction; dotted line, expected bliss independence; shaded areas, 90% prediction intervals.

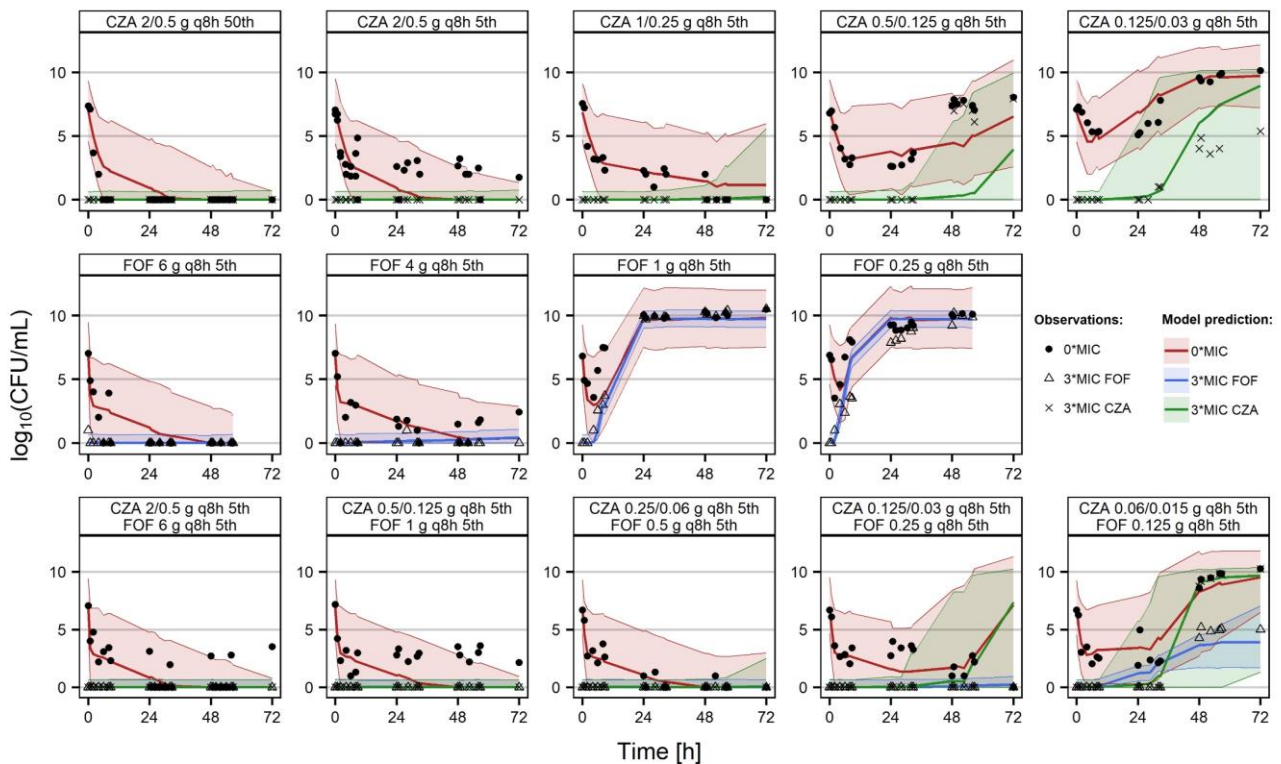


FIG 2 Stratified VPC ($n = 1,000$) on the PKPD model describing the bacterial count in \log_{10} (CFU/mL) of the hollow fiber experiments of the clinical *E. coli* isolate against CZA and FOF ($MIC_{CZA} = 0.125$ mg/L; $MIC_{FOF} = 16$ mg/L). The percentiles (50th or 5th) of the doses correspond to the distribution of pharmacokinetic profiles, which would be expected from simulations of 1,000 patients given the defined dose. Dots, observations of different subpopulations; solid line, median prediction of different subpopulations; shaded areas, 90% prediction intervals of different subpopulations.

The bioanalytical quantification of ceftazidime, avibactam, and FOF confirmed that the planned pharmacokinetic profiles in the HFIM experiment were adequately mimicked (Fig. S1). Therefore, the nominal pharmacokinetics were used for modeling and simulations of the HFIM data.

PKPD modeling to quantify synergy and the tripartite effect relationship between CZA and FOF

The effects of ceftazidime, avibactam, and FOF in the static time-kill curves were well described by a two-compartment model with a susceptible and a joint resistant subpopulation against CZA and FOF (Fig. 3). The individual bacterial killing effects against both subpopulations were mainly implemented as sigmoidal maximum effect models. Power models were only used to describe the drug effects of FOF on the susceptible subpopulation and of avibactam on the resistant subpopulation (Text S5). The general pharmacodynamic interaction (GPDl) model was able to capture synergies beyond bliss independence (12). In detail, those drug interactions were described best by a reduction of the EC_{50} on the susceptible and resistant populations of ceftazidime by avibactam by >99% and a reduction of the EC_{50} on the resistant population of FOF by ceftazidime by >99%. Interexperimental variability was implemented as exponential interindividual variability on the inoculum of the resistant population and on its growth rate. Visual predictive checks (VPCs) confirmed a high predictive performance of the static time-kill experiments (Fig. 1) but revealed a lack of predictability of the dynamic HFIM data, especially with regard to the rapid regrowth in the early phase of the experiments (0–12 h) or later when less susceptible subpopulations emerged and drove the regrowth profile (>30 h) (Fig. S2). Therefore, the model was further developed to fit the HFIM data by the addition of compartments describing the 3× MIC-resistant

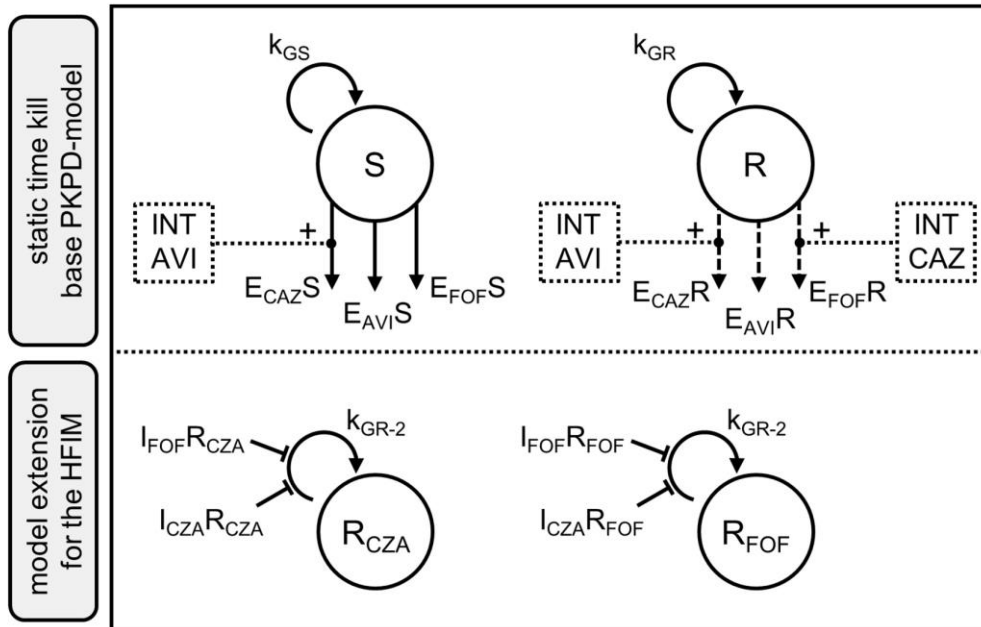


FIG 3 PKPD model structure combining elements of semi-mechanistic and subpopulation synergy. Upper part: model describing the static time-kill experiments. Lower part: model extension on the dynamic hollow fiber data. AVI, avibactam; CAZ, ceftazidime; CFU, sum of $S + R$ (static time-kill curves) or sum of $S + R + R_{CZA} + R_{FOF}$ (HFIM data); E_{CAZS} , E_{AVIS} , E_{FOFS} , effects on the susceptible bacteria by the respective drugs; E_{CAZR} , E_{AVIR} , E_{FOFR} , effects on the resistant bacteria by the respective drugs; $I_{CZAR_{FOF}}$, $I_{FOFR_{FOF}}$, growth inhibition of the phenotypic FOF less susceptible bacteria by the respective drugs; $I_{FOFR_{CZA}}$, $I_{CZAR_{CZA}}$, growth inhibition of the phenotypic CZA less susceptible bacteria by the respective drugs; INT, interaction; k_{GR} , growth rate of the resistant bacteria; k_{GR-2} , growth rate of the phenotypic-resistant bacteria; k_{GS} , growth rate of the susceptible bacteria; R_{CZA} , R_{FOF} , phenotypic-resistant bacteria against the respective drugs. Dotted line, interaction direction; bold arrow, drug effects on the susceptible bacteria; dashed arrow, drug effects on the resistant bacteria; inhibition arrow, growth inhibition.

subpopulations and the suppression of those resistances in combination via subpopulation synergy (Fig. 2 and 3). Interexperimental differences in the regrowth behavior were captured by exponential interindividual variability on the inoculum of the resistant population and on the inoculum of the CZA less susceptible subpopulation. Details on the results of the modeling and the full-model parameters can be obtained from Text S5 and Tables S3 and S4.

PKPD simulations to translate the synergy between CZA and FOF in the clinical perspective

The dose-response surface of the simulations of additional HFIM experiments revealed the possibility for a dose reduction in combination to achieve the same outcome as the monotherapy (Fig. 4). In particular, a combination of 0.5-g q8h FOF and 0.25-/0.06-g q8h CZA would lead to a suppression of the bacterial count, while a 12 times higher dose of FOF (6 g q8h) or a six times higher dose of CZA (1.5/0.375 g q8h) would lead to the same effects in monotherapy.

DISCUSSION

This PKPD study translated the strong synergy of CZA and FOF in a representative multidrug-resistant clinical *E. coli* from static into dynamic pharmacokinetic conditions. In opposite to an endpoint-driven evaluation of drug interactions, this study follows a translational approach based on clinical pharmacokinetics and evaluates the synergy of CZA and FOF in wide dose ranges with outcomes from suppression to regrowth of

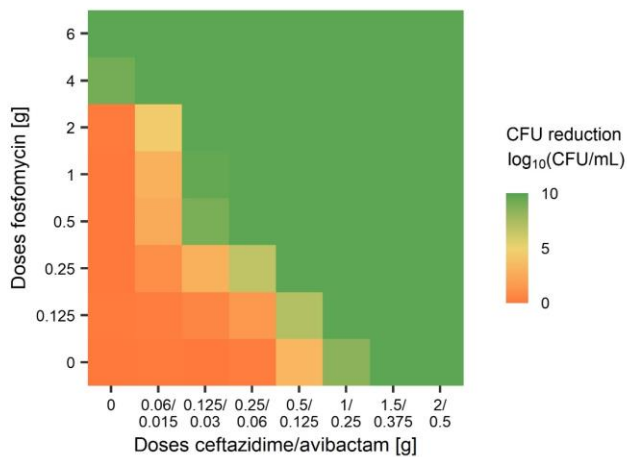


FIG 4 Dose-response surface of the outcome of hollow fiber experiments simulated with the dynamic PKPD model. Effect sizes are calculated as \log_{10} (CFU/mL) reductions compared to no treatment after 72 h.

bacteria in static and dynamic time-kill experiments (13). Concentration-dependent emergence of resistance was identified as a missing link for the translation from static time kill to the HFIM. The emergence of resistance in the HFIM as well as the regrowth of bacteria after an initial decay in the static time-kill experiments occurred within the first 2 days of the experiments. This emphasizes the importance of an efficacious treatment away from the start of therapy. However, it cannot be ruled out that also doses suppressing the regrowth for 72 h would have allowed a delayed regrowth as a total eradication of bacteria was not investigated. Nevertheless, the suppression of the emergence of resistance in the static time-kill experiments as well as in the HFIM played a major role in the increased efficacy of the antibiotic drug combination and could potentially be explained by collateral sensitivity mechanisms and increased uptake of antibiotics when cell wall-interfering drugs are combined or by suppressed mutation frequencies (14–16). Commonly, higher mutation frequencies against FOF than against CZA are reported in Enterobacterales (17, 18). This nature was already confirmed for the evaluated *E. coli* in this study (*E. coli* YAL_AMA in Kroemer et al. (8)). Additionally, reduced mutation frequencies were identified against the combination of CZA and FOF. This is in line with the observed earlier resistance development against FOF in the hollow fiber experiments and, therefore, the significantly higher estimate of the inoculum of the phenotypically less susceptible subpopulation compared to CZA. The lower resistance development against CZA was additionally subjected to a higher variability. Therefore, interexperimental variability was needed in the model to describe the data. This led to relatively wide prediction intervals in the VPC plots covering the observed less susceptible bacteria against CZA. When implementing avibactam in PKPD models with ceftazidime, three major modes of action are conceivable: (i) own killing effect, (ii) potentiation of the ceftazidime effect, and (iii) suppression of beta-lactamase-mediated ceftazidime degradation. PKPD models have been developed including those three mechanisms (19, 20). In the present study, the bioanalysis identified no degradation of ceftazidime in the presence of the avibactam concentrations studied. Therefore, a permanent inhibition of the beta-lactamases by avibactam was assumed in this study, and a concentration-dependent inhibition was not implemented in the model. To reduce the complexity of the model, the avibactam effects were also simplified when modeling the suppression of the less susceptible subpopulations, and the combined suppressive effect of CZA was only described as a function of the ceftazidime concentrations. The results of the hollow fiber study and the simulations with the PKPD model emphasize enhanced killing effects leading to maintained high drug effects in combination at subinhibitory monotherapy exposures. This offers different potential benefits of a rational combination therapy. A

rational combination therapy exploiting the synergistic effects could use lower doses while still being efficacious. Thereby, reduced drug exposures would avoid concentration-driven adverse effects such as neurotoxicity mediated by ceftazidime or hypokalemia mediated by FOF. In the presented study, the enhanced killing effects also prevented regrowth and the emergence of resistance. Thereby, also the combination of CZA and FOF against susceptible bacteria can be used to prolong the shelf life of CZA before resistances occur. Additionally, combination therapy could ensure maintained target site efficacy in critically ill patients with reduced drug exposures or altered target site pharmacokinetics. Lastly, synergistic drug effects could also contribute in re-sensitizing *E. coli* strains that are already resistant against monotherapy. In this context, it is important to note that the results of the HFIM study agree with the breakpoints for resistance set by EUCAST of >8 mg/L for CZA and >32 mg/L for FOF IV (11). The investigated *E. coli* strain is deemed susceptible to FOF and CZA according to EUCAST, and standard-dose monotherapies killed the bacteria and suppressed regrowth successfully.

We acknowledge the following limitations of our study: the dosing schemes were simplified for the HFIM experiments. The application of bolus injections in deviation to the clinical practice of 2-h infusions for CZA or 0.5-h infusions of FOF was driven by practicability reasons. Additionally, the focus on the reproduction of the peak (C_{max}) and trough (C_{min}) concentrations of the pharmacokinetic profiles enabled a simplified control of the elimination of all three drugs with a then-joint elimination half-life of approximately 2 h. This matches the clinically observed half-life for ceftazidime and avibactam, but the clinical half-life of FOF was shortened by 50% (21, 22). It could be expected to even increase the efficacy of the drug combination further, when also the dosing regimens have become a subject of optimization. So far, this study adds a conceptual approach to translating this drug interaction from static time-kill experiments into dynamic HFIM experiments.

This study was solely conducted as a single experiment in one clinical *E. coli* strain. However, previous research highlighted that the interactions of CZA and FOF behave relatively consistent among different clinical *E. coli* strains without an identified influence of the expressed genes (8). Hence, this study adds a conceptual demonstration of the synergy of CZA and FOF in an exemplary strain, but a confirmation of the synergy and further extrapolation to less susceptible or resistant strains would be desirable. The simulated pharmacokinetics were derived from published plasma pharmacokinetic models. Therefore, the target site exposition might be different, and additionally, host-bacteria interactions (e.g., the immune system) need to be considered when a clinical outcome is discussed. Nevertheless, clinical exploitation of the drug interaction might increase the robustness of the antibiotic therapy with regard to efficacy, prevention of the emergence of resistance, and tolerability against pharmacokinetic variability even in infections where a monotherapy could be sufficient.

To conclude, the presented translational *in vitro* study outlined the potential clinical benefit of the drug interaction of CZA and FOF in a clinical *E. coli* isolate. If the synergy demonstrated in *in vitro* experiments can be corroborated clinically, the combination of CZA and FOF comes with the potential for dose reductions or increased treatment success due to enhanced killing effects and suppression of the emergence of resistance. Perspectively, advanced dosing schemes as prolonged or continuous infusions should be evaluated to further benefit from the prevailing synergy of CZA and FOF. To be finally able to translate the drug interaction from "bench to bedside," the development of a rational guidance like breakpoints of the drug combination or PKPD indices is required to advise clinical combination therapy.

MATERIALS AND METHODS

Strains, media, and antimicrobials

One clinical *E. coli* isolate carrying genes coding for both ESBL and carbapenemase was used. The strain was isolated from a rectal swab in a routine screening for multi-drug-resistant bacteria in the Henri-Mondor Hospital in the East of Paris region. The genomes were assembled with shovill v1.0.4 (<https://github.com/tseemann/shovill>), and the resistome was identified using the ResFinder database available on the Center for Genomic Epidemiology platform (<https://www.genomicepidemiology.org/>).

Ceftazidime (Sigma-Aldrich, USA), avibactam (Sigma-Aldrich, USA), FOF (Sigma-Aldrich, USA), and glucose-6-phosphate (Sigma-Aldrich, USA) stock solutions were freshly prepared in sterile 0.9% NaCl solution and stored short term at -80°C .

The bacteria were cultivated on Columbia agar (Carl Roth, Germany). Serial dilution of bacterial samples and plating on Columbia agar plates containing no drug were used to determine total bacterial counts. Agar plates supplemented with $3\times$ MIC were used for monitoring of emergence of phenotypically less susceptible subpopulations during the HFIM. Ceftazidime-containing agar plates were supplemented with a constant concentration of 4-mg/L avibactam. 25-mg/L glucose-6-phosphate was added to agar plates containing FOF corresponding to EUCAST recommendations.

The experiments were conducted in cation-adjusted Mueller-Hinton broth 2 (MHB) (Sigma-Aldrich, USA). In addition to the agar plates, MHB containing FOF was supplemented with glucose-6-phosphate. The final concentration of glucose-6-phosphate after all the dilution steps was kept at 25 mg/L.

Susceptibility testing

Broth microdilution according to the CLSI guideline was applied for MIC determination (23). Turbidity endpoints were read for ceftazidime, CZA, and FOF after 24 h. Although microdilution is not the reference method for FOF susceptibility testing, threefold of the MIC determined by microdilution was used to monitor the emergence of phenotypic-resistant subpopulations of the *E. coli* strain in liquid growth medium during the hollow fiber experiments. To account for the elevated variability, the MIC determination was performed in triplicate, and the modal value was reported. Additionally, the MIC of FOF was determined by agar dilution.

Static time-kill experiments

Static time-kill experiments over 30 h at 37°C ambient air were conducted to explore the pharmacodynamics of ceftazidime, avibactam, and FOF alone and in combination. The concentrations were selected covering full effect ranges from eradication to regrowth as well as clinically relevant concentrations. The time-kill experiments were performed with a total volume of 10 mL and were inoculated with 10^6 CFU/mL. After 2 h of preincubation, the drugs were added. The bacterial counts were quantified at 0, 2, 4, 8, 24, and 30 h after addition of the drugs by serial dilution, plating, and manual colony counting. The lower limit of quantification for this method was around 10^1 – 10^2 CFU/mL. Not quantifiable bacterial counts were empirically set to 1 CFU/mL and included in the model-based data evaluation. The experiments were performed as duplicates.

Dynamic HFIM

Dynamic HFIM experiments over 72 h at 37°C ambient air were utilized to investigate the pharmacodynamics of CZA and FOF and their drug interactions mimicking human pharmacokinetics (24). MHB was circulated from a central compartment through a hollow fiber cartridge (C2011; FiberCell Systems Inc., USA). Peristaltic pumps pumped fresh MHB from a reservoir into the central compartment, and the same volume was removed to control the pharmacokinetics of the drugs. The 40-mL extra-capillary space of the hollow fiber cartridge was inoculated with 10^6 CFU/mL. After 2 h of preincubation, the first dose was administered by a syringe driver.

The total and phenotypic-resistant bacterial count against $3\times$ MIC was quantified by sampling from the bacterial compartment, serial dilution, and plating of the dilutions on agar plates followed by manual counting. Alike in the static time-kill experiments, not quantifiable bacterial counts were empirically set to 1 CFU/mL and included in the model-based data evaluation. Samples to confirm the drug pharmacokinetics within the HFIM were drawn from the central compartment and stored at -80°C until analysis. Details on the HFIM experiments and the used equipment are described in Text S1.

Pharmacokinetics

Pharmacokinetic profiles of different CZA and FOF doses were simulated from published pharmacokinetic models derived from clinically observed drug concentrations (21, 22). From simulations of 1,000 virtual patients, defined percentiles were calculated to ensure that the mimicked pharmacokinetics profiles in the HFIM cover the clinically relevant concentration ranges. Simulated 50th percentiles thereby represent the antibiotic exposure within a typical patient, whereas the simulation of 5th percentiles represents the lower end of the exposure distribution in an inhomogeneous patient population, for example, due to altered pharmacokinetics by increased volume of distribution and/or clearance. In addition to standard doses, subtherapeutic doses were mimicked to evaluate the potential clinical relevance of the synergies. Dosing regimens with thrice daily doses q8h were focused, and for simplification, the drugs were administered to the HFIM as bolus injection maintaining the simulated peak (C_{\max}) and trough (C_{\min}) concentrations. The planned pharmacokinetics profiles are illustrated on Fig. 5, and the key pharmacokinetic properties are summarized in Table 1.

Protein binding for FOF is reported to be neglectable (25). For avibactam, a fraction unbound of 92% was assumed, and for ceftazidime, 85% fraction unbound was presumed as a compromise of the compared literature (21, 25).

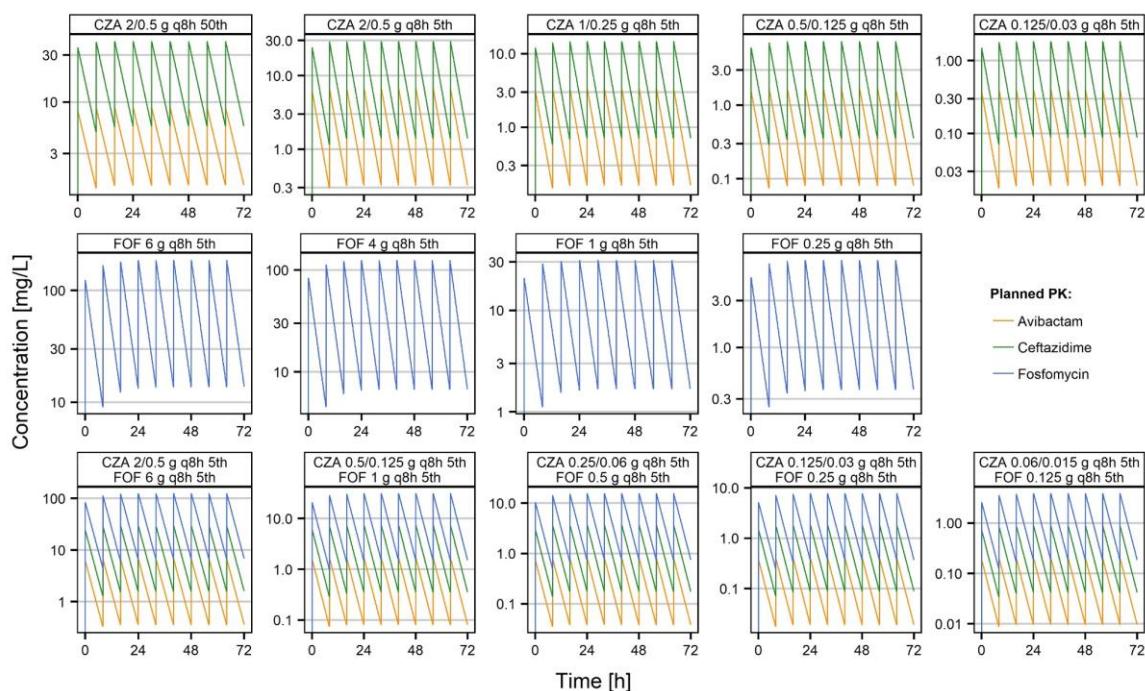


FIG 5 Overview of the simulated pharmacokinetics for the different hollow fiber experiments against CZA and FOF alone and in combination. The percentiles (50th or 5th) of the doses correspond to the distribution of pharmacokinetic profiles that would be expected from simulations of 1,000 patients given the defined dose. C_{\max} , maximum concentration at steady state; C_{\min} , minimum concentration at steady state.

TABLE 1 Overview of the simulated pharmacokinetics for the different hollow fiber experiments against CZA and FOF alone and in combination^a

Hollow fiber experiment	Avibactam (mg/L)		Ceftazidime (mg/L)		FOF (mg/L)		Simulated half-life (h)
	C _{min}	C _{max}	C _{min}	C _{max}	C _{min}	C _{max}	
CZA 2/0.5 g q8h 50th	1.43	8.71	5.70	41.11	-	-	3.03
CZA 2/0.5 g q8h 5th	0.32	6.69	1.40	29.06	-	-	1.81
CZA 1/0.25 g q8h 5th	0.16	3.34	0.71	14.66	-	-	1.81
CZA 0.5/0.125 g q8h 5th	0.08	1.67	0.35	7.33	-	-	1.81
CZA 0.125/0.03 g q8h 5th	0.02	0.40	0.09	1.83	-	-	1.81
FOF 6 g q8h 5th	-	-	-	-	13.67	185.37	2.10
FOF 4 g q8h 5th	-	-	-	-	6.74	124.31	1.88
FOF 1 g q8h 5th	-	-	-	-	1.68	31.08	1.88
FOF 0.25 g q8h 5th	-	-	-	-	0.37	7.72	1.81
CZA 2/0.5 g q8h 5th FOF 6 g q8h 5th	0.36	6.63	1.59	29.26	6.74	124.31	1.88
CZA 0.5/0.125 g q8h 5th							
FOF 1 g q8h 5th	0.08	1.67	0.35	7.33	1.50	31.12	1.81
CZA 0.25/0.06 g q8h 5th							
FOF 0.5 g q8h 5th	0.04	0.80	0.18	3.65	0.75	15.56	1.81
CZA 0.125/0.03 g q8h 5th							
FOF 0.25 g q8h 5th	0.02	0.40	0.09	1.83	0.37	7.72	1.81
CZA 0.06/0.015 g q8h 5th							
FOF 0.125 g q8h 5th	0.01	0.20	0.04	0.87	0.19	3.86	1.81

^aThe percentiles (50th or 5th) of the doses correspond to the distribution of pharmacokinetic profiles that would be expected from simulations of 1,000 patients given the defined dose. C_{max}, maximum concentration at steady state; C_{min}, minimum concentration at steady state.

Bioanalysis

To confirm the pharmacokinetics of ceftazidime, avibactam, and FOF in the HFIM, samples covering the time course of the experiment were analyzed by ultra-high performance liquid chromatography-mass spectrometry (Text S2).

PKPD modeling

In the first step, a semi-mechanistic PKPD model describing the static time-kill experiments was developed in NONMEM 7.5.0. (ICON, Gaithersburg, MD, USA) using second-order conditional estimation with interaction (LAPLACIAN-I). In brief, the monodrug effects of ceftazidime, avibactam, and FOF were modeled as sigmoidal maximum effect (E_{max}) or power models on a two-compartment base model with susceptible and resistant subpopulations. Additivity was calculated by bliss independence (26, 27). Sequentially, drug interactions were introduced by the GPDI model (12). An increase of the ceftazidime potency mediated by avibactam and mono- and bidirectional drug interactions of ceftazidime and FOF was tested. Model selection was guided based on the Akaike information criterion, visual model fit, model stability, and condition number (28). To describe interexperimental variability, interindividual variability was tested on different growth parameters of the resistant population. The model was then evolved for the dynamic HFIM data. The pharmacodynamic parameters determined from the static experiments were fixed, and the model was extended to capture regrowth, which could not be mapped by the static time-kill PKPD model. Therefore, a submodel describing the emergence of phenotypic-resistant subpopulations against 3× MIC CZA or FOF was added. Drug effects were implemented as inhibition of the emergence of the resistances, and the drug interaction of ceftazidime and FOF was described by subpopulation synergy (29). Adjustments of the variability model with regard to interexperimental variability were again tested on growth parameters of the resistant population and the newly introduced subpopulations. Parameter uncertainty for both models was assessed by the sampling importance resampling routine implemented in Perl-speaks-NONMEM 5.0 (Uppsala University, Sweden) with the relative standard error calculated in the

covariance step as proposal distribution (30). Details on the PKPD model building are described in Text S3.

PKPD simulations

The dynamic PKPD model was then used for simulations of additional HFIM experiments. To evaluate the outcome of different dose combinations, the median reduction of the bacterial count after 72 h compared to no treatment was calculated.

ACKNOWLEDGMENTS

This project resulted from a German-French research cooperation called "CO-PROTECT" and was supported by a grant from the Federal Ministry of Education and Research (BMBF), Germany, with grant agreement number 16GW0249K, and by a grant from the National Agency of Research (ANR), France, with grant agreement number R19094GG.

S.G.W. and N.K. planned the study; N.K., L.F.A., A.F., C.P. M.M., J.-W.D., N.G., P.N., and S.G.W. contributed to the research; N.K. wrote the original draft; and all authors wrote, reviewed, edited, and approved the final manuscript.

AUTHOR AFFILIATIONS

¹Institute of Pharmacy, University of Hamburg, Hamburg, Germany

²Dynamic Team – EA 7380, Faculté de Santé, Université Paris-Est-Créteil Val-De-Marne, Créteil, France

³Inserm U1070, Poitiers, France

⁴UFR de Médecine Pharmacie, Université de Poitiers, Poitiers, France

⁵Laboratoire de Toxicologie-Pharmacologie, CHU de Poitiers, Poitiers, France

⁶Medical and Molecular Microbiology, University of Fribourg, Fribourg, Switzerland

AUTHOR ORCIDs

Niklas Kroemer  <http://orcid.org/0000-0002-6941-1647>

Lisa F. Amann  <http://orcid.org/0000-0002-1274-9276>

Jean-Winoc Decousser  <http://orcid.org/0000-0001-7105-6202>

Nicolas Grégoire  <http://orcid.org/0000-0001-6436-3757>

Patrice Nordmann  <http://orcid.org/0000-0002-1343-1622>

Sebastian G. Wicha  <http://orcid.org/0000-0002-8773-4845>

FUNDING

Funder	Grant(s)	Author(s)
Bundesministerium für Bildung und Forschung (BMBF)	16GW0249K	Sebastian G. Wicha
Agence Nationale de la Recherche (ANR)	R19094GG	Jean-Winoc Decousser

ADDITIONAL FILES

The following material is available [online](#).

Supplemental Material

Supplemental material (Spectrum03318-23-S0001.docx). Text S1 to S5, Fig. S1 and S2, and Tables S1 to S4.

REFERENCES

1. Tängdén T, Giske CG. 2015. Global dissemination of extensively drug-resistant carbapenemase-producing enterobacteriaceae: clinical perspectives on detection, treatment and infection control. *J Intern Med* 277:501–512. <https://doi.org/10.1111/joim.12342>

2. Tyers M, Wright GD. 2019. Drug combinations: a strategy to extend the life of antibiotics in the 21st century. *Nat Rev Microbiol* 17:141–155. <https://doi.org/10.1038/s41579-018-0141-x>
3. Dijkmans AC, Zacarias NVO, Burggraaf J, Mouton JW, Wilms EB, Van Nieuwkoop C, Touw DJ, Stevens J, Kamerling IMC. 2017. Fosfomycin: pharmacological, clinical and future perspectives. 4:24. <https://doi.org/10.3390/antibiotics6040024>
4. Albur MS, Noel A, Bowker K, MacGowan A. 2015. The combination of colistin and fosfomycin is synergistic against NDM-1-producing enterobacteriaceae in *in vitro* pharmacokinetic/pharmacodynamic model experiments. *Int J Antimicrob Agents* 46:560–567. <https://doi.org/10.1016/j.ijantimicag.2015.07.019>
5. Avery LM, Sutherland CA, Nicolau DP. 2019. Prevalence of *in vitro* synergistic antibiotic interaction between fosfomycin and nonsusceptible antimicrobials in carbapenem-resistant *Pseudomonas aeruginosa*. *J Med Microbiol* 68:893–897. <https://doi.org/10.1099/jmm.0.000984>
6. Ojdana D, Gutowska A, Sacha P, Majewski P, Wiecek P, Tryniszewska E. 2019. Activity of ceftazidime-avibactam alone and in combination with ertapenem, fosfomycin, and tigecycline against carbapenemase-producing *Klebsiella pneumoniae*. *Microb Drug Resist* 25:1357–1364. <https://doi.org/10.1089/mdr.2018.0234>
7. Mikhail S, Singh NB, Kebriaei R, Rice SA, Stamper KC, Castanheira M, Rybak MJ. 2019. Evaluation of the synergy of ceftazidime-avibactam in combination with meropenem, amikacin, aztreonam, colistin, or fosfomycin against well-characterized multidrug-resistant *Klebsiella pneumoniae* and *Pseudomonas aeruginosa*. *Antimicrob Agents Chemother* 63:e00779-19. <https://doi.org/10.1128/AAC.00779-19>
8. Kroemer N, Martens M, Decousser JW, Grégoire N, Nordmann P, Wicha SG. 2023. Evaluation of *in vitro* pharmacodynamic drug interactions of ceftazidime/avibactam and fosfomycin in *Escherichia coli*. *J Antimicrob Chemother* 78:2524–2534. <https://doi.org/10.1093/jac/dkad264>
9. Friberg LE. 2021. Pivotal role of translation in anti-infective development. *Clin Pharmacol Ther* 109:856–866. <https://doi.org/10.1002/cpt.2182>
10. Nielsen EI, Cars O, Friberg LE. 2011. Predicting *in vitro* antibacterial efficacy across experimental designs with a semimechanistic pharmacokinetic-pharmacodynamic model. *Antimicrob Agents Chemother* 55:1571–1579. <https://doi.org/10.1128/AAC.01286-10>
11. European Committee on Antimicrobial Susceptibility Testing (EUCAST). 2023. Clinical breakpoint tables v. 13.0
12. Wicha SG, Chen C, Clewe O, Simonsson USH. 2017. A general pharmacodynamic interaction model identifies perpetrators and victims in drug interactions. *Nat Commun* 8:2129. <https://doi.org/10.1038/s41467-017-01929-y>
13. Sullivan GJ, Delgado NN, Maharjan R, Cain AK. 2020. How antibiotics work together: molecular mechanisms behind combination therapy. *Curr Opin Microbiol* 57:31–40. <https://doi.org/10.1016/j.mib.2020.05.012>
14. Wang Y, Wang J, Wang R, Cai Y. 2020. Resistance to ceftazidime-avibactam and underlying mechanisms. *J Glob Antimicrob Resist* 22:18–27. <https://doi.org/10.1016/j.jgar.2019.12.009>
15. Papp-Wallace KM, Zeiser ET, Becka SA, Park S, Wilson BM, Winkler ML, D'Souza R, Singh I, Sutton G, Fouts DE, Chen L, Kreiswirth BN, Ellis-Grosse EJ, Drusano GL, Perlin DS, Bonomo RA. 2019. Ceftazidime-avibactam in combination with fosfomycin: a novel therapeutic strategy against multidrug-resistant *Pseudomonas aeruginosa*. *J Infect Dis* 220:666–676. <https://doi.org/10.1093/infdis/jiz149>
16. Aulin LBS, Liakopoulos A, van der Graaf PH, Rozen DE, van Hasselt JGC. 2021. Design principles of collateral sensitivity-based dosing strategies. *Nat Commun* 12:5691. <https://doi.org/10.1038/s41467-021-25927-3>
17. Karageorgopoulos DE, Wang R, Yu XH, Falagas ME. 2012. Fosfomycin: evaluation of the published evidence on the emergence of antimicrobial resistance in Gram-negative pathogens. *J Antimicrob Chemother* 67:255–268. <https://doi.org/10.1093/jac/dkr466>
18. Livermore DM, Warner M, Jamroz D, Mushtaq S, Nichols WW, Mustafa N, Woodford N. 2015. *In vitro* selection of ceftazidime-avibactam resistance in enterobacteriaceae with KPC-3 carbapenemase. *Antimicrob Agents Chemother* 59:5324–5330. <https://doi.org/10.1128/AAC.00678-15>
19. Kristoffersson AN, Bissantz C, Okujava R, Haldimann A, Walter I, Shi T, Zampaloni C, Nielsen EI. 2020. A novel mechanism-based pharmacokinetic-pharmacodynamic (PKPD) model describing ceftazidime/avibactam efficacy against β -lactamase-producing Gram-negative bacteria. *J Antimicrob Chemother* 75:400–408. <https://doi.org/10.1093/jac/dkz440>
20. Sy SKB, Zhuang L, Xia H, Beaudoin M-E, Schuck VJ, Nichols WW, Derendorf H. 2018. A mathematical model-based analysis of the time-kill kinetics of ceftazidime/avibactam against *Pseudomonas aeruginosa*. *J Antimicrob Chemother* 73:1295–1304. <https://doi.org/10.1093/jac/dkx537>
21. Sy SKB, Zhuang L, Sy S, Derendorf H. 2019. Clinical pharmacokinetics and pharmacodynamics of ceftazidime-vibactam combination: a model-informed strategy for its clinical development. *Clin Pharmacokinet* 58:545–564. <https://doi.org/10.1007/s40262-018-0705-y>
22. Pfausler B, Spiss H, Dittrich P, Zeitlinger M, Schmutzhard E, Joukhar C. 2004. Concentrations of fosfomycin in the cerebrospinal fluid of neurointensive care patients with ventriculostomy-associated ventriculitis. *J Antimicrob Chemother* 53:848–852. <https://doi.org/10.1093/jac/dkh158>
23. Clinical and Laboratory Standards Institute. 2012. Methods for dilution antimicrobial susceptibility tests for bacteria that grow aerobically; approved standard—ninth edition. Clinical and laboratory Standards Institute - CLSI.
24. Cadwell JJS. 2015. Advances in antibiotics and antibodies the hollow fiber infection model: principles and practice. *Adv Antibiot Antibodies* 1:1–5.
25. Gonzalez D, Schmidt S, Derendorf H. 2013. Importance of relating efficacy measures to unbound drug concentrations for anti-infective agents. *Clin Microbiol Rev* 26:274–288. <https://doi.org/10.1128/CMR.00092-12>
26. Goldoni M, Johansson C. 2007. A mathematical approach to study combined effects of toxicants *in vitro*: evaluation of the bliss independence criterion and the loewe additivity model. *Toxicol In Vitro* 21:759–769. <https://doi.org/10.1016/j.tiv.2007.03.003>
27. Bliss CI. 1939. The toxicity of poisons applied jointly. *Ann of Appl Biol* 26:585–615. <https://doi.org/10.1111/j.1744-7348.1939.tb06990.x>
28. Akaike H. 1974. A new look at the statistical model identification. *IEEE Trans Automat Contr* 19:716–723. <https://doi.org/10.1109/TAC.1974.1100705>
29. Landersdorfer CB, Ly NS, Xu H, Tsuji BT, Bulitta JB. 2013. Quantifying subpopulation synergy for antibiotic combinations via mechanism-based modeling and a sequential dosing design. *Antimicrob Agents Chemother* 57:2343–2351. <https://doi.org/10.1128/AAC.00092-13>
30. Dosne AG, Bergstrand M, Harling K, Karlsson MO. 2016. Improving the estimation of parameter uncertainty distributions in nonlinear mixed effects models using sampling importance resampling. *J Pharmacokinet Pharmacodyn* 43:583–596. <https://doi.org/10.1007/s10928-016-9487-8>

4 Discussion

The following chapters provide a summarising and overarching discussion of the results presented in the Publications I, II and III.

The aim of the present PhD project as well as of the parent 'CO-PROTECT' project was to elucidate *in vitro* pharmacodynamic drug interactions of ceftazidime/avibactam and fosfomycin and to derive the clinical potential of this combination. Alike the project, the discussion follows a bottom-up approach. The outcomes of the three publications are discussed from a technical perspective with regard to the experimental designs, the applied *in vitro* assays, identified interactions and from a clinical perspective with regard to the therapeutic and translational relevance and current therapeutic strategies.

4.1 Design of experiments

D-optimised designs for interaction screening

Rational and efficient planning of experiments was crucial while performing the extensive *in vitro* research presented in this PhD project. The efforts of design rationalisation culminated in the development and evaluation of dynamic checkerboard designs to enable an efficient pharmacodynamic interaction screening.[86], [87] The optimisation based on the D-optimal design theorem identified innovative rhombic checkerboard designs. Those were based on drug potencies (i.e. effective concentrations (EC) leading to fractions of the maximum effect) rather than on standard concentrations. A design comprising four drug combinations of EC08/EC44, EC44/EC08, EC44/EC82 and EC82/EC44 was evaluated as the best compromise between a reduced workload and high performance with regard to the identification of interactions. Among the evaluated designs, this fixed rhombic design was the most straightforward and efficient experimental layout. Hence, it was subsequently applied in various *in vitro* experiments (see 3.2).[86], [89]–[94]

The significant reduction of the experimental layout led to a lack in precision and accuracy with regard to the estimation of interaction parameters compared to considerably more labour-intensive reference designs. However, the experimental

design was designed as a screening tool and therefore those losses during the estimation were accepted under the premise of the designs being highly efficient when it comes to the correct classification of pharmacodynamic drug interactions. The subsequent *in vitro* application and confirmation studies supported the properties of the experimental design, but they also attested its theoretically foreseen weaknesses. In Publication I, it was already anticipated that strong drug interaction magnitudes can exceed the adaptive concentration ranges.[86] To account for this limitation the interaction potency in the checkerboard experiments was fixed to very small concentrations during the estimation of the drug interactions in Publication II.[87] A comparison of the maximum interaction shift estimates from the checkerboard experiments with those of the static time kill experiments reveals that this adjustment led to an underestimation of the maximum synergistic effect sizes of ceftazidime/avibactam and fosfomycin. In detail, the maximum EC50 reductions in the checkerboard experiments against the three clinical *E. coli* isolates YAL_AMA, JUM_JEA and MER_MIL were estimated to range from 16% to 42% whereas the static time kill experiments identified higher maximum EC50 reductions of > 89%.

In general, the experimental design captured the drug interactions well for the majority of the evaluated bacterial strains and antibiotic agents during the checkerboard screening. However, also such strong synergistic interactions were detected, that additional experiments at lower concentrations were required to properly inform the estimation of exposure-response-surfaces.[92]

Model assumptions for D-optimal design approaches

Since the checkerboard designs reduced the workload and streamlined the interaction screening, the argument might arise, why the D-optimal design theorem was not used for the planning of the subsequent static and dynamic time kill experiments. As introduced (see 1.6.3), D-optimality minimises the variance of parameter estimates of a mathematical model with respect to design variables. Therefore, it is the nature of D-optimal designs to rely heavily on the prior assumption of a mathematical model.

That implies that a developed design will perform weaker, when the PK/PD model used for data evaluation differs significantly from the prior model assumption.[95], [96] In exploratory research, a model is not always known yet and its structure might be driven from an evolving hypothesis, when further data is acquired.[61] Consequently, the optimal design techniques are predestined for specified straightforward research questions, where the mathematical model and an idea of the experimental design is already defined rather than exploratory research. Conversely, exploratory research questions, in which models are developed based on data patterns like for the time kill experiments in Publication II and III, are less suited for D-optimal design approaches.[97] In those cases, translational studies including simulations with preliminary PK/PD models can serve as a rational to guide efficient planning of experimental series. In particular, the dosing choices of 1 g q8h fosfomycin and 0.5/0.125 g q8h ceftazidime/avibactam in Publication III have been derived from the model developed from the static time kill assays. Its predictions guided the dose finding to observe therapy failure and regrowth, which was then experimentally corroborated.[88] The experiments were thereby not only rationalised and optimised based on mathematical criteria, but also by gained knowledge and experience. Nevertheless, both approaches lead to increased efficiency and their value can be clearly emphasised as shown in Publications II and III.

4.2 Evaluation of drug interactions

The identified drug interactions presented in the Publications II and III were investigated with different *in vitro* assays. The following chapter discusses and compares those techniques to alternative *in vitro* assays for interaction testing. Additionally, the presented findings will be contrasted to previous published knowledge on the drug interaction of ceftazidime/avibactam and fosfomycin.

Potential of model-based evaluation

As already introduced (see 1.7.3), there is no defined 'gold standard' for *in vitro* interaction testing.[78] Therefore, a variety of test-methods are applied. They all have in common, that detailed elucidation of drug interactions requires lots of data and is most insightful with regard to the information of mechanistic relationships, when it is supported by pharmacometric modelling and simulation techniques.[4], [64], [65], [98] Since pharmacometrics require complex skills and software, which are not available to all research groups, other (more straightforward) strategies compared to the development of full PK/PD models are often applied.[98]

However, also the approaches of the quantitative modelling of the 'dynamic' checkerboard and time kill experiments presented in Publications II and III differ in their levels of semi-mechanistic insights into the observed drug interactions. The different applied methods unite, that they are able to quantify drug interactions and add information on the relevant interaction concentration ranges. This understanding can either be directly derived from the GPDI model parameter estimates (e.g. the maximum interaction shifts of PD parameters such as E_{max} and EC_{50} or the corresponding potencies of the interaction) or by investigating meaningful graphics such as comparisons of model predictions including the quantified interactions against expected additivity or exposure-response-surface plots. In particular, exposure-response-surface analyses are powerful tools to investigate concentration-effect relations in a multidimensional fashion. Originating from process improvement within the chemical industry, the application of exposure-response-surfaces on drug interactions can help to identify and understand at which concentrations the drug interactions become most apparent.[99]

Additionally to the advantageous parametrisation, the GPDI modelling approach adds semi-mechanistic layers by allowing allosteric and/or competitive interactions.[16] Especially, the missing possibility for description of allosteric interactions with increased effect sizes beyond the maximum effect of a single drug is a limitation of many other interaction models.[65], [100] But it has to be acknowledged, that the parametric

modelling approaches are highly complex and require an appropriate data base to inform the different model parameters. However, the quantification and direct interpretability of the GPDI model parameters represent advantages compared to empiric models, which quantify interactions solely by a factor describing a deviation from the calculated additive effects.[16], [101], [102] Unlike the interaction parameters included in the GPDI model those deviation parameters cannot be interpreted directly. Additionally, those models are not able to distinguish between interactions affecting EC50 or Emax and do not consider a directionality of drug interaction.

For all modelling approaches, it is important to note, that the type of the model is crucial for the interpretation of the model parameters. The different models developed for the Publications II and III can be divided in static endpoint driven evaluations (i.e. the calculation of exposure-response-surfaces of the checkerboard experiments at a defined timepoint) or time-resolved models (i.e. the dynamic description of the time kill experiments). The inclusion of time as a variable when solving time-resolved models has to be considered when comparing different model parameters. A prominent example is Emax. For time-resolved models Emax describes a kill rate over time (h^{-1}) whereas it displays a \log_{10} reduction of the bacterial count compared to uninhibited growth in frame of the checkerboard exposure-response-surfaces. This needs to be considered, when it comes to communication or translation of the results.

Impact of the additivity criterion

Unlike to the development of pharmacometric models, less complex approaches like 'conventional' checkerboard experiments or Etest cross methods are easier to perform and commonly evaluated by the calculation of an FIC index. Thus, they can be easier implemented in routine diagnostics. However, the calculation of FIC indices lacks semi-mechanistical insights, reproducibility, sensitivity and does not provide information whether the concentration, at which the interaction is observed, is actually clinically relevant.[78], [81]–[83] Furthermore, the calculation of an FIC index assumes Loewe additivity, which might not always be considered and can become problematic.[103] As

introduced earlier, Loewe additivity (see 1.3) hypothesises similar or equal agents with same sites of action, which might not always be the case for antibiotics with different modes of action.[19], [20], [22], [103] In essence, Bliss Independence (see 1.3) might be the more suitable additivity criterion for the independently acting ceftazidime/avibactam and fosfomycin. Hence, Bliss Independence was applied for the calculation of expected additivities in the present PhD project. As drug interactions are defined as deviations of the combined drug effect from additivity, the choice of the additivity criterion will directly influence the identification of drug interactions and will also affect their interstudy comparability.[18], [83] Therefore, the careless assumption of Loewe Additivity when calculating an FIC index can hinder the final translation of the findings into the clinical setting.[103]

Influence of the in vitro testing method

The method of *in vitro* interaction testing must be considered, when comparing the results of *in vitro* studies.[4], [83] For example, Mikhail *et al.* conclude antibacterial activity based on shifts of the MIC and recommend the combination of ceftazidime/avibactam and fosfomycin against *K. pneumoniae*.[28] Conversely, Romanelli *et al.* and Avery *et al.* conclude solely additivity or indifferent interactions in *K. pneumoniae* and other selected *Enterobacteriaceae* based on Etests.[104], [105] On the opposite, data was also published identifying synergy rates of nearly 50% in *K. pneumoniae* evaluated by Etest.[106] In concordance to those ambiguous results, a study based on ‘dynamic’ checkerboard experiments, conducted in this PhD project, identified strain dependent additive or synergistic drug interactions in carbapenemase producing and fosfomycin resistant *K. pneumoniae*.[94] The different outcomes highlight a general consensus with regard to the identification of similar interactions for *K. pneumoniae* and selected *Enterobacteriaceae* and indicate uniformity of the results from different methods. Nevertheless, even if this agreement is encouraging, it remains unclear, whether a mechanistic explanation (e.g. genetic disposition of the

different investigated strains) can be found or whether the differences can be traced back to the different *in vitro* assays and evaluation methods.

An additional layer in the evaluation of drug interactions can be provided by the determination of mutation frequencies against the different antibiotics alone and in combination. They were calculated in Publication II and a comparable approach was performed in Publication III, when the phenotypic emergence of resistant subpopulations against ceftazidime/avibactam and fosfomycin was monitored. The results in both publications indicate a suppression of the emergence of resistances in combination, which was already shown for a *P. aeruginosa* strain by measurements of decreased mutation frequencies in combination compared to a mono treatment.[107]

Comparing the evaluation of the data, the different assays have different sensitivities. Conventional checkerboard experiments are relatively insensitive due to the high turbidity threshold of $> 10^7$ cfu/mL, whereas model-based evaluations of bacterial concentrations are highly sensitive.[80] This increased sensitivity might require the necessity to introduce additivity margins or measures of interaction parameter uncertainty (e.g. confidence intervals) to not overinterpret the data and report false positive drug interactions.[16] To avoid this, additivity margins were applied and 95% confidence intervals of the interaction parameter estimates were calculated during the experimental design development in Publication I and for the evaluation of the interaction screening presented in Publication II. Subsequently, the drug interactions were then evaluated under the condition of a non-overlap of the confidence intervals with zero.

Nevertheless, the purposes and the desired applications must be considered, when comparing the different methods. Exploratory research has different requirements than routine or high-throughput testing and vice versa.

4.3 Extrapolation of *in vitro* results

Extrapolation of preclinical research from 'bench to bedside' and deriving conclusions for the clinical setting are the ultimate goals of the present PhD project. However, it is a

great challenge, due to major differences in the experimental conditions between different *in vitro* assays, variability between different laboratories and wide extrapolations from *in vitro* experiments into living organisms.[2], [108] The following sections focus on the translational challenges, the values of the results obtained in the *in vitro* studies published in Publications II and III as well as which constraints might remain.

4.3.1 *In vitro-in vitro* transfer

The transfer of findings between different *in vitro* assays and laboratories becomes important, when it comes to the extrapolation of knowledge from more basic *in vitro* assays into complex and more meaningful experiments. Yet, it can provide major challenges with regard to reproducibility and consistencies of outcomes throughout different experimental conditions.[98] *In vitro-in vitro* transfer is inevitable, because of the different purposes of the available *in vitro* assays. For instance, the MIC determination is a simple diagnostic measure, but does not picture dynamic antibiotic effects. It cannot distinguish between bactericidal and bacteriostatic effects, which might be needed for research purposes and could be provided by time kill experiments.[109]

Impact of the experimental conditions

The most apparent influence factors on the experimental outcome and therefore potential challenges for transfer of findings can be summarised as those of the general experimental conditions. Instable incubation temperatures, different pH values, carbon dioxide concentrations, experimental volumes and incubation times directly impact the experimental outcome and can vary between different laboratories.[20], [76] To reduce those influences, especially for diagnostic measures (i.e. MIC determination), standardised reference methods with reduced variability were established to improve interlaboratory reproducibility.[20] To obtain comparable results and evaluate the susceptibility with regard to clinical guidelines the MIC determinations included in

Publications II and III were based on the guidance of the Clinical and Laboratory Standards Institute (CLSI) and EUCAST.[110]

Additionally, the growth medium influences the experimental outcome and affects observed growth as well as killing effects.[111] Even though Mueller Hinton Broth is commonly used, it is not fully standardised and its composition may vary.[20] In the context of *in vitro* experiments with fosfomycin, it is also important to note that its effect is directly influenced by the concentration of inorganic phosphates, which could conceivably vary between different culture media.[112] To reduce this influence the Mueller Hinton Broth for all of the experiments conducted in this PhD project was purchased from one distinct supplier.

Besides the external influences the bacterial inoculum has a known influence on the *in vitro* effect sizes. The so-called inoculum effect describes reduced drug effect sizes correlating to elevated bacterial counts at the start of an experiment. The phenomenon is frequently observed for beta-lactam antibiotics against bacteria expressing beta-lactamase enzymes.[113] Additionally, the inoculum effect was also captured for fosfomycin.[114]

During the *in vitro* assays in Publications II and III, the broth microdilution MIC tests were inoculated with 5×10^5 cfu/mL. For the EC50 determinations, the static and dynamic time kill experiments the inoculum was increased to 10^6 cfu/mL and a preincubation was introduced. Those adjustments changed the total number of bacteria as well as their growth phase at the beginning of the experiments. Consequently, that influenced the elevated determined EC50s in Publication II compared to the determined MICs. Those adjustments for the EC50 determination were necessary to enable a direct *in vitro-in vitro* transfer of the pharmacodynamics to checkerboard assays and time kill experiments, which are commonly conducted with higher inocula compared to MIC determinations.[20] Thus, a mergeable database (i.e. data generated under the same experimental conditions) was generated to plan the adaptive checkerboard experiments and the amount of data to estimate the exposure-response-surfaces was increased.[87]

Influence of biological variability

The variability of fosfomycin effect sizes in *in vitro* testing is enhanced by a higher mutation frequency of many bacteria against fosfomycin compared to ceftazidime/avibactam.[47], [107], [115] Spontaneous and random mutants, especially in combination with elevated inocula, make the reproducibility of experiments conducted in liquid growth medium more challenging. Therefore, fosfomycin is the only agent EUCAST deviates from the general directive and recommends agar dilution as reference method for MIC testing instead of broth dilution.[116] However, the disagreements of agar and broth dilution are still subject for discussions in the scientific community, because their comparability seems highly variable and strongly dependent on the bacterial species.[43], [114], [117]–[119] Most MICs in the present PhD project were determined by broth dilution to provide comparable experimental growth conditions between the MIC determination and the subsequent checkerboard and time kill experiments, which were inevitably performed in liquid growth medium.

The alignment of the inocula and growth conditions build the foundation for the transfer from the EC50 determinations over the checkerboard assays to the time kill experiments in Publications II and III. Finally, the static time kill experiments confirmed those considerations by corroborating the synergies and the variable interaction directions observed in the checkerboard experiment. Additionally, the detailed static time kill experiments performed in Publication II confirmed the higher variability of the fosfomycin effects and the PK/PD models had to be expanded by variability components describing the interexperimental differences.

Importance of pharmacokinetics

The most important change between the static time kill experiments and the Hollow Fiber experiments was the addition of dynamic pharmacokinetics. Dynamic pharmacokinetics can enhance the emergence of resistant subpopulations, when the concentrations fall below certain thresholds. That can be correlated to the concepts of

mutant selection windows and mutant prevention concentrations as upper boundaries of the resistance selection range.[19]

Earlier pharmacometric approaches indicated a limited impact of the pharmacokinetics for several beta-lactam and non-beta-lactam antibiotics. Nielsen *et al.* demonstrate the prediction of bacterial counts in a dynamic experiment from static PK/PD models.[120] The simulations of dynamic Hollow Fiber experiments from the static model in Publication III cannot fully confirm those findings. The static PK/PD model developed for ceftazidime, avibactam and fosfomycin was always able to pick up the general trend of the bacterial dynamics, but lacked the ability to capture rapid regrowth mechanisms accurately.[88]. Hence, static time kill curves can indeed help to predict and reduce cumbersome Hollow Fiber experiments, but cannot replace them.[120]

Summarising the aspects of *in vitro-in vitro* transfer of the present PhD project, the observed drug interactions were consistent throughout the different *in vitro* assays within the species of *E. coli* as well as in the distinct evaluated strains. Those agreements encourage to derive quantitative and mechanistic knowledge from less labour-intensive *in vitro* assays to predict and spare complex experiments. However, a successful *in vivo* translation into the clinics is not guaranteed and is discussed in the following section.

4.3.2 *In vitro-in vivo* translation

The ultimate leap of preclinical studies is the translation into *in vivo* animal models and finally patients. The following section focuses on challenges regarding a translation of *in vitro* findings into the *in vivo* clinical setting and neglects special features related to the translation into animal models as they were out of the scope of this thesis.

Impact of the bacterial growth conditions

Many of the aspects related to the *in vitro-in vitro* transfer can be applied directly onto the *in vitro-in vivo* translation. Especially, the physiological growth conditions differ significantly from the optimised growth conditions *in vitro*. This includes already

discussed influencing factors (see 4.3.1) on the bacterial growth as well as the inoculum effect.[113] For instance, the already discussed Mueller Hinton Broth is optimised for *in vitro* experiments. It displays a very rich growth medium and provides optimal conditions for bacteria, which does not apply for a physiological *in vivo* infection site.[20], [111] Therefore approaches were developed to perform *in vitro* testing in biological media or close imitations.[108], [121]

The experiments presented in Publication III indicate a rapid emergence of resistance, when fosfomycin is used in monotherapy. This phenomenon is commonly observed *in vitro* but cannot be fully translated into the clinics.[41], [42], [47], [48], [122] A potential explanation for that discrepancy between the resistance development *in vitro* and *in vivo* are the optimised *in vitro* growth conditions. In detail, different rates of mutations in the fosfomycin inactivating enzyme MurA are discussed as a consequence of those different conditions.[122]

Influence of in vitro testing conventions

A series of *in vitro* testing conventions display additional challenges for the *in vitro*-*in vivo* translation. Two of them proposed by EUCAST were mainly faced in the present PhD project: I) applying a standard concentration of 4 mg/L avibactam, when performing *in vitro* susceptibility testing with ceftazidime/avibactam and II) the supplementation of fosfomycin in *in vitro* experiments with 25 mg/L glucose-6-phosphate. Both assumptions are discussed in the following paragraphs.

- I) The recommendation of the standard concentration of 4 mg/L avibactam is justified by EUCAST with a full inhibition of beta-lactamases and restauration of the ceftazidime activity to wild-type level.[123], [124] A comparison with the mimicked pharmacokinetic profiles in Publication III reveals that 4 mg/L is indeed an arbitrary concentration which is not permanently achieved in patients. Therefore, the avibactam effects could get overestimated in standard *in vitro* testing. For the particular *E. coli* strain included in

Publication III, a concentration of 4 mg/L avibactam did not have an own killing effect in static time kill experiments, but was also not always sufficient to potentiate the ceftazidime effect to a maximum.

- II) The second convention is the addition of 25 mg/L glucose-6-phosphate for *in vitro* activation of the UhpT transporter system to observe *in vitro* antibacterial effects of fosfomycin (see 1.4.2).[116] Similar to the avibactam convention, the glucose-6-phosphate concentration is based on a maximum activation of the transporter system and intended to display a maximum potentiation of the fosfomycin effects.[43], [125] *In vivo*, glucose-6-phosphate is physiologically present, but its concentrations are strongly dependent from the tissue and infection site and are assumed to be lower than 25 mg/L.[108], [125] Hence, the plausibility and the clinical correlations of the addition of glucose-6-phosphate are subject to debate.[42], [43], [108], [125], [126] The *in vitro* experiments conducted in the present PhD project followed the recommendation of the addition of 25 mg/L glucose-6-phosphate. A series of static time kill experiments (data not shown) indicate an influence of glucose-6-phosphate on the fosfomycin effects but not on the synergy of ceftazidime and fosfomycin. This outcome is encouraging when considering the glucose-6-phosphate concentration as limitation for a clinical translation.

In vitro-in vivo pharmacokinetic differences

Another, apparent translational challenge between most standard *in vitro* assays and patients are the pharmacokinetics and whether the evaluated *in vitro* concentrations are clinically relevant.[24], [106] As discussed above (see 4.3.1), dynamic time kill experiments such as the Hollow Fiber system can overcome those limitations. Nevertheless, those experiments require detailed prior knowledge on the pharmacokinetics of the researched drugs. In early stages of research and development of new agents physiologically based pharmacokinetic (PBPK) models or allometric scaling can be tools to predict human pharmacokinetics from *in vitro* or animal

models.[60] In an ideal world also target site pharmacokinetics, which can alter from plasma pharmacokinetics, are available for the design of the *in vitro* study.[127] Special features of the drugs such as nonlinear protein binding, active metabolites or prodrugs will challenge the *in vitro* Hollow Fiber system.[85], [128] Additionally, the standard set up of the Hollow Fiber system lacks the simulation of bacteria-host interactions (i.e. the patient's immune system).[85] There are advances to include neutrophil granulocytes in *in vitro* experiments with bacteria in order to mimic parts of the immune system, but eukaryotic cells in combination with bacteria are very fastidious to cultivate and have short survival half-lives.[129]

Clinical relevance of the evaluated strains

The impact of the evaluated bacterial strains on public health needs to be considered for a clinical translation. Often times not a specific strain or species takes advantage of an infection.[98] Therefore, studies with series of strains with clinically relevant susceptibilities add more valuable knowledge for the development of clinical dosing regimens.[4] The evaluated strains in the present PhD project were selected based on their clinical relevance. Various isogenic strains carrying genes coding for different extended-spectrum beta-lactamases and carbapenemases were included as well as clinical counterparts. Das *et al.* identified an MIC₉₀, which defines the MIC for 90% of the evaluated isolates, for ceftazidime/avibactam against clinically isolated *Enterobacteriaceae* of 0.25 mg/L to 0.5 mg/L.[130] This corresponds to the MIC₉₀ of the evaluated clinical *E. coli* strains in Publication II (MIC₉₀: 0.5 mg/L). Hence, despite the relatively small selection of strains evaluated in the present PhD project, this selection might still depict the clinical susceptibilities of *E. coli* against ceftazidime/avibactam and helps to draw conclusions for the clinical application of the combination therapy of ceftazidime/avibactam and fosfomycin.

4.4 Combination therapy in clinical practice

Antibiotic combination therapy is frequently used in clinical practice.[20], [98] The origins reach back more than 70 years for the therapy of tuberculosis. As already introduced (see 1.2), the four main purposes for antibiotic combination therapy are the following: I) expansion of the antibacterial spectrum in an early phase of an empiric treatment, when the pathogen causing the infection is not identified yet, II) the suppression of the emergence of resistance in combination in contrast to monotherapy, III) exploitation of drug interactions for increased efficacy or IV) the re-sensitisation of bacteria which would be resistant against monotherapy.[3], [15], [24], [98]

The following paragraphs discuss the results obtained in the present PhD project in frame of the mentioned four main purposes and how the identified synergies of ceftazidime/avibactam and fosfomycin could be beneficial for the clinical practice.

- I) The screening of the interactions of ceftazidime/avibactam and fosfomycin in the present PhD project identified mainly synergistic and fewer additive interactions across different strains and species.[87], [94] Additionally, no relation between the genotype of the strains and the interaction type or directionality could be identified.[87] Those results encourage the use of the combination in an empiric therapy for *E. coli* independently from the expression of a certain extended-spectrum beta-lactamase or carbapenemase.
- II) Increased drug effect sizes often come with a suppression of resistance. Mechanistic explanations are the efficient decrease of the total count of bacteria, which could mutate and become resistant, or a shortening of the time frame for the pathogens to develop a resistance before they become eradicated. Moreover, the combination of different modes of action increases the biological cost to develop resistances against both drugs and a high likelihood remains, that a second agent stays active, when a resistance is developed against the first.[20] For ceftazidime/avibactam-fosfomycin combinations, fosfomycin does not share the limitations of avibactam not being able to overcome an emergence of

resistance against ceftazidime mediated by an alteration in drug uptake (i.e. mutations of porins or increased efflux mechanisms).[5], [35], [44]

The phenotypical resistance development in the present PhD project was surveyed during the checkerboard and dynamic time kill experiments. In both assays the drug combination was able to suppress resistance development and the semi-mechanistic PK/PD modelling confirmed those effects by enhanced killing mechanisms. Especially, the emergence of fosfomycin resistances was suppressed in combination. Therefore, less regrowth of phenotypic resistant bacteria or regrowth at significant lower concentrations was observed in comparison to the monotherapy.

- III) The calculated exposure-response-surfaces and comparisons of additivity against interaction model predictions in Publications II and III visualize that the synergy mainly promotes effect sizes at sub-inhibitory concentrations. Therefore, a possibility for dose reductions in combination can be discussed. Dose reductions could positively contribute to avoid exposure driven adverse events such as neurotoxicity by beta-lactams or electrolyte imbalances by fosfomycin-sodium.[33], [46] Additionally, maintained high effect levels at decreased drug exposures can be beneficial for critically ill patients with altered pharmacokinetics undergoing standard dosing and no therapeutic drug monitoring.[131] In particular, critically ill patients often times suffer from increased volumes of distribution as a result of altered fluid balances.[132] Hence, hydrophilic drugs such as fosfomycin or beta-lactams might be under-dosed and thereby promote treatment failure or the development of resistances.[34], [132], [133] The observed synergies could ensure sufficient effect sizes in those patients or at reduced target site exposures.
- IV) The investigated *E. coli* strains in Publication II and III express clinically relevant extended-spectrum beta-lactamases and carbapenemases, but were all considered to be susceptible against ceftazidime/avibactam and fosfomycin with regard to the EUCAST classifications.[87], [116] This was confirmed by successful standard dose monotherapies in the Hollow Fiber infection model.[88]

Considering the simulated potential for a dose reduction also a re-sensitisation seems conceivable, however, remains subject to speculation. It might also depend on the expression of additional resistance mechanisms such as Ambler class B beta-lactamases, which are not inhibited by avibactam, or glutathione *S*-transferases degrading fosfomycin.[44] Nevertheless, a re-sensitisation was observed for the clinical *E. coli* YAL_AMA strain included in the Hollow Fiber experiments with regard to the drug combination of ceftazidime and avibactam. An MIC of 16 mg/L against ceftazidime without avibactam was determined for the particular *E. coli* strain and hence, it was classified as resistant according to EUCAST ($R > 4$ mg/L).[116] Conversely, an MIC of 0.125 mg/L was determined for the combination of ceftazidime/avibactam and categorised the strain as susceptible (i.e. $S \leq 8$ mg/L).[116] Thus, in this scenario, the potentiation of avibactam re-sensitised the *E. coli* against ceftazidime.

4.5 Guidance of clinical decision making

To support clinical decision making and to guide the treatment of infectious disease different concepts were established. Traditional PK/PD indices (see 1.6.1) are used to define pharmacokinetic targets which are then evaluated in probability-of-target-attainment analyses with regard to different doses, dosing regimens or modes of application.[68] Based on that exploratory knowledge EUCAST defines MIC breakpoints (i.e. classification of pathogens in susceptible against standard dose (S), susceptible against increased exposure (I) and resistant (R)) to support clinicians in their choice for the right antibacterial agent and therapeutic regimen.[116] Usually, a detailed database is required to derive those clinical breakpoint parameters. The systematic interaction screening performed in Publication II adds valuable data for a high-level evaluation of the synergy of ceftazidime/avibactam and fosfomycin in *E. coli*. To the author's knowledge, no other systematic studies of the drug interactions of ceftazidime/avibactam and fosfomycin against *E. coli* were conducted yet. As discussed above (see 4.2), extensive interaction testing was performed in *P. aeruginosa* or other

Enterobacteriaceae species such as *K. pneumoniae* with varying results identifying synergy and/or additivity.[28], [94], [104]–[106], [134], [135] In combination with those results, the present PhD project adds valuable data about broad synergistic interactions of *E. coli* and identifies an independency of the interactions from the expression of specific extended-spectrum beta-lactamases or carbapenemases. Thus, a general additive and synergistic effect against *Enterobacteriaceae* and *P. aeruginosa* could be assumed. That would be especially relevant as infections are not always caused by one defined pathogen.[98] Additionally, the broad effects facilitate the recruiting of patients for potential clinical studies compared to the cumbersome recruitment of patients infected by highly defined pathogens and/or genotypes.

However, standardised methods for interaction testing such as the reference methods for MIC determination to generate a universal database are still lacking. But more important, the traditional PK/PD indices and MIC breakpoints which commonly provide clinical guidance cannot be directly transferred onto drug combinations. The calculations of PK/PD indices require an MIC as fixpoint, which can be highly dynamic and dependent on the concentration of the combination partner. The most accurate method might be the calculation of an instantaneous MIC, i.e. the computation of an MIC as a function of the concentration of the combination partner. [136], [137] However, this approach is considerably more laborious and might not be suitable for clinical routine diagnostics.

Transferring this argument to the MIC breakpoints set by EUCAST, the determination of measures for combinations dependent from pathogen and combination partner would inflate breakpoint tables and leave them inappropriately complex. Those challenges were noticed by EUCAST and scientific discussions were launched, but no appropriate solution is defined yet. An example for the initiative of a discussion about breakpoints in combination is fosfomycin. Due to its mainly exclusive use in combination therapy, EUCAST questioned the definition of breakpoints for the monotherapy against some pathogens and initiated the scientific exchange, how to handle breakpoints for drug combinations.[138]

Summarising, the insights in the synergy of ceftazidime/avibactam and fosfomycin are a valuable expansion of the existing knowledge on the drug combination in *K. pneumoniae* and *P. aeruginosa*. However, further confirmations of the findings and the development of a format or index to compile clinical treatment recommendations of combinations are required to derive general clinical guidance.

5 Limitations and Perspectives

The present PhD project comprised a translational *in vitro* study and thoroughly elucidated the synergy of ceftazidime/avibactam and fosfomycin in different *E. coli* strains expressing clinically relevant extended-spectrum beta-lactamases and carbapenemases. The application of mathematical and statistical methods in form of D-optimal design theorem and pharmacometric modelling and simulation techniques played a paramount role in streamlining *in vitro* screening experiments, providing in-depth mechanistical insights into drug pharmacodynamics as well as in contributing to the transfer of findings from simplistic to complex *in vitro* assays.

Nonetheless, some limitations have to be acknowledged for the present PhD project.

The optimal experimental checkerboard designs were very condensed and highly specific for the aimed application in a pharmacodynamic interaction study. They successfully enabled a fast and target-oriented evaluation of drug combinations, but already the SSE study in Publication I indicated that unforeseen scenarios such as a potentiation or coalism in highly resistant strains would exceed the limits of the designs.[86] Additionally, those designs were developed with a focus solely on the identification of drug interactions neglecting clinically achievable concentration ranges. A future compromise unifying those two elements seems to be even more promising with regard to a clinical translation of the findings. Nevertheless, the drug interactions identified in the checkerboard experiments were corroborated in more elaborate static and dynamic time kill experiments, but a clinical *in vivo* translation is still lacking. As discussed (see 4.5), broad evidence of beneficial drug interactions of ceftazidime/avibactam and fosfomycin in *E. coli* besides the results presented in this PhD project is missing. Therefore, a further evaluation of the combination in an extended set of bacterial strains is desirable. Especially, the hypothesis of a potential re-sensitisation of resistant strains remained unmet as the main *E. coli* strain of the analysis was indeed resistant against ceftazidime alone but susceptible against ceftazidime/avibactam and fosfomycin, respectively.[88], [116]

The dynamic Hollow Fiber experiments in Publication III remained conceptual and simplified all dosing regimens to bolus injections. Hence, additional benefits of the synergy could be exploited by the development of optimised dosing regimens and focus on target site pharmacokinetics, which were out of scope for the present PhD project. In the context of optimised dosing regimens prolonged infusions as well as the application of loading doses or pulsed dosing would be conceivable.

This study was not able to identify detailed hypotheses for the appearance and the strength of the observed interactions. Therefore, further genomic and metabolomic investigations are warranted to elucidate the mechanistic cores of the interactions. A detailed understanding would be valuable for the development of rapid molecular diagnostics, which could already identify patients benefiting from combination therapy in the critical first hours of treatment.

But to steer a rational combination therapy, clinical guidance parameters categorising drug interactions in a handy manner like PK/PD indices or clinical breakpoints are still missing (see 4.5). The development of such measures could be supported by the assignment of a standard assay and evaluation tool for combination testing. Although the MIC has its superficialities and limitations, it can be an example with regard to assay simplicity and method standardisation.

To finally conclude, owning the principles of rapid molecular diagnostics and pharmacometric model-guided treatment, modern rational combination therapy of antibiotics has the potential to fight the bacteria back and improve the clinical position in the global chess match of science against pathogens.[6]

6 References

- [1] E. Tacconelli *et al.*, 'Discovery, research, and development of new antibiotics: the WHO priority list of antibiotic-resistant bacteria and tuberculosis', *The Lancet Infectious Diseases*, vol. 18, no. 3, pp. 318–327, 2018, doi: 10.1016/S1473-3099(17)30753-3.
- [2] U. Theuretzbacher, K. Outterson, A. Engel, and A. Karlén, 'The global preclinical antibacterial pipeline', *Nature Reviews Microbiology*, vol. 18, no. 5, Art. no. 5, 2020, doi: 10.1038/s41579-019-0288-0.
- [3] M. Tyers and G. D. Wright, 'Drug combinations: a strategy to extend the life of antibiotics in the 21st century', *Nature Reviews Microbiology*, vol. 17, no. 3, pp. 141-155, 2019, doi: 10.1038/s41579-018-0141-x.
- [4] G. G. Rao and C. B. Landersdorfer, 'Antibiotic pharmacokinetic/pharmacodynamic modelling: MIC, pharmacodynamic indices and beyond', *International Journal of Antimicrobial Agents*, vol. 58, no. 2, p. 106368, 2021, doi: 10.1016/j.ijantimicag.2021.106368.
- [5] Y. Wang, J. Wang, R. Wang, and Y. Cai, 'Resistance to ceftazidime–avibactam and underlying mechanisms', *Journal of Global Antimicrobial Resistance*, vol. 22, pp. 18–27, 2020, doi: 10.1016/j.jgar.2019.12.009.
- [6] E. J. Zasowski, J. M. Rybak, and M. J. Rybak, 'The β -Lactams Strike Back: Ceftazidime-Avibactam', *Pharmacotherapy: The Journal of Human Pharmacology and Drug Therapy*, vol. 35, no. 8, pp. 755–770, 2015, doi: 10.1002/phar.1622.
- [7] A. S. Michalopoulos, I. G. Livaditis, and V. Gougoutas, 'The revival of fosfomycin', *International Journal of Infectious Diseases*, vol. 15, no. 11, pp. e732–e739, 2011, doi: 10.1016/j.ijid.2011.07.007.
- [8] Alexander Fleming, 'Penicillin – Nobel Lecture', Dec. 1945, Accessed: Dec. 13, 2022. Available: <https://www.nobelprize.org/prizes/medicine/1945/fleming/lecture/>
- [9] C. J. L. Murray *et al.*, 'Global burden of bacterial antimicrobial resistance in 2019: a systematic analysis', *The Lancet*, vol. 399, no. 10325, pp. 629–655, 2022, doi: 10.1016/S0140-6736(21)02724-0.

- [10] R. Laxminarayan, 'The overlooked pandemic of antimicrobial resistance', *The Lancet*, vol. 399, no. 10325, pp. 606–607, 2022, doi: 10.1016/S0140-6736(22)00087-3.
- [11] European Centre for Disease Prevention and Control, 'Antimicrobial resistance in the EU/EEA (EARS-Net) - Annual Epidemiological Report 2021', ECDC, Stockholm, 2022. Accessed: Jan. 24, 2023. Available: https://www.ecdc.europa.eu/sites/default/files/documents/AER-EARS-Net-2021_2022-final.pdf
- [12] N. Hassoun-Kheir and S. Harbarth, 'Estimating antimicrobial resistance burden in Europe—what are the next steps?', *The Lancet Public Health*, vol. 7, no. 11, pp. e886–e887, 2022, doi: 10.1016/S2468-2667(22)00250-X.
- [13] N. Singh and P. J. Yeh, 'Suppressive drug combinations and their potential to combat antibiotic resistance', *Journal of Antibiotics*, vol. 70, no. 11, pp. 1033–1042, 2017, doi: 10.1038/ja.2017.102.
- [14] World Health Organization (WHO), '2021 Antibacterial agents in clinical and preclinical development: an overview and analysis', 2022.
- [15] J. G. C. V. Hasselt and R. Iyengar, 'Systems pharmacology: Defining the interactions of drug combinations', *Annual Review of Pharmacology and Toxicology*, vol. 59, pp. 21–40, 2019, doi: 10.1146/annurev-pharmtox-010818-021511.
- [16] S. G. Wicha, C. Chen, O. Clewe, and U. S. H. Simonsson, 'A general pharmacodynamic interaction model identifies perpetrators and victims in drug interactions', *Nature Communications*, vol. 8, no. 1, p. 2129, 2017, doi: 10.1038/s41467-017-01929-y.
- [17] H. Derendorf, S. Schmidt, M. Rowland, and T. N. Tozer, *Rowland and Tozer's clinical pharmacokinetics and pharmacodynamics: concepts and applications*, Fifth edition. Philadelphia: Wolters Kluwer, 2020.
- [18] G. G. Rao, J. Li, S. M. Garonzik, R. L. Nation, and A. Forrest, 'Assessment and modelling of antibacterial combination regimens', *Clinical Microbiology and Infection*, vol. 24, no. 7, pp. 689–696, 2018, doi: 10.1016/j.cmi.2017.12.004.

- [19] P. J. Yeh, M. J. Hegreness, A. P. Aiden, and R. Kishony, 'Drug interactions and the evolution of antibiotic resistance', *Nature Reviews Microbiology*, vol. 7, no. 6, pp. 460–466, 2009, doi: 10.1038/nrmicro2133.
- [20] J. C. Rotschafer, D. R. Andes, and K. A. Rodvold, Eds., *Antibiotic pharmacodynamics*. in *Methods in pharmacology and toxicology*. New York: Humana Press, 2016. doi: 10.1007/978-1-4939-3323-5.
- [21] C. I. Bliss, 'The Toxicity of Poisons Applied Jointly', *Annals of Applied Biology*, vol. 26, no. 3, pp. 585–615, 1939, doi: 10.1111/j.1744-7348.1939.tb06990.x.
- [22] S. Loewe, 'The problem of synergism and antagonism of combined drugs.', *Arzneimittel-Forschung*, vol. 3, no. 6, pp. 285–290, 1953.
- [23] K. R. Roell, D. M. Reif, and A. A. Motsinger-Reif, 'An Introduction to Terminology and Methodology of Chemical Synergy—Perspectives from Across Disciplines', *Frontiers in Pharmacology*, vol. 8, p. 158, 2017, doi: 10.3389/fphar.2017.00158.
- [24] G. J. Sullivan, N. N. Delgado, R. Maharjan, and A. K. Cain, 'How antibiotics work together: molecular mechanisms behind combination therapy', *Current Opinion in Microbiology*, vol. 57, pp. 31–40, 2020, doi: 10.1016/j.mib.2020.05.012.
- [25] A. C. Dijkmans *et al.*, 'Fosfomycin: Pharmacological, Clinical and Future Perspectives', *Antibiotics*, vol. 6, no. 4, Art. no. 4, Oct. 2017, doi: 10.3390/antibiotics6040024.
- [26] M. E. Falagas, E. K. Vouloumanou, G. Samonis, and K. Z. Vardakas, 'Fosfomycin', *Clinical Microbiology Reviews*, vol. 29, no. 2, pp. 321–347, 2016, doi: 10.1128/CMR.00068-15.
- [27] J. Albiero *et al.*, 'Pharmacodynamic evaluation of the potential clinical utility of fosfomycin and meropenem in combination therapy against KPC-2-producing *Klebsiella pneumoniae*', *Antimicrobial Agents and Chemotherapy*, vol. 60, no. 7, pp. 4128–4139, 2016, doi: 10.1128/AAC.03099-15.

- [28] S. Mikhail *et al.*, 'Evaluation of the Synergy of Ceftazidime-Avibactam in Combination with Meropenem, Amikacin, Aztreonam, Colistin, or Fosfomycin against Well-Characterized Multidrug-Resistant *Klebsiella pneumoniae* and *Pseudomonas aeruginosa*', *Antimicrobial Agents and Chemotherapy*, vol. 63, no. 8, pp. 1–10, 2019, doi: 10.1128/AAC.00779-19.
- [29] T. Olay, A. Rodriguez, L. E. Oliver, M. V. Vicente, and M. C. R. Quecedo, 'Interaction of fosfomycin with other antimicrobial agents: in vitro and in vivo studies', *Journal of Antimicrobial Chemotherapy*, vol. 4, no. 6, pp. 569–576, 1978, doi: 10.1093/jac/4.6.569.
- [30] A. C. Kastoris, P. I. Rafailidis, E. K. Vouloumanou, I. D. Gkegkes, and M. E. Falagas, 'Synergy of fosfomycin with other antibiotics for Gram-positive and Gram-negative bacteria', *European Journal of Clinical Pharmacology*, vol. 66, no. 4, pp. 359–368, 2010, doi: 10.1007/s00228-010-0794-5.
- [31] EMA, 'Zavicefta', European Medicines Agency. Accessed: Feb. 14, 2023. Available: <https://www.ema.europa.eu/en/medicines/human/EPAR/zavicefta>
- [32] G. G. Zhanel *et al.*, 'Ceftazidime-Avibactam: a Novel Cephalosporin/ β -lactamase Inhibitor Combination', *Drugs*, vol. 73, no. 2, pp. 159–177, 2013, doi: 10.1007/s40265-013-0013-7.
- [33] V. Pingue, R. Penati, A. Nardone, and D. Franciotta, 'Ceftazidime/avibactam neurotoxicity in an adult patient with normal renal function', *Clinical Microbiology and Infection*, vol. 27, no. 5, pp. 795–796, 2021, doi: 10.1016/j.cmi.2020.11.031.
- [34] R. P. Veiga and J.-A. Paiva, 'Pharmacokinetics–pharmacodynamics issues relevant for the clinical use of beta-lactam antibiotics in critically ill patients', *Critical Care*, vol. 22, no. 1, p. 233, 2018, doi: 10.1186/s13054-018-2155-1.
- [35] P. Lagacé-Wiens, A. Walkty, and J. Karlowsky, 'Ceftazidime-avibactam: an evidence-based review of its pharmacology and potential use in the treatment of Gram-negative bacterial infections', *Core Evidence*, vol. 9, pp. 13-25, 2014, doi: 10.2147/CE.S40698.

- [36] D. Yahav, C. G. Giske, A. Grāmatniece, H. Abodakpi, V. H. Tam, and L. Leibovici, 'New β -Lactam- β -Lactamase Inhibitor Combinations', *Clinical Microbiology Reviews*, vol. 34, no. 1, 2020, doi: 10.1128/CMR.00115-20.
- [37] A. N. Kristoffersson *et al.*, 'A novel mechanism-based pharmacokinetic-pharmacodynamic (PKPD) model describing ceftazidime/avibactam efficacy against β -lactamase-producing Gram-negative bacteria', *Journal of Antimicrobial Chemotherapy*, vol. 75, no. 2, pp. 400–408, 2019, doi: 10.1093/jac/dkz440.
- [38] S. K. B. Sy *et al.*, 'In vitro pharmacokinetics/pharmacodynamics of the combination of avibactam and aztreonam against MDR organisms', *Journal of Antimicrobial Chemotherapy*, vol. 71, no. 7, pp. 1866–1880, 2016, doi: 10.1093/jac/dkw082.
- [39] K. M. Papp-Wallace, 'The latest advances in β -lactam/ β -lactamase inhibitor combinations for the treatment of Gram-negative bacterial infections', *Expert Opinion on Pharmacotherapy*, vol. 20, no. 17, pp. 2169–2184, 2019, doi: 10.1080/14656566.2019.1660772.
- [40] C. Adembri, I. Cappellini, and A. Novelli, 'The role of PK/PD-based strategies to preserve new molecules against multi-drug resistant gram-negative strains', *Journal of Chemotherapy*, vol. 32, no. 5, pp. 219–225, 2020, doi: 10.1080/1120009X.2020.1786634.
- [41] B. Grabein, W. Graninger, J. Rodríguez Baño, A. Dinh, and D. B. Liesenfeld, 'Intravenous fosfomycin—back to the future. Systematic review and meta-analysis of the clinical literature', *Clinical Microbiology and Infection*, vol. 23, no. 6, pp. 363–372, 2017, doi: 10.1016/j.cmi.2016.12.005.
- [42] S. Parker, J. Lipman, D. Koulenti, G. Dimopoulos, and J. A. Roberts, 'What is the relevance of fosfomycin pharmacokinetics in the treatment of serious infections in critically ill patients? A systematic review', *International Journal of Antimicrobial Agents*, vol. 42, no. 4, pp. 289–293, 2013, doi: 10.1016/j.ijantimicag.2013.05.018.
- [43] M. Díez-Aguilar and R. Cantón, 'New microbiological aspects of fosfomycin.', *Revista española de quimioterapia: publicacion oficial de la Sociedad Española de Quimioterapia*, vol. 32 Suppl 1, no. 1, pp. 8–18, May 2019.

- [44] Y. Doi, 'Treatment Options for Carbapenem-resistant Gram-negative Bacterial Infections', *Clinical Infectious Diseases*, vol. 69, no. Supplement_7, pp. S565–S575, 2019, doi: 10.1093/cid/ciz830.
- [45] M. F. Mojica, M.-A. Rossi, A. J. Vila, and R. A. Bonomo, 'The urgent need for metallo- β -lactamase inhibitors: an unattended global threat', *The Lancet Infectious Diseases*, vol. 22, no. 1, pp. e28–e34, 2022, doi: 10.1016/S1473-3099(20)30868-9.
- [46] K. S. Kaye *et al.*, 'Fosfomycin for Injection (ZTI-01) Versus Piperacillin-tazobactam for the Treatment of Complicated Urinary Tract Infection Including Acute Pyelonephritis: ZEUS, A Phase 2/3 Randomized Trial', *Clinical Infectious Diseases*, vol. 69, no. 12, pp. 2045–2056, 2019, doi: 10.1093/cid/ciz181.
- [47] D. E. Karageorgopoulos, R. Wang, X. -h. Yu, and M. E. Falagas, 'Fosfomycin: evaluation of the published evidence on the emergence of antimicrobial resistance in Gram-negative pathogens', *Journal of Antimicrobial Chemotherapy*, vol. 67, no. 2, pp. 255–268, 2011, doi: 10.1093/jac/dkr466.
- [48] A. I. Nilsson, O. G. Berg, O. Aspevall, G. Kahlmeter, and D. I. Andersson, 'Biological Costs and Mechanisms of Fosfomycin Resistance in *Escherichia coli*', *Antimicrobial Agents and Chemotherapy*, vol. 47, no. 9, pp. 2850–2858, 2003, doi: 10.1128/AAC.47.9.2850-2858.2003.
- [49] EMA, 'Fosfomycin-containing medicinal products', European Medicines Agency. Accessed: Feb. 14, 2023. Available: <https://www.ema.europa.eu/en/medicines/human/referrals/fosfomycin-containing-medicinal-products>
- [50] S. J. Enna and M. Williams, 'Defining the Role of Pharmacology in the Emerging World of Translational Research', in *Advances in Pharmacology*, vol. 57, S. J. Enna and M. Williams, Eds., in Contemporary Aspects of Biomedical Research, vol. 57., Academic Press, 2009, pp. 1–30. doi: 10.1016/S1054-3589(08)57001-3.
- [51] A. Talevi and P. A. M. Quiroga, Eds., *ADME Processes in Pharmaceutical Sciences: Dosage, Design, and Pharmacotherapy Success*. Cham: Springer International Publishing, 2018. doi: 10.1007/978-3-319-99593-9.
- [52] R. I. Ogilvie, 'An introduction to pharmacokinetics', *Journal of Chronic Diseases*, vol. 36, no. 1, pp. 121–127, 1983, doi: 10.1016/0021-9681(83)90051-6.

- [53] P. J. Williams, A. Desai, and E. Ette, 'The Role of Pharmacometrics in Cardiovascular Drug Development', in *Cardiac Drug Development Guide*, New Jersey: Humana Press, 2003, pp. 365–388. doi: 10.1385/1-59259-404-2:365.
- [54] J. S. Barrett, M. J. Fossler, K. D. Cadieu, and M. R. Gastonguay, 'Pharmacometrics: A Multidisciplinary Field to Facilitate Critical Thinking in Drug Development and Translational Research Settings', *The Journal of Clinical Pharmacology*, vol. 48, no. 5, pp. 632–649, 2008, doi: 10.1177/0091270008315318.
- [55] E. I. Ette and P. J. Williams, *Pharmacometrics*. New Jersey: John Wiley & Sons, Inc., Hoboken, 2007.
- [56] J. V. S. Gobburu, 'Pharmacometrics 2020', *The Journal of Clinical Pharmacology*, vol. 50, no. S9, pp. 151S-157S, 2010, doi: 10.1177/0091270010376977.
- [57] L. B. Sheiner, S. Beal, B. Rosenberg, and V. V. Marathe, 'Forecasting individual pharmacokinetics', *Clinical Pharmacology & Therapeutics*, vol. 26, no. 3, pp. 294-305, 1979, doi: 10.1002/cpt1979263294.
- [58] E. I. Nielsen and L. E. Friberg, 'Pharmacokinetic-pharmacodynamic modeling of antibacterial drugs', *Pharmacological Reviews*, vol. 65, no. 3, pp. 1053–1090, 2013, doi: 10.1124/pr.111.005769.
- [59] L. B. Sheiner, B. Rosenberg, and V. V. Marathe, 'Estimation of population characteristics of pharmacokinetic parameters from routine clinical data', *Journal of Pharmacokinetics and Biopharmaceutics*, vol. 5, no. 5, pp. 445–479, 1977, doi: 10.1007/BF01061728.
- [60] S. Schmidt and H. Derendorf, *Applied Pharmacometrics*. in AAPS advances in the pharmaceutical sciences series, no. 14. New York: Springer, 2014.
- [61] P. L. Bonate, *Pharmacokinetic-Pharmacodynamic Modeling and Simulation*. Boston, MA: Springer US, 2011. doi: 10.1007/978-1-4419-9485-1.
- [62] L. B. Sheiner, B. Rosenberg, and K. L. Melmon, 'Modelling of individual pharmacokinetics for computer-aided drug dosage', *Computers and Biomedical Research*, vol. 5, no. 5, pp. 441–459, 1972, doi: 10.1016/0010-4809(72)90051-1.

- [63] J. S. Owen and J. Fiedler-Kelly, *Introduction to Population Pharmacokinetic / Pharmacodynamic Analysis with Nonlinear Mixed Effects Models*, vol. 50, no. 1. Hoboken, New Jersey: John Wiley & Sons, Inc, 2014. doi: 10.1002/9781118784860.
- [64] L. E. Friberg, 'Pivotal Role of Translation in Anti-Infective Development', *Clinical Pharmacology and Therapeutics*, vol. 109, no. 4, pp. 856–866, 2021, doi: 10.1002/cpt.2182.
- [65] M. J. E. Brill, A. N. Kristoffersson, C. Zhao, E. I. Nielsen, and L. E. Friberg, 'Semi-mechanistic pharmacokinetic–pharmacodynamic modelling of antibiotic drug combinations', *Clinical Microbiology and Infection*, vol. 24, no. 7, pp. 697–706, 2018, doi: 10.1016/j.cmi.2017.11.023.
- [66] C. B. Landersdorfer, N. S. Ly, H. Xu, B. T. Tsuji, and J. B. Bulitta, 'Quantifying subpopulation synergy for antibiotic combinations via mechanism-based modeling and a sequential dosing design', *Antimicrobial Agents and Chemotherapy*, vol. 57, no. 5, pp. 2343–2351, 2013, doi: 10.1128/AAC.00092-13.
- [67] S. Shiffman, M. Zettler-Segal, J. Kassel, J. Paty, N. L. Benowitz, and G. O'Brien, 'Nicotine elimination and tolerance in non-dependent cigarette smokers', *Psychopharmacology*, vol. 109, no. 4, pp. 449–456, 1992, doi: 10.1007/BF02247722.
- [68] Y. Yu, D. Rüppel, W. Weber, and H. Derendorf, 'PK/PD Approaches', in *Drug Discovery and Evaluation: Methods in Clinical Pharmacology*, F. J. Hock and M. R. Gralinski, Eds., Cham: Springer International Publishing, 2020, pp. 1047–1069. doi: 10.1007/978-3-319-68864-0_26.
- [69] E. I. Nielsen, O. Cars, and L. E. Friberg, 'Pharmacokinetic/Pharmacodynamic (PK/PD) Indices of Antibiotics Predicted by a Semimechanistic PKPD Model: a Step toward Model-Based Dose Optimization', *Antimicrobial Agents and Chemotherapy*, vol. 55, no. 10, pp. 4619–4630, 2011, doi: 10.1128/AAC.00182-11.
- [70] A. Abdulla *et al.*, 'Failure of target attainment of beta-lactam antibiotics in critically ill patients and associated risk factors: a two-center prospective study (EXPAT)', *Critical Care*, vol. 24, no. 1, p. 558, 2020, doi: 10.1186/s13054-020-03272-z.

- [71] S. Retout, S. Duffull, and F. Mentré, 'Development and implementation of the population Fisher information matrix for the evaluation of population pharmacokinetic designs', *Computer Methods and Programs in Biomedicine*, vol. 65, no. 2, pp. 141–151, 2001, doi: 10.1016/S0169-2607(00)00117-6.
- [72] G. Hendeby and F. Gustafsson, 'Detection Limits for Linear Non-Gaussian State-Space Models', in *Fault Detection, Supervision and Safety of Technical Processes 2006*, Elsevier, 2007, pp. 282–287. doi: 10.1016/B978-008044485-7/50048-8.
- [73] F. Mentré, A. Mallet, and D. Baccar, 'Optimal design in random-effects regression models', *Biometrika*, vol. 84, no. 2, pp. 429–442, 1997, doi: 10.1093/biomet/84.2.429.
- [74] A. C. Atkinson and A. N. Donev, *Optimum Experimental Designs*. Oxford: Oxford University Press, 1992.
- [75] B. Jones, K. Allen-Moyer, and P. Goos, 'A-optimal versus D-optimal design of screening experiments', *Journal of Quality Technology*, vol. 53, no. 4, pp. 369–382, 2020, doi: 10.1080/00224065.2020.1757391.
- [76] P. F. McDermott, D. G. White, S. Zhao, S. Simjee, and R. D. Walker, 'Antimicrobial Susceptibility Testing', *Preharvest and Postharvest Food Safety*, pp. 189–200, 2004, doi: 10.1002/9780470752579.ch15.
- [77] D. F. J. Brown and L. Brown, 'Evaluation of the E test, a novel method of quantifying antimicrobial activity', *Journal of Antimicrobial Chemotherapy*, vol. 27, no. 2, pp. 185–190, 1991, doi: 10.1093/jac/27.2.185.
- [78] C. D. Doern, 'When does 2 plus 2 equal 5? A review of antimicrobial synergy testing', *Journal of Clinical Microbiology*, vol. 52, no. 12, pp. 4124–4128, 2014, doi: 10.1128/JCM.01121-14.
- [79] J. H. Jorgensen and M. J. Ferraro, 'Antimicrobial Susceptibility Testing: A Review of General Principles and Contemporary Practices', *Clinical Infectious Diseases*, vol. 49, no. 11, pp. 1749–1755, 2009, doi: 10.1086/647952.

- [80] S. G. Wicha, M. G. Kees, J. Kuss, and C. Kloft, 'Pharmacodynamic and response surface analysis of linezolid or vancomycin combined with meropenem against *Staphylococcus aureus*', *Pharmaceutical Research*, vol. 32, no. 7, pp. 2410–2418, 2015, doi: 10.1007/s11095-015-1632-3.
- [81] F. C. Odds, 'Synergy, antagonism, and what the checkerboard puts between them', *Journal of Antimicrobial Chemotherapy*, vol. 52, no. 1, p. 1, 2003, doi: 10.1093/jac/dkg301.
- [82] C. R. Bonapace, J. A. Bosso, L. V. Friedrich, and R. L. White, 'Comparison of methods of interpretation of checkerboard synergy testing', *Diagnostic Microbiology and Infectious Disease*, vol. 44, no. 4, pp. 363–366, 2002, doi: 10.1016/S0732-8893(02)00473-X.
- [83] N. R. Twarog, M. Connelly, and A. A. Shelat, 'A critical evaluation of methods to interpret drug combinations', *Scientific Reports*, vol. 10, no. 1, pp. 1–13, 2020, doi: 10.1038/s41598-020-61923-1.
- [84] C. Chen, S. G. Wicha, R. Nordgren, and U. S. H. Simonsson, 'Comparisons of Analysis Methods for Assessment of Pharmacodynamic Interactions Including Design Recommendations', *The AAPS Journal*, vol. 20, no. 4, p. 77, 2018, doi: 10.1208/s12248-018-0239-0.
- [85] J. J.S. Cadwell, 'The Hollow Fiber Infection Model for Antimicrobial Pharmacodynamics and Pharmacokinetics', *Advances in Pharmacoepidemiology & Drug Safety*, vol. 01, no. S1, pp. 1–5, 2012, doi: 10.4172/2167-1052.S1-007.
- [86] N. Kroemer, R. Aubry, W. Couet, N. Grégoire, and S. G. Wicha, 'Optimized Rhombic Experimental Dynamic Checkerboard Designs to Elucidate Pharmacodynamic Drug Interactions of Antibiotics', *Pharmaceutical Research*, no. 39, pp. 3267–3277, 2022, doi: 10.1007/s11095-022-03396-7.
- [87] N. Kroemer, M. Martens, J.-W. Decusser, N. Grégoire, P. Nordmann, and S. G. Wicha, 'Evaluation of *in vitro* pharmacodynamic drug interactions of ceftazidime/avibactam and fosfomycin in *Escherichia coli*', *Journal of Antimicrobial Chemotherapy*, vol. 78, no. 10, pp. 2524–2534, 2023, doi: 10.1093/jac/dkad264.

- [88] N. Kroemer *et al.*, ‘Pharmacokinetic/pharmacodynamic analysis of ceftazidime/avibactam and fosfomycin combinations in an *in vitro* hollow fiber infection model against multidrug-resistant *Escherichia coli*’, *Microbiology Spectrum*, pp. e03318-23, 2024, doi: 10.1128/spectrum.03318-23.
- [89] N. Kroemer, J. W. Decousser, J. Buyck, N. Gregoire, P. Nordmann, and S. G. Wicha, ‘Systematic interaction screening of ceftazidime/avibactam and fosfomycin against eight isogenic *Escherichia coli* strains’, in *ECCMID*, Online, 2021.
- [90] N. Kroemer, R. Aubry, N. Gregoire, W. Couet, and S. G. Wicha, ‘Development and evaluation of D-optimal 2x2 checkerboard designs for identification of pharmacodynamic drug interactions’, in *PAGE*, online, 2021.
- [91] N. Kroemer, J. W. Decousser, J. Buyck, N. Gregoire, P. Nordmann, and S. G. Wicha, ‘Systematic “dynamic” checkerboard screening of eight isogenic *E. coli* strains against ceftazidime-avibactam and fosfomycin’, in *DPhG*, online, 2021.
- [92] N. Kroemer, J. W. Decousser, J. Buyck, N. Gregoire, P. Nordmann, and S. G. Wicha, ‘Systematic pharmacodynamic interaction screening of meropenem/vaborbactam and fosfomycin in isogenic and clinical *E. coli* and *K. pneumoniae* isolates expressing ESBL or carbapenemases’, in *ECCMID*, Lisbon, 2022.
- [93] A. Farooq *et al.*, ‘Interaction screening of ceftazidime-avibactam and tigecycline against six clinical and nine isogenic *E. coli* and *K. pneumoniae* strains expressing carbapenemases’, in *ECCMID*, Lisbon, 2022.
- [94] N. Kroemer, J.-W. Decousser, J. Buyck, P. Nordmann, and S. Wicha, ‘34: SYSTEMATIC IN VITRO INTERACTION STUDY ON CEFTAZIDIME/AVIBACTAM AND FOSFOMYCIN’, *Journal of Global Antimicrobial Resistance*, vol. 31, pp. S21–S22, 2022, doi: 10.1016/S2213-7165(22)00313-7.
- [95] F. Loingeville, T. T. Nguyen, M. K. Riviere, and F. Mentré, ‘Robust designs in longitudinal studies accounting for parameter and model uncertainties—application to count data’, *Journal of Biopharmaceutical Statistics*, vol. 30, no. 1, pp. 31–45, 2020, doi: 10.1080/10543406.2019.1607367.

- [96] J. Seurat, T. T. Nguyen, and F. Mentré, 'Robust designs accounting for model uncertainty in longitudinal studies with binary outcomes', *Statistical Methods in Medical Research*, vol. 29, no. 3, pp. 934–952, 2020, doi: 10.1177/0962280219850588.
- [97] J. Gabrielsson, B. Meibohm, and D. Weiner, 'Pattern Recognition in Pharmacokinetic Data Analysis', *The AAPS Journal*, vol. 18, no. 1, pp. 47–63, 2016, doi: 10.1208/s12248-015-9817-6.
- [98] W. Couet, 'Pharmacokinetics/pharmacodynamics characterization of combined antimicrobial agents: a real challenge and an urgent need', *Clinical Microbiology and Infection*, vol. 24, no. 7, pp. 687–688, 2018, doi: 10.1016/j.cmi.2018.03.047.
- [99] A. Dean, D. Voss, and D. Draguljić, 'Response Surface Methodology', in *Design and Analysis of Experiments*, A. Dean, D. Voss, and D. Draguljić, Eds., in Springer Texts in Statistics. Cham: Springer International Publishing, 2017, pp. 565–614. doi: 10.1007/978-3-319-52250-0_16.
- [100] V. H. Tam, A. N. Schilling, R. E. Lewis, D. A. Melnick, and A. N. Boucher, 'Novel approach to characterization of combined pharmacodynamic effects of antimicrobial agents', *Antimicrobial Agents and Chemotherapy*, vol. 48, no. 11, pp. 4315–4321, 2004, doi: 10.1128/AAC.48.11.4315-4321.2004.
- [101] W. R. Greco, H. S. Park, and Y. M. Rustum, 'Application of a New Approach for the Quantitation of Drug Synergism to the Combination of cis-Diamminedichloroplatinum and 1- θ -d-Arabinofuranosylcytosine', *Cancer Research*, vol. 50, no. 17, pp. 5318–5327, 1990.
- [102] M. Cokol *et al.*, 'Systematic exploration of synergistic drug pairs', *Molecular Systems Biology*, vol. 7, no. 1, p. 544, 2011, doi: 10.1038/msb.2011.71.
- [103] A. N. Boucher and V. H. Tam, 'Mathematical formulation of additivity for antimicrobial agents', *Diagnostic Microbiology and Infectious Disease*, vol. 55, no. 4, pp. 319–325, 2006, doi: 10.1016/j.diagmicrobio.2006.01.024.
- [104] F. Romanelli *et al.*, 'In Vitro Activity of Ceftazidime/Avibactam Alone and in Combination With Fosfomycin and Carbapenems Against KPC-producing *Klebsiella Pneumoniae*.' , *The new microbiologica*, vol. 43, no. 3, pp. 136–138, 2020.

- [105] L. M. Avery, C. A. Sutherland, and D. P. Nicolau, 'In vitro investigation of synergy among fosfomicin and parenteral antimicrobials against carbapenemase-producing Enterobacteriaceae', *Diagnostic Microbiology and Infectious Disease*, vol. 95, no. 2, pp. 216–220, 2019, doi: 10.1016/j.diagmicrobio.2019.05.014.
- [106] D. Ojdana, A. Gutowska, P. Sacha, P. Majewski, P. Wieczorek, and E. Trynieszewska, 'Activity of Ceftazidime-Avibactam Alone and in Combination with Ertapenem, Fosfomicin, and Tigecycline Against Carbapenemase-Producing *Klebsiella pneumoniae*', *Microbial Drug Resistance*, vol. 25, no. 9, pp. 1357–1364, 2019, doi: 10.1089/mdr.2018.0234.
- [107] K. M. Papp-Wallace *et al.*, 'Ceftazidime-Avibactam in Combination With Fosfomicin: A Novel Therapeutic Strategy Against Multidrug-Resistant *Pseudomonas aeruginosa*', *The Journal of Infectious Diseases*, vol. 220, no. 4, pp. 666–676, 2019, doi: 10.1093/infdis/jiz149.
- [108] I. J. Abbott, E. van Gorp, R. A. Wijma, J. Meletiadis, J. W. Mouton, and A. Y. Peleg, 'Evaluation of pooled human urine and synthetic alternatives in a dynamic bladder infection in vitro model simulating oral fosfomicin therapy', *Journal of Microbiological Methods*, vol. 171, p. 105861, 2020, doi: 10.1016/j.mimet.2020.105861.
- [109] J. W. Mouton and A. A. Vinks, 'Pharmacokinetic/Pharmacodynamic Modelling of Antibacterials In Vitro and In Vivo Using Bacterial Growth and Kill Kinetics', *Clinical Pharmacokinetics*, vol. 44, no. 2, pp. 201–210, 2005, doi: 10.2165/00003088-200544020-00005.
- [110] Clinical and Laboratory Standards Institute (CLSI), *M07-A10: Methods for Dilution Antimicrobial Susceptibility Tests for Bacteria That Grow Aerobically; Approved Standard*, vol. 35, no. 2. 2015.
- [111] J. W. Mouton, 'Soup with or without meatballs: Impact of nutritional factors on the MIC, kill-rates and growth-rates', *European Journal of Pharmaceutical Sciences*, vol. 125, pp. 23–27, 2018, doi: 10.1016/j.ejps.2018.09.008.

- [112] M. Ortiz-Padilla *et al.*, 'Role of inorganic phosphate concentrations in in vitro activity of fosfomycin', *Clinical Microbiology and Infection*, vol. 28, no. 2, p. 302.e1-302.e4, 2022, doi: 10.1016/j.cmi.2021.09.037.
- [113] J. R. Lenhard and Z. P. Bulman, 'Inoculum effect of β -lactam antibiotics', *Journal of Antimicrobial Chemotherapy*, vol. 74, no. 10, pp. 2825–2843, 2019, doi: 10.1093/jac/dkz226.
- [114] M. Ballesterro-Télez *et al.*, 'Role of inoculum and mutant frequency on fosfomycin MIC discrepancies by agar dilution and broth microdilution methods in Enterobacteriaceae', *Clinical Microbiology and Infection*, vol. 23, no. 5, pp. 325–331, 2017, doi: 10.1016/j.cmi.2016.12.022.
- [115] D. M. Livermore *et al.*, 'In Vitro Selection of Ceftazidime-Avibactam Resistance in Enterobacteriaceae with KPC-3 Carbapenemase', *Antimicrobial Agents and Chemotherapy*, vol. 59, no. 9, pp. 5324–5330, 2015, doi: 10.1128/AAC.00678-15.
- [116] European Committee on Antimicrobial Susceptibility Testing (EUCAST), 'Clinical Breakpoint Tables v. 13.0', 13.0, Jan. 2023. Accessed: Feb. 22, 2023. Available: https://www.eucast.org/fileadmin/src/media/PDFs/EUCAST_files/Breakpoint_tables/v_13.0_Breakpoint_Tables.pdf
- [117] P. C. Fuchs, A. L. Barry, and S. D. Brown, 'Susceptibility testing quality control studies with fosfomycin tromethamine', *European Journal of Clinical Microbiology and Infectious Diseases*, vol. 16, no. 7, pp. 538–540, 1997, doi: 10.1007/BF01708240.
- [118] M. F. Mojica *et al.*, 'Performance of disk diffusion and broth microdilution for fosfomycin susceptibility testing of multidrug-resistant clinical isolates of Enterobacterales and *Pseudomonas aeruginosa*', *Journal of Global Antimicrobial Resistance*, vol. 21, pp. 391–395, 2020, doi: 10.1016/j.jgar.2020.01.003.
- [119] J. V. Pereira, A. K. Bari, R. Kokare, and A. Poojary, 'Comparison of in vitro fosfomycin susceptibility testing methods with agar dilution for carbapenem resistant *Klebsiella pneumoniae* and *Escherichia coli*', *Indian Journal of Medical Microbiology*, vol. 42, pp. 39–45, 2023, doi: 10.1016/j.ijmmb.2023.01.005.

- [120] E. I. Nielsen, O. Cars, and L. E. Friberg, 'Predicting In Vitro Antibacterial Efficacy across Experimental Designs with a Semimechanistic Pharmacokinetic-Pharmacodynamic Model', *Antimicrobial Agents and Chemotherapy*, vol. 55, no. 4, pp. 1571–1579, 2011, doi: 10.1128/AAC.01286-10.
- [121] W. van Os *et al.*, 'Impact of individual ascitic fluids on growth of *Escherichia coli* and antimicrobial effect of ceftriaxone', in *ECCMID*, Online, 2021.
- [122] M. E. Falagas, F. Athanasaki, G. L. Voulgaris, N. A. Triarides, and K. Z. Vardakas, 'Resistance to fosfomycin: Mechanisms, Frequency and Clinical Consequences', *International Journal of Antimicrobial Agents*, vol. 53, no. 1, pp. 22–28, 2019, doi: 10.1016/j.ijantimicag.2018.09.013.
- [123] European Committee on Antimicrobial Susceptibility Testing (EUCAST), 'Important considerations for breakpoint setting of antibiotic-inhibitor combinations v. 2', 2021. Accessed: Feb. 22, 2023.
Available: https://www.eucast.org/fileadmin/src/media/PDFs/EUCAST_files/Guidance_documents/Inhibitor_combinations_-_Guidance_for_drug_developers_v2_20211214.pdf
- [124] J. Berkhout, M. J. Melchers, A. C. van Mil, W. W. Nichols, and J. W. Mouton, 'In Vitro Activity of Ceftazidime-Avibactam Combination in In Vitro Checkerboard Assays', *Antimicrobial Agents and Chemotherapy*, vol. 59, no. 2, pp. 1138–1144, 2015, doi: 10.1128/AAC.04146-14.
- [125] G. A. Detter, H. Knothe, B. Schönenbach, and G. Plage, 'Comparative study of fosfomycin activity in Mueller–Hinton media and in tissues', *Journal of Antimicrobial Chemotherapy*, vol. 11, no. 6, pp. 517–524, 1983, doi: 10.1093/jac/11.6.517.
- [126] S. S. Patel, J. A. Balfour, and H. M. Bryson, 'Fosfomycin Tromethamine', *Drugs*, vol. 53, no. 4, pp. 637–656, 1997, doi: 10.2165/00003495-199753040-00007.
- [127] R. Dimelow, J. G. Wright, M. MacPherson, P. Newell, and S. Das, 'Population Pharmacokinetic Modelling of Ceftazidime and Avibactam in the Plasma and Epithelial Lining Fluid of Healthy Volunteers', *Drugs in R and D*, vol. 18, no. 3, pp. 221–230, 2018, doi: 10.1007/s40268-018-0241-0.

- [128] A. N. Deitchman, R. S. P. Singh, and H. Derendorf, 'Nonlinear Protein Binding: Not What You Think', *Journal of Pharmaceutical Sciences*, vol. 107, no. 7, pp. 1754–1760, 2018, doi: 10.1016/j.xphs.2018.03.023.
- [129] Y. Li, A. Karlin, J. D. Loike, and S. C. Silverstein, 'A critical concentration of neutrophils is required for effective bacterial killing in suspension', *Proceedings of the National Academy of Sciences*, vol. 99, no. 12, pp. 8289–8294, 2002, doi: 10.1073/pnas.122244799.
- [130] S. Das, D. Zhou, W. W. Nichols, A. Townsend, P. Newell, and J. Li, 'Selecting the dosage of ceftazidime–avibactam in the perfect storm of nosocomial pneumonia', *European Journal of Clinical Pharmacology*, vol. 76, no. 3, pp. 349–361, 2020, doi: 10.1007/s00228-019-02804-z.
- [131] T. Tängdén *et al.*, 'The role of infection models and PK/PD modelling for optimising care of critically ill patients with severe infections', *Intensive Care Medicine*, vol. 43, no. 7, pp. 1021–1032, 2017, doi: 10.1007/s00134-017-4780-6.
- [132] J. A. Roberts *et al.*, 'Individualised antibiotic dosing for patients who are critically ill: Challenges and potential solutions', *The Lancet Infectious Diseases*, vol. 14, no. 6, pp. 498–509, 2014, doi: 10.1016/S1473-3099(14)70036-2.
- [133] P. Gaibani *et al.*, 'Suboptimal drug exposure leads selection of different subpopulations of ceftazidime/avibactam-resistant KPC-producing *Klebsiella pneumoniae* in a critically ill patient', *International Journal of Infectious Diseases*, pp. 0–13, 2021, doi: 10.1016/j.ijid.2021.10.028.
- [134] H. Hayami, T. Goto, M. Kawahara, and Y. Ohi, 'Activities of β -lactams, fluoroquinolones, amikacin and fosfomycin alone and in combination against *Pseudomonas aeruginosa* isolated from complicated urinary tract infections', *Journal of Infection and Chemotherapy*, vol. 5, no. 3, pp. 130–138, 1999, doi: 10.1007/s101560050022.
- [135] M. Okazaki *et al.*, 'Effectiveness of fosfomycin combined with other antimicrobial agents against multidrug-resistant *Pseudomonas aeruginosa* isolates using the efficacy time index assay', *Journal of Infection and Chemotherapy*, vol. 8, no. 1, pp. 37–42, 2002, doi: 10.1007/s101560200004.

- [136] P. Bhagunde, K.-T. Chang, E. B. Hirsch, K. R. Ledesma, M. Nikolaou, and V. H. Tam, 'Novel Modeling Framework To Guide Design of Optimal Dosing Strategies for β -Lactamase Inhibitors', *Antimicrobial Agents and Chemotherapy*, vol. 56, no. 5, pp. 2237–2240, 2012, doi: 10.1128/AAC.06113-11.
- [137] A. Chauzy, J. Buyck, B. L. M. de Jonge, S. Marchand, N. Grégoire, and W. Couet, 'Pharmacodynamic modelling of β -lactam/ β -lactamase inhibitor checkerboard data: illustration with aztreonam–avibactam', *Clinical Microbiology and Infection*, vol. 25, no. 4, p. 515.e1-515.e4, 2019, doi: 10.1016/j.cmi.2018.11.025.
- [138] European Committee on Antimicrobial Susceptibility Testing (EUCAST), 'EUCAST General Consultation on Fosfomycin IV breakpoints', 2022. Accessed: Dec. 12, 2022. Available: https://www.eucast.org/fileadmin/src/media/PDFs/EUCAST_files/Consultation/2022/EUCAST_General_Consultation_on_Fosfomycin_IV_final__20220514.pdf

7 Appendix

7.1 Supplementary material of Publication I

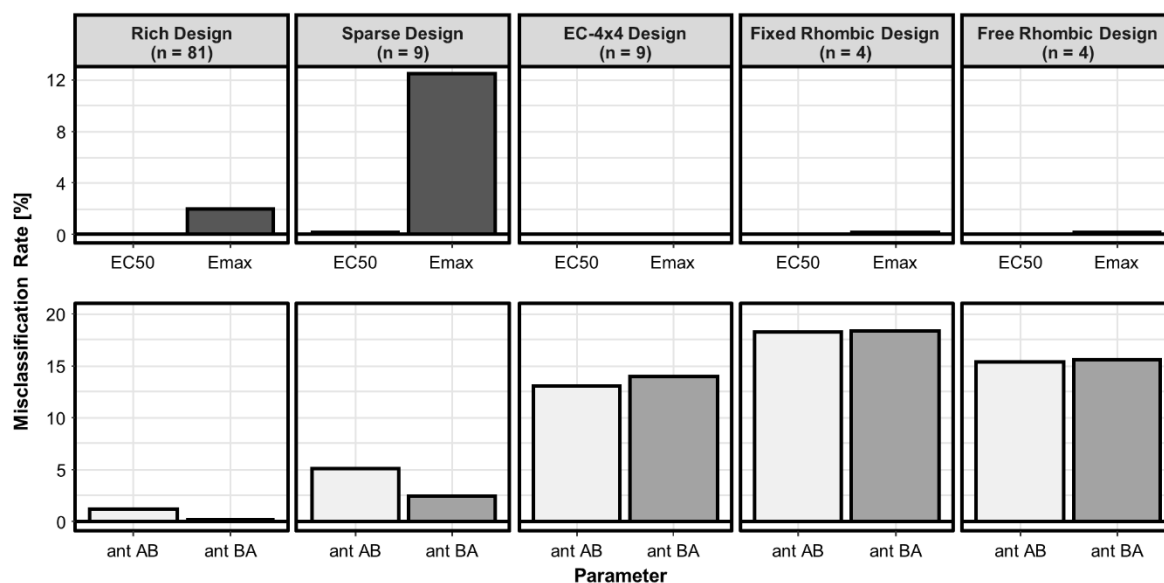
Supplement Text 1: Materials and Methods: SSE for strong monodirectional antagonisms

To evaluate the different experimental designs in their ability to identify very strong monodirectional antagonistic interactions where one drug fully suppresses the effect of the companion drug an SSE with the following adjustments was conducted: the INT-parameters for one drug was set to 99 for competitive EC50 interactions or to -0.99 for allosteric Emax antagonisms. The INT parameter of the combination partner was set to 0. To account for the monodirectional interactions the criterion for a correct classified interaction was adjusted and a conservative additivity margin for the INT parameter of -0.2 to 0.2 was added. In this case an additivity margin means a threshold value of an INT parameter that is necessary to identify a synergistic or antagonistic interaction over additivity.

Supplement Text 2: Results: SSE for strong monodirectional antagonisms

The misclassification rates for the SSE evaluating strong monodirectional antagonistic interactions are displayed on Supplement Figure 1. The misclassification of EC50 or Emax interactions are similar to interactions with more moderate interaction effect sizes. The identification of Emax interactions by the conventional sparse design was worst, which corresponded to the very small AIC differences when discriminating both types of interactions (Supplement Table I).

Comparing the misclassification rates of the antagonistic interactions, the two groups of conventional and EC-based designs clearly differed. While the conventional rich and sparse designs display misclassification rates < 5.08%, all EC-based designs misclassified > 12.99% of the antagonistic interactions.



Supplement Figure 1: Misclassification rates of the different checkerboard designs in the SSE study investigating strong monodirectional antagonistic interactions. Classification rates for discriminating competitive (EC50) or allosteric (Emax) interactions were calculated as well as for identifying the correct type of the interaction (ant AB: antagonism drug A affected by drug B, ant BA: antagonism drug B affected by drug A). n represents the number of combination scenarios included in the respective experimental design.

Supplement Table I: SSE statistics on the ability of the different experimental designs to discriminate between EC50 and Emax interactions when analyzing strong antagonistic interactions.

	Reference designs			Rhombic designs	
	conventional		EC 4x4	fixed	free
	rich	spars e			
Combination scenarios	81	9	9	4	4
Min. AIC^a difference for interaction discrimination (EC50, Emax) in $\geq 95\%$ of the simulations	19.05	1.03	28.85	18.05	14.10

^aAIC, Akaike Information criterion

Supplement Text 3: Discussion: SSE for strong monodirectional antagonisms

Very strong interactions as full antagonism can be challenging for experimental designs. Especially EC-based designs showed inferior classification of the interactions, because their flexible and adaptive layout is linked to the drug potencies in opposite to wider standard concentrations as the conventional rich or conventional sparse design. Therefore, the concentrations to quantify very strong interactions can lay outside the concentration range of the experimental design, which is less likely to happen in an unspecific design with standardized concentration levels. Therefore, it would always be recommended to check the results for biological plausibility and consider retesting, when strong interactions occur.

7.2 Supplementary material of Publication II

Text S1: Pharmacometric modelling of the EC_{50-24h}

The EC₅₀ after 24 h was determined by description of the cfu/mL using a sigmoidal Emax model (Eq. (1)), with Baseline being the bacterial count without antibiotic exposure, Emax the maximum log₁₀(cfu/mL) reduction, C the concentration of the drug (mg/L), H the sigmoidicity parameter and the EC₅₀ being the concentration at which the effect is half-maximum.

$$E(C) = \text{Baseline} - \frac{\text{Emax} \cdot C^H}{\text{EC}_{50}^H + C^H} \quad (1)$$

Parameter estimation was performed by minimizing the negative log-likelihood (-LL) objective function criterion (Eq. (2)) using 'optim' from the R package stats (version 3.6.3). The criterion was calculated as follows:

$$\text{OF}_{-LL} = 0.5 \cdot \sum_{j=1}^n \left[\frac{(\text{obs}_j - \text{pred}_j)^2}{\sigma_j^2} + \ln \sigma_j^2 \right] \quad (2)$$

with obs_j being the jth observation, pred_j the respective jth model prediction and σ² being the residual variability. To guide the minimization the pharmacodynamic (PD) parameters were estimated in four different implementations of the sigmoidal Emax model (Eq. (1)): i) all parameters were freely estimated, ii) the Baseline value was fixed to the median of the bacterial count without antibiotic exposure, iii) the Baseline and Emax value were fixed to the median of the bacterial count without antibiotic exposure and iv) Emax value and Baseline were estimated as one parameter value. The initials for the parameter estimation were based on the data of the respective antibiotic and bacterial strain. Model selection was based on the -LL, graphical model fit and biological plausibility (e.g. Emax not higher than Baseline value).

Text S2: Pharmacometric modelling of drug interactions of the ‘dynamic’ checkerboard experiments

The mono drug PD parameters were updated after the checkerboard experiment as outlined above and fixed for the estimation of the drug interactions. No interaction was described by Bliss Independence with single drug effects normalised to 1 for calculation of the probabilistic Bliss Independence term and then scaled back to the effect scale (Eqs. (3)-(4)), drug interactions were assessed in a naive pooling data approach using the general pharmacodynamic interaction (GPDI) model implemented in R.¹⁻³

$$E_{\max} = \max(E_{\max,A}, E_{\max,B}) \quad (3)$$

$$E_{\text{comb}} = \left(\frac{E_A}{E_{\max}} + \frac{E_B}{E_{\max}} - \frac{E_A}{E_{\max}} \cdot \frac{E_B}{E_{\max}} \right) \cdot E_{\max} \quad (4)$$

The GPDI model describes interactions directionally by the insertion of a GPDI-term. Depending on the polarity of the INT-parameter synergistic, antagonistic or no drug interactions can be described and the GPDI model enables a discrimination between interactions on EC_{50} (competitive) or E_{\max} (allosteric).

As for the bactericidal drug effects of ceftazidime/avibactam and fosfomycin without combination a total killing was observed, it applied that $E_{\max} = \text{Baseline}$. Therefore, interactions on level of E_{\max} were not possible and solely competitive interactions as shifts of the drugs potency (EC_{50}) of a victim drug by a perpetrator were considered (Eq. (5)).

$$EC_{50\text{GPDI}} = EC_{50} \cdot \left(1 + \frac{\text{INT} \cdot C^{\text{H}_{\text{INT}}}}{EC_{50-\text{INT}}^{\text{H}_{\text{INT}}} + C^{\text{H}_{\text{INT}}}} \right) \quad (5)$$

with EC_{50} being the potency of the victim drug, INT the maximum fractional shift of the interaction, C the concentration of the perpetrator of the interaction, $EC_{50-\text{INT}}$ the potency of the interaction and H_{INT} the sigmoidicity of the interaction. For simplification H_{INT} was fixed to 1 and as very strong PD drug interactions were observed the $EC_{50-\text{INT}}$ was not only fixed to the perpetrators EC_{50} but to a small fraction of the lowest checkerboard concentration ($0.05 \cdot EC_{08}$). Alternatively, the GPDI could be collapsed to $EC_{50-\text{GPDI}} = EC_{50} \times (1 + \text{INT})$ to account strong PD interactions. Parameter estimation was performed by minimizing the -LL objective function criterion (Eq. (2)) using ‘optim’ from

the R package stats (version 3.6.3). To guide the minimization no or mono- and bidirectional interactions were tested and the Akaike Information Criterion (AIC) was calculated. After estimation of the INT parameters the Hessian was calculated within the 'optim' function. The standard errors of the estimates (SE's) were derived as square roots of the diagonal values on the inverse Hessian matrix. 95% confidence intervals (CI) of the INT parameter estimates were calculated as INT-parameter $\pm 1.96 \cdot SE$. The model selection was based on the model with the lowest AIC and CIs of the INT parameters not overlapping with 0. The INT parameters were reported as fractional interaction shifts at the EC_{50} of the perpetrator drug.

Text S3: Pharmacometric modelling of the time kill experiments

PD models for the static time kill data were developed sequentially for the three different clinical *E. coli* strains. The lower limit of quantification (LLOQ) for bacterial counts by serial dilution and plating on agar plates was at 10^1 - 10^2 cfu/mL. Below limit of quantification (BLOQ) data was empirically set to 1 cfu/mL and included in the modelling. Base for the model was a two compartmental ordinary differential equation (ODE) system describing a susceptible (S) and a resistant (R) subpopulation experiencing different drug effects (E_S and E_R). Both subpopulations were described with separate inocula as initial conditions, separate growth rates (k_{GS} and k_{GR}) and a global bacterial capacity limit B_{max} of the system. To capture biological variability with regard to resistance development inter-experimental variability was introduced as exponential coefficient of variation on the inoculum of the (R) subpopulation.

$$\frac{dS}{dt} = S \cdot k_{GS} \cdot \left(1 - \frac{S+R}{B_{max}}\right) - S \cdot E_S \quad (6)$$

$$\frac{dR}{dt} = R \cdot k_{GR} \cdot \left(1 - \frac{S+R}{B_{max}}\right) - S \cdot E_R \quad (7)$$

In a first step the mono drug effects were introduced separately for each subpopulation preferred as sigmoidal Emax models (with or without sigmoidicity parameter fixed to 1) or power function (Eqs. (8)-(9)).

$$E(C) = \frac{E_{max} \cdot C^H}{EC_{50}^H + C^H} \quad (8)$$

$$E(C) = \text{Slope} \cdot C^H \quad (9)$$

Model selection was made on graphical model fit, model stability, AIC and biological plausibility.

After estimation of the mono drug PD parameters, they were fixed and the model was applied on combination experiment data. For description of no interaction Bliss Independence with single drug effects normalised to 1 for calculation of the probabilistic Bliss Independence term and then scaled back to the effect scale was used to calculate the combined drug effects on the S or R subpopulations (Eqs. (3)-(4)). In case of effects were described by a power function effect sizes below 50% of a presumable Emax were assumed. In these cases, effect addition was applied as an approximation of Bliss

Independence as the probabilistic correction becomes neglectable for small effect sizes (Eq. (10)).⁴

$$E_{\text{comb}} = E_A + E_B \quad (10)$$

Drug interactions were introduced using the GPDI model outlined above (Eq. (5)).¹ Beside Bliss Independence four different mono- and bidirectional interactions affecting the EC_{50} or E_{max} of the drugs on the R subpopulation utilizing the GPDI model were evaluated: i) monodirectional interaction with ceftazidime/avibactam as perpetrator affecting fosfomycin EC_{50} or E_{max} (ceftazidime/avibactam \rightarrow fosfomycin), ii) monodirectional interaction with fosfomycin as perpetrator affecting ceftazidime/avibactam EC_{50} or E_{max} (ceftazidime/avibactam \leftarrow fosfomycin), iii) bidirectional interactions with ceftazidime/avibactam and fosfomycin being perpetrator and victim at the same time with the same INT-parameter (ceftazidime/avibactam \leftrightarrow fosfomycin one INT), iv) bidirectional interactions with ceftazidime/avibactam and fosfomycin being perpetrator and victim at the same time with different INT-parameters (ceftazidime/avibactam \leftrightarrow fosfomycin separate INT). The model describing the combination data best was chosen based on graphical model fit, AIC, model stability and condition number.

The model fit was evaluated by visual predictive checks based on 1000 simulations and plotting of the 90% prediction interval (Fig. 3-5)

Parameter uncertainty was assessed using the SIR algorithm implemented by PsN 5.0 (Uppsala University, Sweden) with 10% inflated relative standard errors (RSE) produced by the covariance step in NONMEM as proposal distribution. M/m was increased to 20 to reach stable differences in objective function value (dOFV) distributions.

Text S4: Results of the pharmacodynamic interaction screening

The drug interaction screening revealed inhomogeneous results with regard to the direction of the drug interaction of ceftazidime/avibactam and fosfomycin. An exploratory graphical analysis was performed to detect correlations between the identified interaction and characteristics of the bacterial strains, the drug effect sizes or ratios of susceptibility (Figure S1). None of the inspected variables could be identified to explain the direction of the interaction. Therefore, no clear conclusion can be drawn and a composite mechanism of interaction with different expressions in different strains is the most likely explanation.

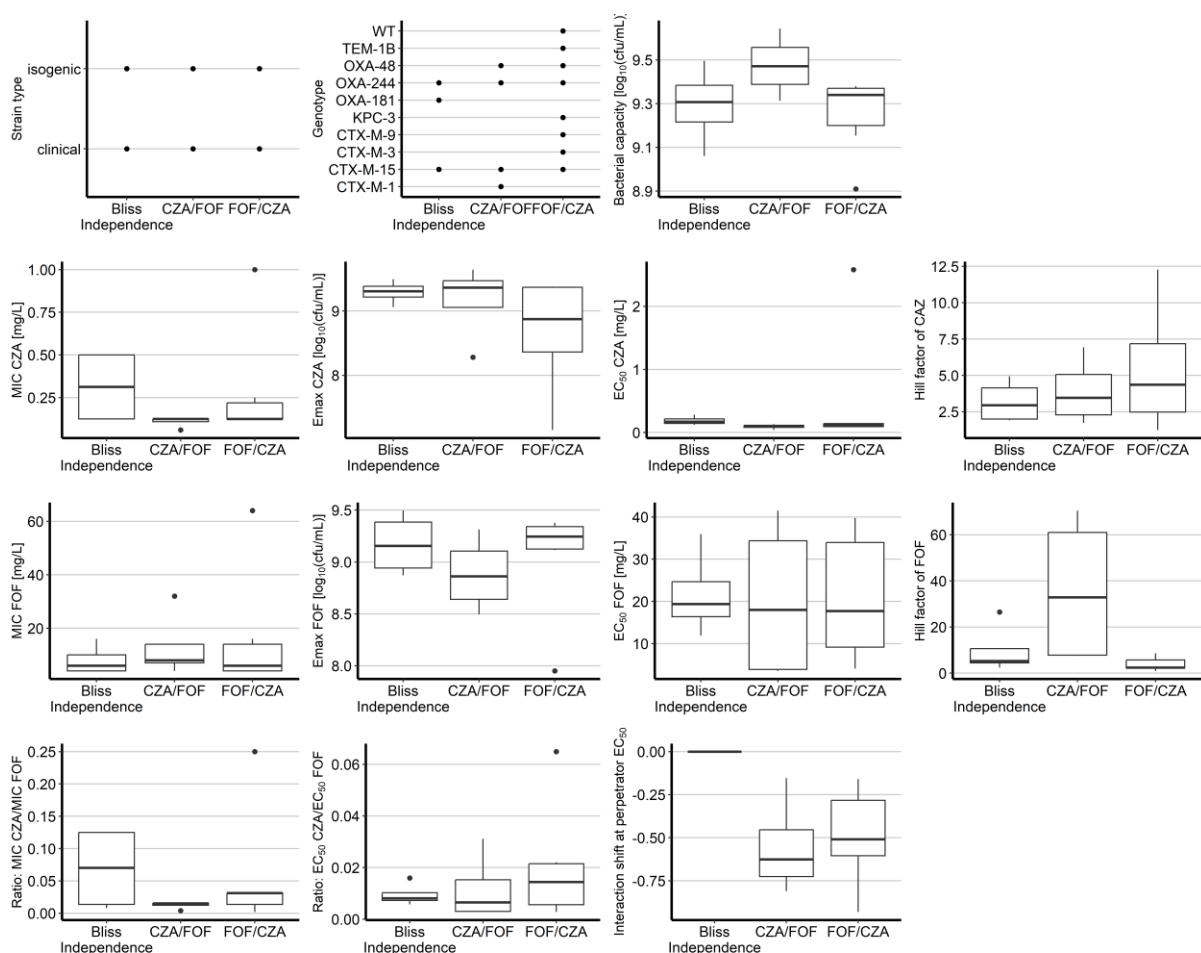


Figure S1: Exploratory graphical analysis to investigate potential correlations of the determined interaction directions (Bliss Independence or drug interaction (victim/perpetrator)) against different parameters of susceptibility and drug effect. CZA, ceftazidime/avibactam; FOF, fosfomycin.

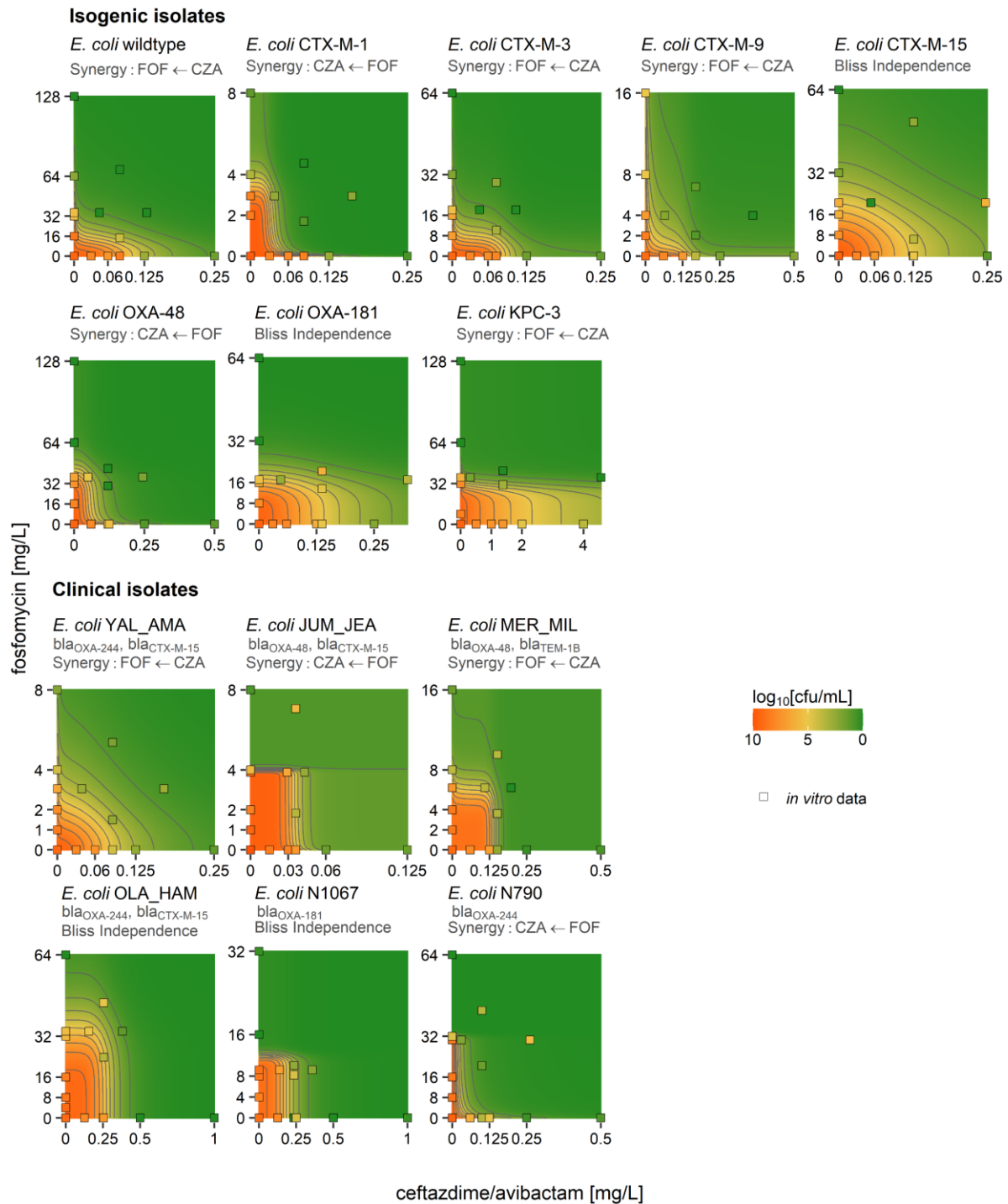


Figure S2: Calculated interaction response surfaces based on Bliss Independence GPDI models for each clinical or isogenic *E. coli* strain presenting the estimated drug interactions. Directions of the interactions are illustrated by arrows (victim ← perpetrator). Calculated combined effects are illustrated as colour gradient. Green areas display areas of high effects and red areas highlight low effect sizes measured in log₁₀[cfu/mL] after 24 h. The squares correspond to obtained *in vitro* data filled with respective colour gradient as outlined above. The avibactam concentration as supplement for ceftazidime was fixed to 4 mg/L. CZA, ceftazidime/avibactam; FOF, fosfomycin.

Text S5: Model selection for modelling of the time kill experiments

The exploratory graphical analysis of the drug combinations suggested drug interactions on EC_{50} because the drug interactions led to maintained drug effects at reduced drug concentrations rather than to stronger killing effects. The implementations of the GPDI model on Emax were not supported by the data and led to instable models, termination of runs and elevated objective function values. Therefore, for *E. coli* YAL_AMA an interaction model with ceftazidime/avibactam altering the fosfomycin EC_{50} described the data best (AIC: Bliss Independence: 6372.316; ceftazidime/avibactam->fosfomycin: 811.179; ceftazidime/avibactam<-fosfomycin: 1069.613; ceftazidime/avibactam<->fosfomycin one INT: 815.958; ceftazidime/avibactam<->fosfomycin separate INT: 815.3). The data for *E. coli* JUM_JEA was described by an interaction with fosfomycin altering the ceftazidime/avibactam EC_{50} (AIC: Bliss Independence: 3606.366; ceftazidime/avibactam->fosfomycin: 934.731; ceftazidime/avibactam<-fosfomycin: 764.334; ceftazidime/avibactam<->fosfomycin one INT: 943.782; ceftazidime/avibactam<->fosfomycin separate INT: 887.009). The interaction of ceftazidime/avibactam-fosfomycin in *E. coli* MER_MIL was described by ceftazidime/avibactam altering the fosfomycin EC_{50} (AIC: Bliss Independence: 1688.836; ceftazidime/avibactam->fosfomycin: 761.448; ceftazidime/avibactam<-fosfomycin: 764.831; ceftazidime/avibactam<->fosfomycin one INT: 768.831; ceftazidime/avibactam<->fosfomycin separate INT: 770.772).

In the last step all model parameters were unfixed and the model was fitted to the whole dataset to obtain final parameter-estimates. Shrinkage of the inter-experimental variability on the inoculum of the (R) subpopulation was < 25% for all three models.

References

1. Wicha SG, Chen C, Clewe O, *et al.* A general pharmacodynamic interaction model identifies perpetrators and victims in drug interactions. *Nat Commun* 2017; **8**: 2129.
2. R Core Team. R: A Language and Environment for Statistical Computing. 2021.
3. Bliss CI. The Toxicity of Poisons Applied Jointly. *Ann Appl Biol* 1939; **26**: 585–615.
4. Chen C, Wicha SG, De Knecht GJ, *et al.* Assessing pharmacodynamic interactions in mice using the multistate tuberculosis pharmacometric and general pharmacodynamic interaction models. *CPT Pharmacomet Syst Pharmacol* 2017; **6**: 787–97.

7.3 Supplementary material of Publication III

Methods

Text S1: Methods of the hollow fiber infection model (HFIM)

The HFIM system was conducted with polysulfone cartridges (C2011) purchased from FiberCell® Systems Inc. The central compartment had a volume of 200 mL and its circulation through the hollow fiber cartridge was ensured by a Duet Pump (FiberCell® Systems Inc., USA) with a flowrate of approximately 80 mL/min. The central compartment was connected with the hollow fiber cartridge by 4 m of oxygenator tubing. An Ismatec® Reglo ICC (12 rolls; VWR, USA) was used to pump fresh Mueller-Hinton-Broth 2 (MHB) (Sigma-Aldrich, USA) from a reservoir into the central compartment with flow-rates ranging from 0.834 mL/min to 1.28 mL/min. The same volume was removed by a Masterflex L/S® digital pump drive (100 RPM, VWR, USA). Doses of the drugs were administered into the central compartment by a programmable syringe driver (Masterflex® Touch-Screen Syringe Pump 74905-54; VWR, USA). Because the elimination half-life of ceftazidime, avibactam and fosfomycin for the chosen conditions were approximately similar the HFIM setup was not augmented by additional dosing compartments (1). Before inoculation of the experiments the sterility of the cartridge and central compartment was checked by plating and incubation of samples of the respective compartments. The retention of the previously identified beta-lactamases CTX-M-15 and OXA-244 in the hollow fiber cartridge was corroborated exemplarily by antigen tests of the bacterial suspension and the central compartment after 2 h of preincubation before the addition of the first dose. To identify the respective beta-lactamases the NG-Test® CTX-M and NG-Test® CARBA-5 (NG Biotech, France) were used. Those tests identify CTX-M and OXA-48 like enzymes.

Up to 20 pharmacokinetic and pharmacodynamic samples were drawn at predetermined timepoints.

Pharmacodynamic samples were serially diluted and plated on drug-free agar plates and plates containing threefold minimum inhibitory concentrations (MIC). The growing

colonies were counted after 24 h and 48 h respectively. The HFIM were performed as single experiments.

Text S2: Methods of the bioanalysis

The bioanalysis of the pharmacokinetic samples from the HFIM was performed to confirm the nominal concentrations and experimental conditions. To confirm the planned pharmacokinetic profiles, the drug concentrations at the beginning of each dosing interval (0.75 h time after dose) and mid-interval concentrations (4 h time after dose) were measured. The samples from the central compartment were stored at -80 °C after collection and thawed immediately before preparation. Calibration curves including seven calibration standards were prepared based on the expected drug concentrations in the HFIM experiments. The calibration curves ranged from 0.1 µg/mL to 40 µg/mL for ceftazidime, from 0.02 µg/mL to 10 µg/mL for avibactam and from 0.5 µg/mL to 50 µg/mL for fosfomycin. Samples expecting a higher fosfomycin concentration than 50 µg/mL were diluted 1:3 with MHB prior to sample preparation. To precipitate proteins 100 µL of sample were mixed with 50 µL internal standard solution (0.2 µg/mL moxifloxacin in methanol) and 300 µL ice-cold acetonitrile. The samples were then centrifuged at 17968 g at 4 °C for 20 min and 2 µL supernatant were directly injected on an Agilent 1290 Infinity 2 (Agilent Technologies, USA) UHPLC system coupled with a QTRAP 5500 (Sciex, USA) electrospray ionization mass spectrometer. Separation was achieved on a reverse phase Nucleodur PFP column (100x2 mm, 3 µm particle size; Macherey-Nagel, Germany) at 35 °C with a gradient elution. Solvents used were water containing 0.1% formic acid (A) and acetonitrile containing 0.1% formic acid (B). The gradient elution was performed as follows: starting conditions were 100% (A). After 0.8 min (B) linearly increased to 20% until 2 min and from there further increased to 40% (B) until 3.5 min, followed by isocratic elution with 40% (B) until 4.5 min and a return to starting conditions of 100% (A) after 4.6 min and reconditioning until 6 min. Fosfomycin and avibactam were detected within the first four minutes with the mass spectrometer operating in negative mode and then switched to positive mode for the detection of

ceftazidime and moxifloxacin. Details on the ion source and detection parameters of the analytes are provided in Tables S1 and S2.

Table S1: Ion source parameters of the two different ESI phases of the method

	Curtain Gas (psi)	Collision Gas	Ion Spray Voltage (volt)	Temperature (°C)	Nebulizer Gas (psi)	Heater Gas (psi)
Phase 1 (0-4 min)	40	Medium	-3500	450	50	50
Phase 2 (4-6 min)	20	Medium	4000	450	50	50

Table S2: Fragments and parameters used for each antibiotic and the internal standard (IS). Individual standard solutions of each analyte and internal standard were directly injected to optimize their mass spectrometry parameters.

Antibiotic	Identifier	ESI mode	Retention time (min)	Q1 (Da)	Q3 (Da)	Dwell Time (msec)	Declustering Potential (volts)	Entrance Potential (volts)	Collision Energy (volts)	Exit Potential (volts)
Fosfomycin	Quantification	-	1.22	136.884	78.9	150	-100	-10	-62	-13
Fosfomycin	Qualification	-	1.22	136.884	81.1	150	-100	-10	-32	-13
Avibactam	Quantification	-	2.60	263.913	80	150	-80	-10	-38	-11
Avibactam	Qualification	-	2.60	263.913	95.8	150	-80	-10	-20	-9
Ceftazidime	Quantification	+	4.29	546.957	468	150	96	10	17	20
Ceftazidime	Qualification	+	4.29	546.957	167.2	150	96	10	33	18
Moxifloxacin (IS)	Quantification	+	5.20	402.118	384.2	150	96	10	33	22
Moxifloxacin (IS)	Qualification	+	5.20	402.118	96.1	150	96	10	79	12

Text S3: Methods of the pharmacokinetic/pharmacodynamic (PKPD) modelling

Static time kill experiments

The PKPD model describing the static time kill data was built sequentially: in a first step the mono drug effects of ceftazidime, avibactam and fosfomycin were estimated, in a second step the mono drug parameters were fixed and solely the drug interaction parameters were estimated and in a final estimation step all parameters were unfixed and estimated together. The CVODES differential equation solver implemented as ADVAN14 in NONMEM® 7.5.0. (ICON, Gaithersburg, MD, USA) was used for model development. The base model consisted of a two-compartment ordinary differential equation system describing a susceptible (S) and a resistant (R) population affected by different drug effects (E_S and E_R) (Eqs. 1-2). The growth kinetics of the bacteria were described by individual inocula of the two compartments and individual growth constants (k_{GS} and k_{GR}). The growth of the bacteria was limited to a global capacity limit (B_{max}).

$$\frac{dS}{dt} = S \cdot k_{GS} \cdot \left(1 - \frac{S + R}{B_{max}}\right) - S \cdot E_S \quad (1)$$

$$\frac{dR}{dt} = R \cdot k_{GR} \cdot \left(1 - \frac{S + R}{B_{max}}\right) - S \cdot E_R \quad (2)$$

The individual drug effects were preferably described by sigmoidal maximum effects models or power functions (Eqs. 3-4).

$$E(C) = \frac{E_{max} \cdot C^H}{EC_{50}^H + C^H} \quad (3)$$

$$E(C) = Slope \cdot C^H \quad (4)$$

with E_{max} being the maximum kill rate of the respective agent (h^{-1}), C the concentration of the drug (mg/L), H the sigmoidicity parameter, the EC_{50} the concentration (mg/L) at which the drug effect is half-maximum and $Slope$ being the linear correlation factor of the concentration to the killing rate of an agent ($L/(mg \times h)$). The model selection was made based on graphical model fit, model stability and Akaike information criterion (AIC).

For combined drug effects the applied additivity criterion was Bliss Independence. To calculate the probabilistic Bliss Independence term for three drugs the single drug

effects were normalized to the maximum drug effect of the combined drugs and afterwards scaled back to the effect scale (Eqs. 5-6) (2, 3).

$$E_{\max} = \max (E_{\max,A}, E_{\max,B}, E_{\max,C}) \quad (5)$$

$$E_{\text{comb}} = \left(\frac{E_A}{E_{\max}} + \frac{E_B}{E_{\max}} + \frac{E_C}{E_{\max}} - \frac{E_A}{E_{\max}} \cdot \frac{E_B}{E_{\max}} - \frac{E_A}{E_{\max}} \cdot \frac{E_C}{E_{\max}} - \frac{E_B}{E_{\max}} \cdot \frac{E_C}{E_{\max}} + \frac{E_A}{E_{\max}} \cdot \frac{E_B}{E_{\max}} \cdot \frac{E_C}{E_{\max}} \right) \cdot E_{\max} \quad (6)$$

In cases, where the drug effects of ceftazidime, avibactam or fosfomycin were described by a power function effect sizes below 50% of the maximum effect were assumed. In these cases the probabilistic correction terms in Bliss Independence become neglectable and criterion collapses to simple addition of the effect sizes (Eq. 7) (3).

$$E_{\text{comb}} = E_A + E_B + E_C \quad (7)$$

Semi-mechanistic modelling of the drug interactions was performed by application of the general pharmacodynamic interaction (GPDI) model (4). The GPDI model describes drug interactions by the insertion of a GPDI-term shifting pharmacodynamic parameters (Θ) like E_{\max} or EC_{50} affected by a present concentration of a combination partner (Eq. 8). Depending on the affected parameter and the polarity of the maximum interaction shift (INT) synergistic or antagonistic drug interactions can be modelled. The magnitude of the shift is depending from the concentration of the perpetrator drug (C; mg/L), the sigmoidicity of the interaction (H_{INT}) and the potency of the interaction ($EC_{50-\text{INT}}$; mg/L).

$$\Theta_{\text{GPDI}} = \Theta \cdot \left(1 + \frac{\text{INT} \cdot C^{H_{\text{INT}}}}{EC_{50-\text{INT}}^{H_{\text{INT}}} + C^{H_{\text{INT}}}} \right) \quad (8)$$

If the GPDI-term is implemented on one combination partner, interactions are monodirectional. They can become bidirectional when the GPDI-term is implemented on both interaction partners. In those cases, both drugs are perpetrator and victim of the interaction at the same time and also asymmetric drug interactions with simultaneous synergy and antagonism are possible. For the drug interaction of avibactam and ceftazidime the interactions were implemented as shifts on the EC_{50} of ceftazidime mediated by avibactam.

For the drug interaction of ceftazidime and fosfomycin four different implementations of the GPDI model were tested before unfixing all mono drug effects for the final simultaneous estimation of all parameters: I) a monodirectional interaction of ceftazidime affecting fosfomycin, II) a monodirectional interaction of fosfomycin affecting ceftazidime, III) a bidirectional interaction described by one shared maximum interaction shift and IV) a bidirectional interaction described by separate maximum interaction shifts.

Uncertainty of the parameters of the static time kill model was assessed by the sampling importance resampling (SIR) routine implemented in Perl-speakes-NONMEM (PsN) 5.0 (Uppsala University, Sweden) with the relative standard errors (RSE) calculated in the covariance step as proposal distribution (5).

Dynamic hollow fiber infection model

The model developed based on the static time kill curve data was further developed to include the HFIM data. All parameters related to the drug effects were fixed. The ODE system was extended by two compartments describing the phenotypic less susceptible subpopulations which emerged against ceftazidime/avibactam or fosfomycin (R_{CZA} and R_{FOF}) (Eqs. 9-12):

$$\frac{dS}{dt} = S \cdot k_{GS} \cdot \left(1 - \frac{S + R + R_{CZA} + R_{FOF}}{B_{max}}\right) - S \cdot E_S \quad (9)$$

$$\frac{dR}{dt} = R \cdot k_{GR} \cdot \left(1 - \frac{S + R + R_{CZA} + R_{FOF}}{B_{max}}\right) - S \cdot E_R \quad (10)$$

$$\frac{dR_{CZA}}{dt} = R_{CZA} \cdot k_{GR_{CZA/FOF}} \cdot \left(1 - \frac{S+R+R_{CZA}+R_{FOF}}{B_{max}}\right) \cdot (1 - E_{CZA_{R_{CZA}}}) \cdot (1 - E_{FOF_{R_{CZA}}}) \quad (11)$$

$$\frac{dR_{FOF}}{dt} = R_{FOF} \cdot k_{GR_{CZA/FOF}} \cdot \left(1 - \frac{S+R+R_{CZA}+R_{FOF}}{B_{max}}\right) \cdot (1 - E_{FOF_{R_{FOF}}}) \cdot (1 - E_{CZA_{R_{FOF}}}) \quad (12)$$

with additional effects of ceftazidime and fosfomycin suppressing the emerging subpopulations (E_{CZA} and E_{FOF}).

For suppression of resistance development, the maximum effect was assumed to be a full inhibition of the growth of the respective subpopulation. Therefore, a simplification of the sigmoidal maximum effect model was applied (Eq. 13).

$$E(C) = \frac{C^H}{EC_{50}^H + C^H} \quad (13)$$

The sigmoidicity parameters were either estimated or fixed to constants (i.e. 1 for model simplification or 20 for steep concentration effect relations). The inhibitory effects of the two drugs ceftazidime and avibactam were merged for the subpopulation synergy and the effect was estimated as a function of the concentration of ceftazidime.

To account for the lower limit of quantification of the less susceptible subpopulations a baseline was set to 0 log₁₀(CFU/mL) and the time points of the emergence of resistance were solely driven by the inoculum of the respective subpopulation and the drug concentrations suppressing their growth.

As described above the uncertainty of the parameters of the dynamic HFIM model was also assessed by the SIR routine implemented in PsN 5.0 (Uppsala University, Sweden) with the relative standard errors (RSE) calculated in the covariance step as proposal distribution (5).

Results

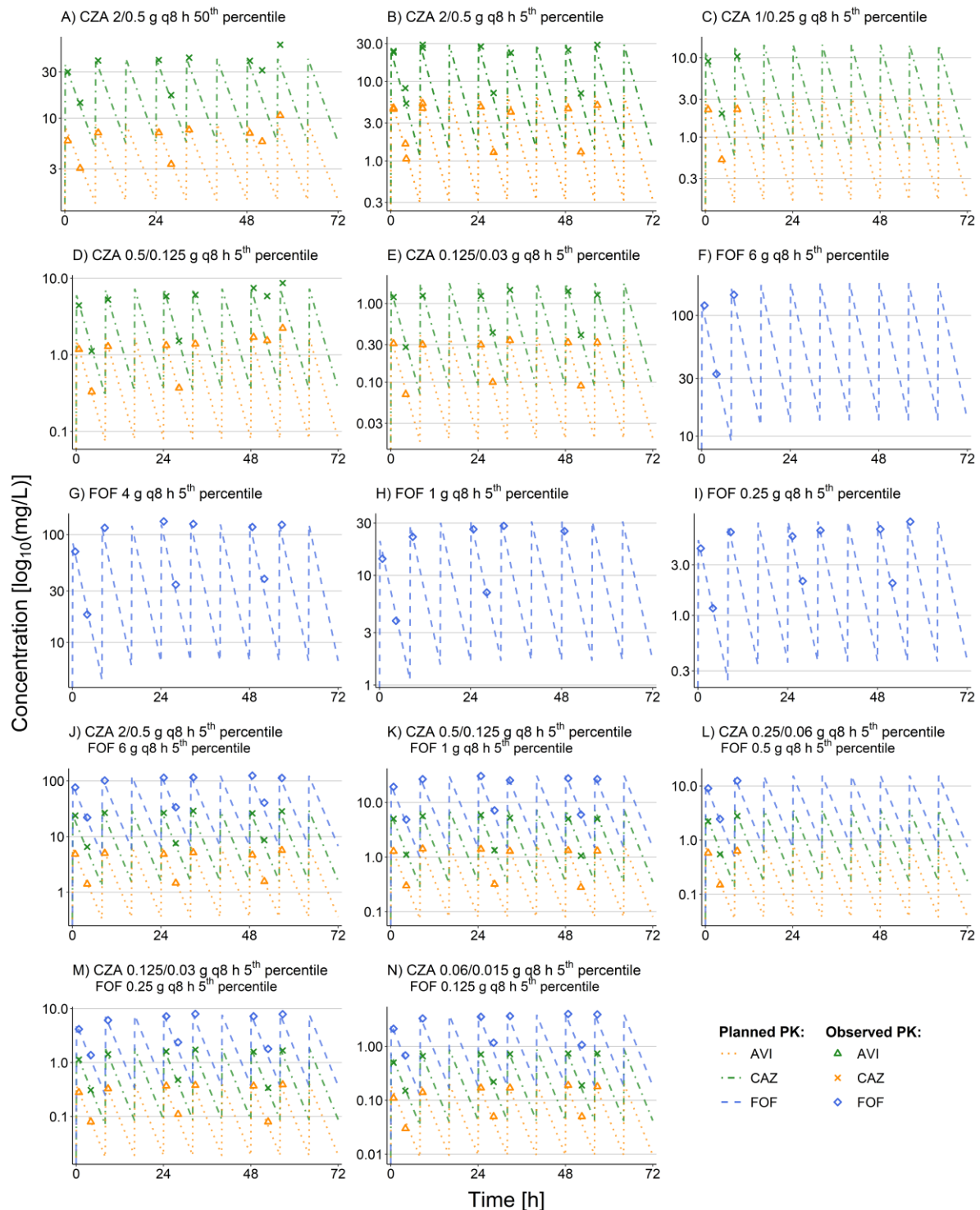


Figure S1: Illustration of the quantified concentrations of ceftazidime (CAZ), avibactam (AVI) and fosfomycin (FOF). Planned pharmacokinetic (PK) profiles (lines) are compared to the measured concentrations (symbols). Facets A to E display the monotherapy simulations of ceftazidime/avibactam, facets F to I display monotherapy simulations of fosfomycin and facets J to N display combination therapy simulations. The percentiles represent the percentage of patients from 1000 simulations achieving the displayed or lower pharmacokinetic profiles.

Text S4: Results of the dynamic hollow fiber infection model

The antigen test against the beta-lactamases CTX-M-15 and OXA-244 after 2 h of preincubation confirmed the expression of the beta-lactamases and their retention in the hollow fiber cartridge.

The quantified drug concentrations matched the planned pharmacokinetic profiles and no extensive degradation of the ceftazidime by beta-lactamases was apparent.

Text S5: Results of the pharmacokinetic/pharmacodynamic modelling**Static time kill experiments**

Comparable regrowth patterns of the bacteria incubated with the different drugs alone and in combination allowed for a combination of the emerging bacteria in one joint resistant (R) subpopulation. Most calculated drug effects of ceftazidime, avibactam and fosfomicin were supported by sigmoidal maximum effect models. Solely the drug effect of fosfomicin on (S) and the drug effect of avibactam on (R) were described by power models. Therefore, for the (S) population the Bliss Independence criterion collapsed to effect addition. Because of the small effect sizes of avibactam compared to ceftazidime and fosfomicin ($E_{max_{CAZ}}$: 0.659 h^{-1} and $E_{max_{FOF}}$: 0.635 h^{-1} compared to the avibactam effect at the highest applied concentration: 0.294 h^{-1}), just the maximum effects of ceftazidime and fosfomicin were considered for the normalization for the calculation of Bliss Independence on the (R) population.

The exploratory graphical analysis of the drug interactions of avibactam with ceftazidime and ceftazidime with fosfomicin indicated maintained drug effects at significantly reduced drug concentrations (e.g. Fig. 1: ceftazidime $0.0625 \mu\text{g/mL}$ + avibactam $8 \mu\text{g/mL}$ had a similar effect as ceftazidime $128 \mu\text{g/mL}$ alone and ceftazidime $2 \mu\text{g/mL}$ + fosfomicin $4 \mu\text{g/mL}$ had a similar effect as fosfomicin $16 \mu\text{g/mL}$ alone). Therefore, the implementation of the drug interaction via the GPDI model was focused on EC_{50} interactions. A pharmacokinetic drug interaction of avibactam and ceftazidime by means of an inhibition of the degradation of ceftazidime by beta-lactamases was neglected, because of the absence of quantitative data for the static time kill experiments.

The drug interaction of ceftazidime and fosfomycin was described best by a mono directional interaction with a potentiation of the fosfomycin EC_{50} on the (R) population. The respective Akaike Information Criteria differences for the different GPDI model implementations computed against Bliss Independence were as follows:

Monodirectional interactions:

I) ceftazidime affecting fosfomycin: -271.991

II) fosfomycin affecting ceftazidime: -2.035

Bidirectional interactions:

III) interactions described by one shared maximum interaction shift: -262.994

IV) interactions described by separate maximum interaction shifts: -251.171

The model estimated strong synergistic interactions with maximum interaction shifts (INT) reducing the EC_{50} by >99% for both interacting drug pairs (i.e. ceftazidime/avibactam and ceftazidime/fosfomycin). Those estimates are in line with the *in vitro* observed interaction effect sizes outlined above. To support the accurate estimation and to avoid boundary issues the INT-parameters and interaction potencies (EC_{50} s of the interaction) were transformed to a logarithmic scale. This rescaling enabled the estimation of the full concentration-interaction-relations without any further assumptions. For example, the interaction of ceftazidime and avibactam is characterised by a very small EC_{50} of the interaction and a Hill factor of 0.266. This leads mathematically to an onset of the potentiation of ceftazidime by avibactam at very small concentrations followed by a less steep concentration-potentiation-relation when the avibactam concentration is further increased. This finding is in line with the *in vitro* observations. The full set of model parameters is displayed on Table S3.

Interexperiment variability was tested as interindividual variability on the inoculum and the growth rate of the (R) population and was implemented on both parameters as exponential coefficient of variation.

Table S3: Typical PD parameters (Θ) of the static PD model developed based on data of static time kill experiments including 95% confidence intervals obtained by the sampling importance resampling (SIR) technique.

Structural model parameters	
Inoculum susceptible bacteria (S) [\log_{10} (CFU/mL)]	6.86 [6.74-6.96]
Inoculum resistant bacteria (R) [\log_{10} (CFU/mL)]	3.14 [2.81-3.43]
Maximum bacterial capacity [\log_{10} (CFU/mL)]	8.92 [8.76-9.06]
Growth rate (S) [h^{-1}]	1.81 [1.61-2.15]
Growth rate (R) [h^{-1}]	0.45 [0.41-0.52]
Mono drug PD parameters	
E _{max} of CAZ on (S) [h^{-1}]	3.40 [3.08-3.87]
EC ₅₀ of CAZ on (S) [mg/L]	5.31 [4.23-6.54]
Hill factor of CAZ on (S)	2.32 [1.77-2.88]
E _{max} of CAZ on (R) [h^{-1}]	0.659 [0.592-0.746]
EC ₅₀ of CAZ on (R) [mg/L]	74.40 [64.25-92.04]
Hill factor of CAZ on (R)	8.45 [5.98-10.95]
Slope of FOF on (S) [L/mg x h^{-1}]	2.71 [2.51-3.09]
Hill factor of FOF on (S)	0.333 [0.292-0.377]
E _{max} of FOF on (R) [h^{-1}]	0.635 [0.582-0.718]
EC ₅₀ of FOF on (R) [mg/L]	4.70 [3.67-5.72]
Hill factor of FOF on (R)	4.08 [2.76-5.79]
E _{max} of AVI on (S) [h^{-1}]	3.3 [2.76-3.98]
EC ₅₀ of AVI on (S) [mg/L]	22.3 [16.50-29.10]
Hill factor of AVI on (S)	1.13 [0.92-1.39]
Slope of AVI on (R) [L/mg x h^{-1}]	0.0787 [0.0554-0.1101]
Hill factor of AVI on (R)	0.317 [0.194-0.420]

Interaction model: avibactam affecting ceftazidime	
INT: maximum change of EC ₅₀ of CAZ on (S) mediated by AVI	-6.70 [-8.13- -5.65] ¹
EC ₅₀ of AVI in the interaction on EC ₅₀ of CAZ on (S) [mg/L]	-16.20 [-18.93- -13.99] ²
Hill factor of AVI in the interaction on EC ₅₀ of CAZ on (S)	0.266 [0.226-0.312]
INT: Maximum change of EC ₅₀ of CAZ on (R) mediated by AVI	-13.50 [-19.43- -9.69] ¹
EC ₅₀ of AVI of the interaction on EC ₅₀ of CAZ on (R) [mg/L]	-5.23 [-5.53- -5.04] ²
Hill factor of AVI in the interaction on EC ₅₀ of CAZ on (R)	1 ³
Interaction model: ceftazidime affecting fosfomycin	
INT: Maximum change of EC ₅₀ of FOF on (R) mediated by CAZ	-7.85 [-10.08- -5.58] ¹
EC ₅₀ of CAZ in the interaction on EC ₅₀ of FOF on (R) [mg/L]	-12.40 [-15.01- -10.50] ²
Hill factor of CAZ in the interaction on EC ₅₀ of FOF on (R)	0.239 [0.179-0.311]
Variability model	
Inter-experimental variability on the inoculum of resistant bacteria (R) [%CV] ⁴	33.9 [27.8-38.9]
Inter-experimental variability on the Growth rate (R) [%CV] ⁴	22.6 [19.9-25.8]
Additive residual variability σ [log(CFU/mL)]	1.30 [1.20-1.38]

Abbreviations: AVI: avibactam; CAZ: ceftazidime; CFU: colony forming units; EC₅₀: drug concentration at which the effect is half-maximum; Emax: maximum effect; FOF: fosfomycin; INT: maximum interaction shift

¹ parameter was estimated on log scale: TV = e⁰-1

² parameter was estimated on log scale: TV = e⁰

³ parameter was fixed to a constant

⁴ %CV was calculated as follows: %CV = $\sqrt{\exp(\omega^2) - 1} \cdot 100\%$

Dynamic hollow fiber infection model

Simulations of the HFIM experiments using the static time kill PKPD model revealed, that the model solely informed by the static time kill experiments missed to capture rapid regrowth in the early phase of the HFIM experiments (0 h - 12 h) or later regrowth profiles (> 30 h) (Figure S2). These regrowth patterns were driven by the emergence of phenotypic 3xMIC resistant subpopulations. Hence, the static time kill PKPD model was further developed to describe the dynamic HFIM experiments by the addition of two bacterial subpopulations describing the CFU growing on agar plates containing each drug at a concentration of 3xMIC. Those subpopulations were assumed to contribute to the total CFU count of the ODE system and allowed to quantify and accurately describe the emergence of 3xMIC resistance against the present antibiotics in the respective experiments.

To account for different growth conditions in the HFIM due to a constant supply of growth medium compared to static time kill experiments where the medium is not replenished, the bacterial inocula of the previous (S) and (R) populations as well as their growth rates and the maximum bacterial capacity were initially attempted to be estimated from the HFIM data. The data was insufficiently able to fully inform all growth parameters and the estimates tended towards the final static time kill PKPD parameter estimates. Therefore, both growth constants of the (S) and (R) populations as well as the inoculum of the (S) population were fixed, following previous studies where the phenomenon of non-diverging growth constants between static and dynamic experiments was also observed (6).

The model parameters are displayed on Table S4. The inoculum of the (R) population was estimated to be lower than for the static time kills curves (i.e. $2.89 \log_{10}(\text{CFU/mL})$ instead of $3.14 \log_{10}(\text{CFU/mL})$), because the newly introduced phenotypic subpopulations covered parts of the regrowth pattern and the (R) population remained to describe lower resistance level besides the 3xMIC resistance. Describing the growth of the additional subpopulations, the additive residual error as well as the growth rates of both phenotypic less susceptible subpopulations were estimated to be similar. Therefore, they were merged to one respective parameter describing the residual error

and growth rate of both phenotypic less susceptible subpopulations. Of note, the final estimate of the growth rate of the less susceptible subpopulations unexpectedly exceeds the growth rate of the (S) population (2.37 h^{-1} against 1.81 h^{-1}) (Tables S3, S4). Nevertheless, the confidence intervals of both estimates overlap, thus, a significant difference of the growth rates cannot be concluded. The relatively similar values indicate a low biological cost of the resistance development against ceftazidime/avibactam and fosfomycin.

The inoculum of the phenotypic resistant bacteria against ceftazidime/avibactam was fixed to the final estimate to stabilize the model. The very low inoculum of 10^{-18} CFU/mL corresponds to the later observed emergence of resistances against ceftazidime/avibactam compared to fosfomycin and allows to describe the higher variability of the emergence of resistance against ceftazidime/avibactam.

Regarding the effects suppressing the growth of the phenotypically resistant bacteria, the sigmoidicity parameters were either fixed to 1 or freely estimated. For very steep concentration effect relations the parameter was empirically fixed to 20.

Adjustments were made to the variability model to explain the observed interexperimental variability especially for the development of phenotypic resistances against ceftazidime/avibactam. The interindividual variability on the growth constant of (R) estimated for the static time kill data was not necessary to adequately describe the HFIM data. In contrast an interindividual variability on the inoculum of the phenotypic less susceptible subpopulation against ceftazidime/avibactam was implemented to capture the observed variability of the resistance development.

Table S4: Typical PD parameters (Θ) of the dynamic time kill model based on data of dynamic hollow fiber experiments evolved from the model developed for static time kill curve (TKC) experiments (Table S3) including 95% confidence intervals obtained by the sampling importance resampling (SIR) technique.

Structural model parameters	
Inoculum susceptible bacteria (S) [\log_{10} (CFU/mL)]	6.86 FIX to TKC parameter
Inoculum resistant bacteria (R) [\log_{10} (CFU/mL)]	2.89 [2.68-2.99]
Maximum bacterial capacity [\log_{10} (CFU/mL)]	9.73 [9.50-9.91]
Growth rate (S) [h^{-1}]	1.81 FIX to TKC parameter
Growth rate (R) [h^{-1}]	0.45 FIX to TKC parameter
Mono drug PD parameters	
E _{max} of CAZ on (S) [h^{-1}]	3.40 FIX to TKC parameter
EC ₅₀ of CAZ on (S) [mg/L]	5.31 FIX to TKC parameter
Hill factor of CAZ on (S)	2.32 FIX to TKC parameter
E _{max} of CAZ on (R) [h^{-1}]	0.659 FIX to TKC parameter
EC ₅₀ of CAZ on (R) [mg/L]	74.40 FIX to TKC parameter
Hill factor of CAZ on (R)	8.45 FIX to TKC parameter
Slope of FOF on (S) [L/mg x h^{-1}]	2.71 FIX to TKC parameter
Hill factor of FOF on (S)	0.333 FIX to TKC parameter
E _{max} of FOF on (R) [h^{-1}]	0.635 FIX to TKC parameter
EC ₅₀ of FOF on (R) [mg/L]	4.70 FIX to TKC parameter
Hill factor of FOF on (R)	4.08 FIX to TKC parameter
E _{max} of AVI on (S) [h^{-1}]	3.3 FIX to TKC parameter
EC ₅₀ of AVI on (S) [mg/L]	22.3 FIX to TKC parameter
Hill factor of AVI on (S)	1.13 FIX to TKC parameter
Slope of AVI on (R) [L/mg x h^{-1}]	0.0787 FIX to TKC parameter
Hill factor of AVI on (R)	0.317 FIX to TKC parameter

Interaction model: avibactam affecting ceftazidime	
INT: maximum change of EC ₅₀ of CAZ on (S) mediated by AVI	-6.70 FIX to TKC parameter ¹
EC ₅₀ of AVI in the interaction on EC ₅₀ of CAZ on (S) [mg/L]	-16.20 FIX to TKC parameter ²
Hill factor of AVI in the interaction on EC ₅₀ of CAZ on (S)	0.266 FIX to TKC parameter
INT: maximum change of EC ₅₀ of CAZ on (R) mediated by AVI	-13.50 FIX to TKC parameter ¹
EC ₅₀ of AVI in the interaction on EC ₅₀ of CAZ on (R) [mg/L]	-5.23 FIX to TKC parameter ²
Hill factor of AVI in the interaction on EC ₅₀ of CAZ on (R)	1 FIX to TKC parameter
Interaction model: ceftazidime affecting fosfomycin	
INT: maximum change of EC ₅₀ of FOF on (R) mediated by CAZ	-7.85 FIX to TKC parameter ¹
EC ₅₀ of CAZ in the interaction on EC ₅₀ of FOF on (R) [mg/L]	-12.40 FIX to TKC parameter ²
Hill factor of CAZ in the interaction on EC ₅₀ of FOF on (R)	0.239 FIX to TKC parameter
Less susceptible subpopulation model	
Inoculum ceftazidime/avibactam less susceptible subpopulation [\log_{10} (CFU/mL)]	-18 ³
Inoculum fosfomycin less susceptible subpopulation [\log_{10} (CFU/mL)]	-2.15 [-2.98- -1.52]
Growth rate less susceptible subpopulations [h ⁻¹]	2.37 [2.09-2.68]
EC ₅₀ of FOF suppressing the FOF less susceptible subpopulation [mg/L]	6.84 [6.48-7.17]
Hill factor of FOF suppressing the FOF less susceptible subpopulation	20 ⁴

EC ₅₀ of CZA suppressing the CZA less susceptible subpopulation [mg/L]	0.576 [0.441-0.765]
Hill factor of CZA suppressing the CZA less susceptible subpopulation	1 ⁴
EC ₅₀ of CZA suppressing the FOF less susceptible subpopulation [mg/L]	0.049 [0.040-0.057]
Hill factor of CZA suppressing the FOF less susceptible subpopulation	2.49 [1.76-4.20]
EC ₅₀ of FOF suppressing the CZA less susceptible subpopulation [mg/L]	1.38 [1.00-2.49]
Hill factor of FOF suppressing the CZA less susceptible subpopulation	20 ⁴
Variability model	
Inter-experimental variability on the inoculum of resistant bacteria (R) [%CV] ⁵	48.2 [40.4-56.9]
Inter-experimental variability on the on the inoculum of the ceftazidime/avibactam less susceptible subpopulation [%CV] ⁵	47.7 [28.6-65.9]
Additive residual variability on the total bacterial count σ [log(CFU/mL)]	3.28 [2.98-3.67]
Additive residual variability on less susceptible σ [log(CFU/mL)]	0.906 [0.837-1.00]

Abbreviations: AVI: avibactam; CAZ: ceftazidime; CFU: colony forming units; CZA: ceftazidime/avibactam; EC₅₀: drug concentration at which the effect is half-maximum; Emax: maximum effect; FOF: fosfomycin; INT: maximum interaction shift; TKC: static time kill curve

¹ parameter was estimated on log scale: TV = e⁰-1

² parameter was estimated on log scale: TV = e⁰

³ parameter was fixed to final estimate

⁴ parameter was fixed to a constant

⁵ %CV was calculated as follows: %CV = $\sqrt{\exp(\omega^2) - 1} \cdot 100\%$

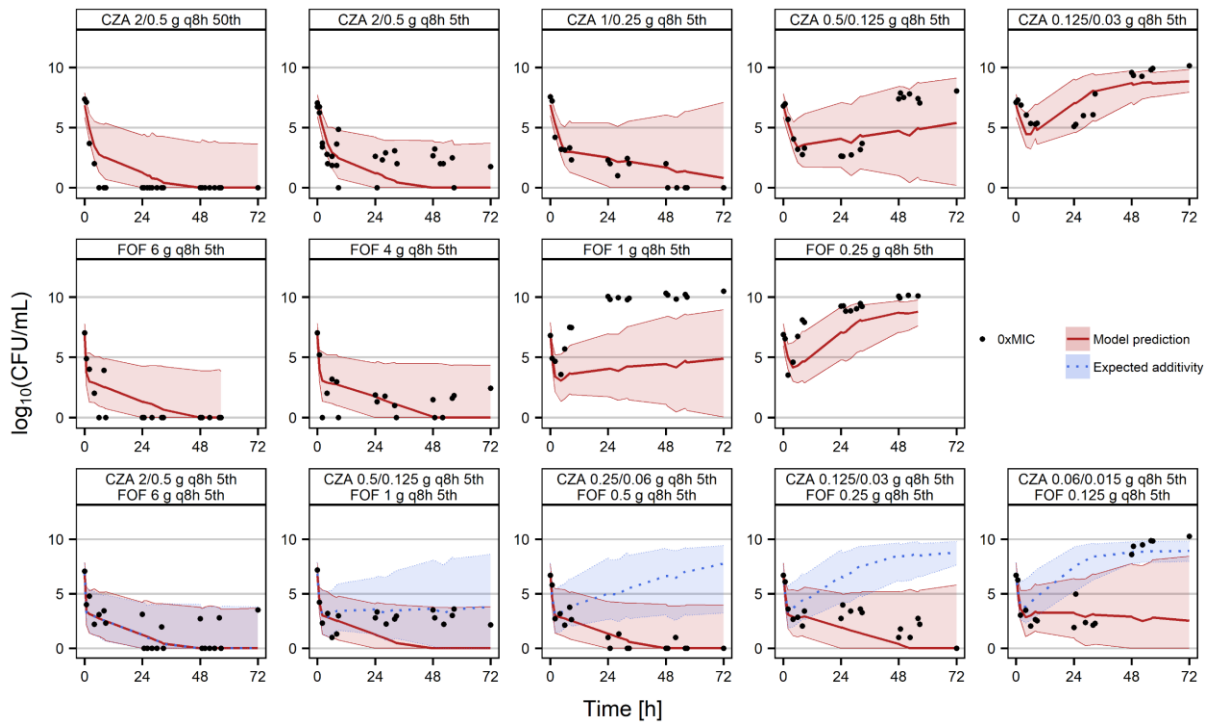









Figure S2: Stratified visual predictive check (VPC) ($n=1000$) on the PKPD model developed on static time kill experiments applied to the experimental data of the dynamic hollow fiber experiments. The percentiles (50^{th} or 5^{th}) of the doses correspond to the distribution of pharmacokinetic profiles which would be expected from simulations of 1000 patients given the defined dose. Dots: observed bacterial count; solid line: median prediction; dotted line: expected Bliss Independence; shaded areas: 90% prediction intervals.








References

1. Sy SKB, Zhuang L, Sy S, Derendorf H. 2019. Clinical Pharmacokinetics and Pharmacodynamics of Ceftazidime–Avibactam Combination: A Model-Informed Strategy for its Clinical Development. *Clin Pharmacokinet* 58:545–564.
2. Goldoni M, Johansson C. 2007. A mathematical approach to study combined effects of toxicants in vitro: Evaluation of the Bliss independence criterion and the Loewe additivity model. *Toxicol In Vitro* 21:759–769.
3. Chen C, Wicha SG, De Knecht GJ, Ortega F, Alameda L, Sousa V, De Steenwinkel JEM, Simonsson USH. 2017. Assessing pharmacodynamic interactions in mice using the multistate tuberculosis pharmacometric and general pharmacodynamic interaction models. *CPT Pharmacomet Syst Pharmacol* 6:787-797.
4. Wicha SG, Chen C, Clewe O, Simonsson USH. 2017. A general pharmacodynamic interaction model identifies perpetrators and victims in drug interactions. *Nat Commun* 8:2129.
5. Dosne AG, Bergstrand M, Harling K, Karlsson MO. 2016. Improving the estimation of parameter uncertainty distributions in nonlinear mixed effects models using sampling importance resampling. *J Pharmacokinet Pharmacodyn* 43:583–596.
6. Nielsen EI, Cars O, Friberg LE. 2011. Predicting In Vitro Antibacterial Efficacy across Experimental Designs with a Semimechanistic Pharmacokinetic-Pharmacodynamic Model. *Antimicrob Agents Chemother* 55:1571–1579.

8 Hazardous materials

Table 1: List of the hazardous substances used in accordance with GHS including the GHS pictograms and hazard and precautionary statements

Substance	GHS pictogram	Signal word	Hazard statements	Precautionary statements
Acetonitrile		Danger	225, 302+312+332, 319	210, 280, 301+312, 303+361+353, P304+340+312, 305+351+338
Amitriptyline		Danger	301, 319, 361d, 410	201, 273, 301+310+330, 305+351+338
Avibactam		Warning	315, 319, 335	261, 264, 271, 280, 302+352, 304+340, 305+351+338, 312, 321, 362+364, 332+313, 337+313, 403+233, 405, 501
Ceftazidime		Danger	317, 334	261, 272, 280, 284, 302+352, 333+313
Ceftolozane		Danger	317, 334	261, 272, 280, 302+352, 333+313, 321, 362+364, 501, 284, 304+340, 342+311
Chloramphenicol		Warning	318, 351, 361fd	202, 280, 305+351+338, 308+313, 405, 501
Ethanol (absolute)		Danger	225, 319	210, 243, 280, 305+351+338, 403+235

Substance	GHS pictogram	Signal word	Hazard statements	Precautionary statements
Formic acid (98%)		Danger	226, 302, 314, 331	210, 280, 301+312, 303+361+353, 304+340+310, 305+351+338
Fosfomycin	The substance is not classified by GHS according to regulation (EC) No 1272/2008.			
Glucose-6-phosphate	The substance is not classified by GHS according to regulation (EC) No 1272/2008.			
Meropenem		Danger	317, 334	261, 272, 280, 284, 302+352, 333+313
Methanol		Danger	225, 301+311+331, 370	210, 233, 280, 301+310, 303+361+353, 304+340+311
Moxifloxacin		Warning	302, 319, 412	264, 270, 273, 280, 301+312, 305+351+338
Sulfadimethoxine		Warning	315, 317, 319, 335	261, 280, 305+351+338
Tazobactam	The substance is not classified by GHS according to regulation (EC) No 1272/2008.			
Tetracycline		Warning	361d, 411	201, 273, 308+313
Vaborbactam		Warning	302	264, 270, 301+312, 330, 501

9 Acknowledgements

In a first place, I want to express my gratitude to my supervisor *Prof. Sebastian G. Wicha. Sebastian*, I feel honored to have gotten the opportunity to be guided by you into the world of pharmacometrics and clinical anti-infectives. The way I was able to learn from your knowledge and your experience was simply impressive. You managed to inspire me for our research field in a very trust- and respectful way. Our eye-level scientific exchange and discussions trained me as the scientist I am today. The tremendous support and chances you created were invaluable for me as a junior scientist.

I am also very grateful to *Dr. Astrid Bröker* who enlightened the spark of pharmacometrics in me and finally tempted me to apply to the Clinical Pharmacy Research Group in Hamburg.

A huge thank you goes to *Dr. Fabian Thielbeer* for all the scientific and moral support and for reviewing parts of this dissertation. Additionally, I thank *David, Emily, Christoph, Christine, Joost* and *Aneeq* for their assistance during the preparation of this thesis.

I would also like to equally thank all colleagues and collaborators within the CO-PROTECT project, namely *Prof. William Couet* as representative for the whole 'Poitiers-Team', *Prof. Patrice Nordmann, Dr. Prasad Phapale* and *Prof. Jean-Winoc Decousser*. I learned a lot from your expertise in PK/PD, clinical microbiology, genomics and metabolomics. The monthly scientific exchange and multidisciplinary discussions expanded my scientific horizon.

A warm thank you goes to all the colleagues and friends from the Clinical Pharmacy Research Group in Hamburg: *Astrid, David, Lisa, Emily, Christoph, Christine K., Khalid, Aneeq, Anna, Tjokosela, Christine B., Julian* and *Antonia* and to all the interns and guest researchers on the way. It was a great journey and a pleasure to explore the fields of pharmacometrics with you!

Finally, I want to thank my *family* and *friends* for backing me and being there for me. Especially, *Malin*, without your unconditional love and support this project would have never been possible.

There is a lot more to come and I will always be curious of what is awaiting.

10 Eidesstattliche Versicherung

Hiermit versichere ich an Eides statt, die vorliegende Dissertation selbst verfasst und keine anderen als die angegebenen Hilfsmittel benutzt zu haben. Die eingereichte schriftliche Fassung entspricht der auf dem elektronischen Speichermedium. Ich versichere, dass diese Dissertation nicht in einem früheren Promotionsverfahren eingereicht wurde.

Biberach, den _____

Niklas Krömer